Cyclical non-linearity, nowcasting and asset allocation

Romain Aumond

INSTITUT POLYTECHNIQUE DE PARIS

NNT : 2024IPPAG008

Thèse de doctorat

ENSAE

IP PARIS

La non-linéarité cyclique, prévision en temps réel et son application à la gestion d'actifs

Thèse de doctorat de l'Institut Polytechnique de Paris
préparée à l'École nationale de la statistique et de l'administration économique

École doctorale n°626 École doctorale de l'Institut Polytechnique de Paris (ED IP Paris)
Spécialité de doctorat : Sciences Economiques

Thèse présentée et soutenue à Palaiseau, le 17 octobre 2024, par

ROMAIN AUMOND

Composition du Jury :

Frédérique Bec Professeure, CY Cergy Paris Université (THEMA)	Présidente
Christophe Hurlin Professeur, Université d'Orléans (LEO)	Rapporteur
Gabriel Pérez Quirós Chef d'Unité, Unité d'analyse macroéconomique, Banco de España	Rapporteur
Jean-Michel Zakoïan Professeur, Université de Lille et ENSAE (CREST)	Examinateur
Anna Simoni Professeure, ENSAE et Ecole Polytechnique (CREST)	Directrice de thèse
Warin Buntrock Directeur adjoint des gestions, BFT IM	Invité
Mabrouk Chetouane Responsable de la stratégie de marché, Natixis IM	Invité

A Denise et Roger Aumond, Anna Margareta et Peter Amend.

Remerciements

Ces quelques mots introductifs ont pour objet l'expression de ma reconnaissance envers toutes les personnes qui ont contribué, par leur bienveillance, leur générosité, leur lumière, leur humour et leur franchise à m'élever autant humainement qu'intellectuellement durant ce long voyage qu'a constitué ma thèse.

Je tiens premièrement à remercier ma Directrice de thèse, Anna Simoni d'avoir été aussi disponible et exigeante, pierre angulaire de la rigueur scientifique de ce manuscrit.

Christian Francq et Jean-Michel Zakoïan ont été déterminants dans le suivi de mes travaux et je les remercie pour les discussions inspirantes relatives à mes progrès.

Comment ne pas exprimer ensuite, ma plus profonde gratitude envers Mabrouk Chetouane, sans qui rien de ce projet de recherche étiré maintenant sur cinq années depuis un encadrement de groupe de travail ENSAE en 2019, n'aurait vu le jour. Une personnalité iconoclaste qui, par la curiosité constante et la recherche inlassable de l'élégance, ne transigeant sur aucun aspect esthétique et moral, m'a transmis le goût pour l'effort, la persévérance et élargi mon horizon culturel – du « froissage élégant » des vêtements à l'œnologie, du sens de la formule façonné dans son creuset urbain à la vision macroéconomique globale et structurante de la société.

Je remercie également chaleureusement Christophe Hurlin et Gabriel Perez-Quiros pour leurs rapports et commentaires alimentant l'amélioration des travaux présentés, ainsi que Frédérique Bec et Jean-Michel Zakoïan d'avoir accepté de prendre part au jury.

I also warmly thank Christophe Hurlin and Gabriel Perez-Quiros for their reports and comments that contributed to improving the presented work, as well as Frédérique Bec and Jean-Michel Zakoïan for agreeing to take part in the jury.

Julien Royer, co-auteur de l'un des chapitres de cette thèse, est une cheville ouvrière de mon succès. Sans lui, sa perspicacité et son entrain remarquables, l'orientation de ces recherches n'eurent été que plus chaotiques. Je lui en suis infiniment reconnaissant. Sa passion pour l'art et ses goûts éclectiques, son parcours de jeune chercheur et son audace ont guidé une grande partie de mes choix et réflexions durant ces trois années.

Je ne peux faire l'économie de remerciements directement adressés à Killian Pluzanski, oreille empathique et partenaire de recherche indéfectible avec lequel j'ai pu, cent fois au moins, verbaliser les difficultés inhérentes à tout travail de recherche honnête et consciencieusement réalisé.

Cette thèse doit par ailleurs beaucoup au support du laboratoire d'économie du CREST, de son personnel administratif, pédagogique ainsi que des doctorants. Je pense ici tout particulièrement à Marion, Margarita, Pauline et Vincent mes collègues de bureau. Ces travaux sont aussi le fruit de trois années riches d'expérience au sein de BFT IM, que je souhaite remercier de m'avoir accueilli ainsi que pour son soutien, en particulier Gilles Guez, Laurent Gonon, Warin Buntrock. Plus globalement, c'est une multitude de personnes qui me viennent à l'esprit dans cette expérience

de franche camaraderie ; tout d'abord l'équipe de recherche, Fabien, Béline, Karen ainsi que les équipes de Gestion dans lesquelles Félicien, Lucas et Julien ont été de véritables appuis. Je remercie au même titre Bastien, Jean-Marie, Hassan et Zakaria pour les riches discussions que nous avons pu avoir.

Mon parcours académique est le produit d'une formation exigeante reçue à l'Université Paris-Dauphine, institution dans laquelle j'ai désormais la chance de transmettre les savoirs qui m'ont été prodigués. A ce titre, j'éprouve un sentiment de profonde reconnaissance envers Philippe Bernard et l'ensemble des enseignants que j'ai eu la chance de rencontrer et qui ont toujours stimulé ma curiosité en érigeant la raison comme rempart à l'obscurantisme. Je souhaite tout particulièrement remercier ici Mabrouk Chetouane (encore), Florian Ielpo, Chafic Merhy et Matthieu Garcin, parangons de ce modèle universitaire.

Ce projet de thèse n'eût été qu'une illusion si je n'avais eu, durant ces trois années, un soutien indéfectible de mes parents, constamment présents à mes côtés afin de m'encourager et à qui je dois bien plus que d'avoir fait de moi ce que je suis ; m'avoir fait devenir ce que j'aurais dû être. Je leur en suis extrêmement redevable et m'efforcerai de transmettre à mon tour, tout l'amour qu'ils ont eu pour moi.

Enfin, j'exprime mes remerciements les plus sincères à mes amis, qui m'ont offert une fenêtre sur un monde différent de celui de la recherche sur les cycles économiques, financiers et de politique monétaire, préservé du tumulte du temps. Ils m'ont, chacun à leur façon, fait grandir et atteindre une certaine forme d'ataraxie. Alice, Arthur, Carmen, Célia, Daphné, Elise, Etienne, Guillaume, Hadrien, Jean-Baptiste, Jeanne-Alice, Justus, Léa, Léna, Marguerite, Marti, Samuel, Sarah, Serah, Tristan, Ugo, Yoluène, MERCI.

Toute cette folle aventure s'est finalement construite sur la base d'une tendresse et d'une affection réciproque au quotidien, véritable forteresse. Son inlassable détermination à me pousser plus loin, à partager ce bout de vie qui fonde un paysage intérieur fleuri, délicieux, curieux, riche de mille influences, ouvert et sincère. A Laurène.

Contents

List of Figures

List of Tables

Chapter 1

Introduction

1.1. Résumé des travaux de thèse en français

Cette thèse se donne pour but d'affiner la détection des phases du cycle économique et d'étendre son application à l'allocation d'actifs. Les économies mondiales, et plus particulièrement les États-Unis, ont traversé récemment la récession la plus brutale de l'histoire au travers de la crise Covid. À la suite de ce choc macroéconomique considérable tant par son amplitude que sa courte durée, l'identification des phases du cycle économique pose problème aux praticiens. Les spécifications traditionnelles de modèles à facteur dynamique non linéaire ne parviennent en effet plus à identifier précisément les récessions de plus faible envergure, les deux dernières récessions (grande crise financière et Covid) ayant "pollué" par leur volatilité l'ensemble d'information historique. Ce travail propose une extension du cadre méthodologique des modèles à facteurs dynamiques à changements de régimes markoviens capable de traiter ces évènements historiques sans nuire à leur capacité de détection des ralentissements macroéconomiques plus modérés. Cela est rendu possible en prenant en compte des processus de volatilité dynamique spécifiques dans le facteur inobservable à changements de régimes synthétisant le cycle macroéconomique.

Identifier la date d'entrée et de sortie d'une récession est crucial pour les décideurs politiques et les investisseurs souhaitant suivre les fluctuations macroéconomiques sur une fréquence hebdomadaire. À cet égard, ce manuscrit montre la valeur ajoutée pour un praticien d'ajouter à son ensemble d'information macroéoconomique traditionnellement utilisé des prix de marchés servant à l'identification des phases du cycle conjoncturel en temps réel. Nous nous concentrons sur une classe spécifique de prix d'actifs, les asset swap spreads sur crédit d'entreprise, qui matérialisent des probabilités de défaut sur les emprunts émis et qui sont révisées continuellement. Le marché évalue la capacité d'un émetteur d'obligations d'entreprise à rembourser à la fois les intérêts et le capital d'un prêt. En agrégant ces probabilités à travers des catégories allant des entreprises au profil le plus risqué ("high yield") à celle de qualité supérieure ("investment grade"), couvrant une large partie des entreprises aux États-Unis, il est possible de capter des mouvements concomitants

du cycle économique. Cela correspond exactement à la définition donnée par Burns and Mitchell (1946) :

> *"Les cycles économiques sont un type de fluctuation que l'on retrouve dans l'activité économique globale des nations qui organisent principalement leur travail en entreprises : un cycle consiste en des expansions concomitantes dans de nombreuses activités économiques, suivies de ralentissement, de contractions et de reprises similaires qui débouchent sur la phase d'expansion du cycle suivant."* (p. 3)

Les asset swap spreads d'emprunts d'entreprise ainsi que les probabilités de défaut sous-jacentes, peuvent être considérés comme une évaluation partielle des dynamiques économiques globales. Partielle parce que toutes les entreprises américaines n'ont pas accès aux marchés financiers pour se financer (selon la Banque des Règlements Internationaux, la dette bancaire des entreprises non financières aux États-Unis représente environ 77% du produit intérieur brut américain tandis qu'en Europe continentale, malgré certaines disparités, la dette bancaire des entreprises représente environ 94,3%, il y aurait donc un accès approfondi des entreprises américaines aux marché financiers désintermédiés), néanmoins, un nombre suffisant d'entreprises de taille importante nous permet d'identifier les régimes du cycle économique de manière efficace. Être capable de détecter en temps réel (par exemple, sur une base hebdomadaire) l'occurence d'une récession économique permet le déploiement d'une stratégie dynamique de couverture efficiente pour un investisseur. Les indices actions ont en effet tendance à réagir aux chocs négatifs affectant le cycle économique en escomptant une dégradation des revenus futurs. Ce travail relie l'évaluation en temps réel du cycle économique à une stratégie de couverture réduisant l'exposition aux actifs risqués proportionnellement à la probabilité d'être en récession. Ce type de stratégie de couverture améliore le rendement ajusté de la volatilité pour un investisseur.

L'identification des phases du cycle économique est cruciale, mais ce n'est pas le seul facteur qu'un investisseur surveille dans le cadre d'une allocation multi-actifs. Certaines tensions de marché surviennent sans aucune dégradation macroéconomique. Les environnements de marché fortement volatiles ont tendance à produire des retournement de prix sévères lors de ventes paniques déclenchées par des rumeurs, des nouvelles exogènes ou par les structures mêmes du marché. Une quantification du sentiment de marché est donc primordiale à intégrer dans une stratégie d'allocation d'actifs afin de réduire les expositions du portefeuille aux actifs risqués lorsqu'un stress apparaît. Un autre segment qu'un investisseur suit dans sa décision d'allocation est la politique monétaire. À cette fin, identifier la posture de la politique monétaire que le marché escompte peut être d'une grande utilité pour les stratégies multi-actifs. Le portefeuille traditionnel 60% actions / 40% obligations, qui vise à maximiser le couple rendement/rique au travers des phases de marché, montre sa vulnérabilité lors de périodes où une politique monétaire restrictive est en place ou est anticipée par le marché. Ce travail consistera également à l'identification, en temps réel, d'une posture de politique monétaire basé sur des prix de marché. L'idée sera le développement d'une solution de couverture du portefeuille traditionnel 60% actions / 40% obligations avec un désinvestissement à chaque fois qu'un régime de politique monétaire restrictive est identifié.

Combiner les signaux de régime du cycle économique, de posture de la politique monétaire avec un sentiment de marché permet à un investisseur d'obtenir des couples rendement/risque robustes à travers diverses périodes de baisse de marché.

1.1.1. Motivations

Les modèles à facteurs dynamiques ont été utilisés pour résumer les sources de variation communes entre des variables économiques et ont connu plusieurs évolutions majeures depuis leur première utilisation (Bai and Ng (2008), Doz and Fuleky (2019), Barigozzi and Hallin (2023), entre autres, proposent une revue exhaustive de l'histoire et des développements majeurs dans ce champ de recherche). L'analyse factorielle a d'abord été introduite en psychologie par Spearman (1904), qui utilisait une composante inobservée pour caractériser les capacités cognitives des individus. Bien que ce cadre méthodologique ait avant tout été développé pour traiter des vecteurs aléatoires indépendamment distribués, Geweke (1977) l'a étendu pour synthétiser des co-mouvements entre séries temporelles économiques. L'intuition prend racine dans la définition du cycle économique de Burns and Mitchell (1946), observable d'après les auteurs à travers des phases d'expansion et de récession dans un grand nombre de séries économiques. Les travaux liminaires de Sargent and Sims (1977) et Stock and Watson (1989), ont montré qu'un petit nombre de composantes communes pouvait expliquer la dynamique conjointe des principaux agrégats économiques. Les indices économiques composites produits ont rapidement été amenés à varier en fonction des phases dans lesquelles se trouve le cycle économique. Les régimes économiques peuvent en effet être intégrés dans un cadre de modèles à changements de régimes markoviens. Kim (1994) et Diebold and Rudebusch (1996) ont été les premiers à incorporer des chaînes de Markov dans des modèles à facteurs dynamiques. Diebold and Rudebusch (1996) ont d'abord considéré un seul facteur résumant l'état sous-jacent de l'économie. Les auteurs définissent une dépendance des paramètres du facteur à une chaîne de Markov latente à deux états. Kim and Nelson (1998) sont les premiers à proposer une approche Bayésienne par le truchement d'un algorithme d'échantillonnage de Gibbs pour estimer les paramètres du modèle ainsi que les deux variables latentes (le facteur et la chaîne de Markov sous-jacente). Un premier volet de la littérature académique s'est concentré sur une approche fréquentiste d'estimation dans laquelle une approximation proposée par Kim (1994) était utilisée dans le calcul de la vraisemblance et du filtre de Kalman afin d'éviter l'écueil du nombre exponentiel de trajectoires (M^T) de la chaîne rendant une solution numérique impossible (avec M le nombre d'états de la chaîne de Markov et T le nombre d'observations). Une autre méthode a été avancée par Diebold and Rudebusch (1996). Ils introduisent une approche en deux étapes dans laquelle un indice coïncident est d'abord construit, puis le modèle Hamiltonien est estimé sur cet indice par la suite. Sur la base de cette intuition, Doz and Fuleky (2019) précisent qu'on peut utiliser une approche en deux étapes similaire à Doz et al. (2011) dans un cadre linéaire. Un modèle à facteurs dynamiques linéaire est d'abord estimé par composantes principales. On estime ensuite sur le facteur un modèle à changements de régimes markoviens, dans l'esprit de Hamilton (1989), par maximum de vraisemblance. Camacho et al. (2015) comparent les deux approches susmentionnées et soulignent la précision de l'approche en une étape lorsque le nombre

de variables utilisées est faible. Camacho et al. (2014) déploient une spécification du modèle prenant en compte des données multifréquentielles et au schéma de publication asynchrone. Dans le reste de ce manuscrit de thèse, nous nous concentrerons sur l'estimation bayésienne et resterons guidés par notre volonté de nous en tenir à des modèles avec un nombre restreint de variables afin de conserver l'interprétabilité des relations (dans l'esprit de Stock and Watson (1989), Kim and Yoo (1995), Doz et al. (2020) ou encore Leiva-Leon et al. (2020)). Chauvet and Piger (2008) démontrent la capacité du modèle à facteurs dynamiques à changements de régimes markoviens estimé à l'aide d'une méthode bayésienne de détecter avec précision les récessions datées par le National Bureau of Economic Research (NBER).

La difficulté que ce manuscrit aborde est l'hétérogénéité croissante des récessions économiques dans le cadre des modèles à facteurs dynamiques à changements de régimes markoviens. Comme le soulignent Leiva-Leon et al. (2020), spécifier des paramètres constants par régime (notamment la constante dans la dynamique du facteur) peut entraîner une identification inexacte des récessions modérées après les épisodes de contraction macroéconomique brutaux engendrés par la grande crise financière et l'épidémie du Covid. Les auteurs définissent une constante du facteur captant le cycle des affaires spécifique à chaque épisode de récession en activant une variable aléatoire au sein de chaque régime récessif. Les récessions hétérogènes peuvent également être captées par la volatilité qui leur est associée. Cette solution est proposée pour la première fois par Chauvet (1998) où une chaîne de Markov détermine à la fois les paramètres de la constante et de la volatilité du cycle écomonomique. Dans des travaux plus récents, Doz et al. (2020) explorent la possibilité de prendre en compte deux chaînes de Markov indépendantes dans la spécification du modèle, l'une déterminant la constante du facteur et l'autre la volatilité, produisant ainsi quatre états : deux régimes d'expansion et de récession à faible volatilité et deux régimes d'expansion et de récession à forte volatilité. Les paramètres restent néanmoins constants dans chaque régime. Le traitement de la récession Covid demeure de ce point de vue-là une question épineuse. On pourrait exclure les données liées à ce choc macroéconomique historique, mais ces valeurs extrêmes ne sont pas dénuées de contenu économique, comme le note Ng (2021). En se concentrant sur les modèles VAR linéaires, l'auteur introduit des variables indicatrices sur la période associée au Covid pour contrôler et distinguer les effets de la pandémie dans l'ensemble d'inforamtion. Carriero et al. (2022) proposent une approche différente et spécifient un VAR à volatilité dynamique pour filtrer les valeurs extrêmes. C'est l'intuition que nous suivrons de près dans le premier chapitre.

Le timing de l'occurrence de la récession est d'un intérêt capital pour les décideurs politiques et les agents de marché. Étant donné la nature des données macroéconomiques caractérisées par des retards et des délais de publication, il est difficile d'évaluer la positon d'une économie donnée dans son cycle. Furno and Giannone (2024) proposent de se concentrer sur l'Indice Composite de Stress Systémique (CISS) ainsi que sur des données d'enquête disponibles rapidement pour inférer de façon simultanée les épisodes de récession. Ils montrent que la prise en compte de données relatives aux conditions de marché, lorsqu'elles sont ajoutées aux indicateurs macroéconomiques, augmentent la capacité d'un modèle logit à identifier les récessions. Cela est en ligne avec Giannone et al. (2008), qui montrent la valeur ajoutée d'inclure des prix d'actifs financiers à un ensemble

d'information macroéconomique afin de réduire l'incertitude dans un cadre de prévision en temps réel et augmenter le contenu informationnel. Ce chemin de recherche motive le deuxième chapitre de ce manuscrit en se concentrant sur la possibilité d'extraire une évaluation hebdomadaire de la position du cycle économique.

Les dynamiques macroéconomiques sont vitales pour un investisseur qui souhaite allouer tactiquement son portefeuille lorsqu'une récession se produit ou déployer des stratégies de couverture. En effet, la littérature académique tend à montrer que les régimes macroéconomiques déterminent les distributions des rendements financiers (Ang and Timmermann (2012)). Les trajectoires prévues des taux de politique monétaire futurs ou les régimes de politique monétaire impactent également les variations des prix des actifs (Rigobon and Sack (2004)). Ang and Bekaert (2004) démontrent que le rendement d'un portefeuille peut être amélioré à travers l'adaptation de l'allocation en fonction de l'identification de régime basée sur des moyennes, corrélations ou volatilités conditionnelles dans le cadre des modèles d'équilibre des actifs financiers. Prendre en compte les phases du cycle économique dans la construction de portefeuilles a été envisagé pour la première fois par Brocato and Steed (1998). Jensen and Mercer (2003) proposent plutôt de considérer les régimes de politique monétaire dans la construction de portefeuilles. Plus récemment, Kollar and Schmieder (2019) préconisent de tenir compte des phases du cycle économique et financier dans la stratégie d'investissement. Kritzman et al. (2012) sont les premiers à développer une identification de régimes composés de la croissance, de l'inflation et des turbulences financières afin de construire une stratégie d'allocation adéquate. Plus récemment, Kim and Kwon (2023) présentent une stratégie d'investissement basée sur les dynamiques de croissance et d'inflation (impliquant une réaction de politique monétaire). De façon similaire, Bouyé and Teiletche (2024) montrent que les portefeuilles basés sur les régimes macroéconomiques (surchauffe, "boucle d'or", stagflation, ralentissement) peuvent surperformer des portefeuilles plus traditionnels. Les références ci-dessus font cependant l'économie d'une identification en "temps réel" des régimes associés. La plupart de ces travaux sont en effet basés sur une identification a posteriori des régimes, éloignée des considérations opérationnelles de gestion de portefeuille. Cette littérature demeure la base du troisième et dernier chapitre : être capable d'évaluer, en temps réel, le sentiment du marché, les phases du cycle économique ainsi que la posture de la politique monétaire afin de pondérer les portefeuilles de façon idoine.

1.1.2. Principaux résultats

Dans le premier chapitre, une extension du cadre des modèles à facteurs dynamiques à changements de régimes markoviens est proposée. Elle permet d'introduire un processus de volatilité dynamique dans le comportement du facteur latent. Un algorithme d'échantillonnage de Gibbs est présenté et le travail montre les bonnes performances de la nouvelle spécification dans l'identification des points de retournement sur données simulées. De plus, l'approche est confrontée à des processus générateurs de données mal spécifiés et à sauts artificiels (pour imiter des chocs exogènes tels que la récession Covid) et parvient à identifier correctement la chaîne de Markov sous-jacente. Nous comparons d'abord les performances de la nouvelle approche à des spécifications plus tradition-

nelles dans un exercice de détection de points de retournement macroéconomique sur la totalité de l'échantillon. Le nouveau modèle fournit une datation précise, robuste à la crise Covid, des récessions datées par le NBER, alors que la plupart des autres spécifications captent difficilement les récessions plus modérées. De plus, un exercice en temps réel est réalisé, montrant la capacité du modèle proposé à identifier de manière concomitante les dates d'entrée en récession, ainsi que sa réactivité dans la détection de futurs ralentissements (forts ou modérés).

Le second chapitre de ce manuscrit se donne pour but de mitiger le délai dans l'identification des récessions attribuable à la nature même des données macroéconomiques : à savoir des délais de publication et l'asynchronicité de l'information disponible. Il démontre l'utilité, pour les investisseurs désireux de suivre de près les phases du cycle économique, d'ajouter à leur ensemble d'information macroéconomique usuellement utilisé les "asset swap spreads" de crédit d'entreprise. La valorisation de ces produits financiers par le bais d'une mise à jour en continu des probabilités de défaut des émetteurs d'emprunts obligataires contient une évaluation en temps réel de la position d'une économie dans son cycle. Nous relions le sentiment du marché du crédit d'entreprise, mesuré par une contraction ou un élargissement des spreads (à travers sept paniers de notes de qualité d'emprunteur, de CCC à AAA), à l'état de l'économie en tenant compte de la variation conjointe entre les asset swap spreads et les variables économiques généralement utilisées dans les modèles de prévision en temps réel. Ce travail vise à évaluer, sur une fréquence hebdomadaire, la position de l'économie dans son cycle. Il souligne la capacité des modèles à facteurs dynamiques à changements de régimes markoviens, incorporant à la fois des variables macroéconomiques et des asset swap spreads de crédit d'entreprise, à identifier avec précision les récessions tant dans l'échantillon historique qu'en temps réel. Les contractions économiques déclenchent habituellement de larges variations négatives de prix sur les marchés actions, car l'aversion au risque augmente chez les investisseurs. A ce titre, ce chapitre montre également que les investisseurs qui souhaitent construire des stratégies assurantielles doivent utiliser les probabilités de récession en temps réel comme règle d'allocation entre un actif risqué (par exemple le S&P500) et un actif sans risque dont le rendement correspond au taux d'intérêt de court terme dans une économie - nous utiliserons par la suite le terme "cash" par un abus de langage fréquent dans la littérature financière. Les stratégies basées sur les probabilités de défaut construites sur un ensemble d'information composé d'indicateurs macroéconomiques classiques et des asset swap spreads surperforment systématiquement un portefeuille investi à 100% sur l'indice S&P500 et créent une utilité économique pour l'investisseur.

Les investisseurs à la recherche de rendements stables à travers les phases économiques, tant du point de vue du cycle économique que de la politique monétaire, font face à des questions complexes dans la construction de leur portefeuille, notamment sur la pondération tactique des actifs le composant. Le troisième chapitre de ce manuscrit introduit une nouvelle approche pour évaluer le régime de politique monétaire à travers les dynamiques des taux d'intérêt réels en utilisant un modèle à facteurs dynamiques à changements de régimes markoviens capturant le co-mouvement des taux réels de long terme. Ce modèle s'avère performant dans l'identification de posture restrictive de la politique monétaire à la fois sur l'historique de l'échantillon mais également en

temps réel, sur une fréquence hebdomadaire. Le chapitre étend ensuite le cadre méthodologique d'identification de régime de marché action haussier et baissier introduit par Maheu et al. (2012) en un modèle à facteurs dynamiques afin de capturer un sentiment de marché boursier multivarié permettant d'identifier des épisodes de marché haussier à forte volatilité et des phases de correction à faible volatilité. Ce signal réussit à capturer un sentiment de marché sous-jacent à travers quatre principaux indices actions américains. Enfin, ce chapitre combine le signal de posture de la politique monétaire avec le sentiment de marché et une évaluation hebdomadaire en temps réel du cycle économique dans un cadre d'allocation d'actifs "long-only", sans possibilité de vente à découvert. L'avantage pour un investisseur de considérer ces trois dimensions est primordial afin de pondérer dynamiquement son portefeuille. La prise en compte de ces trois axes et l'identification de leur régime associées à des dynamiques de prix de marché spécifiques justifient des allocations dynamiques au-delà de la répartition constante traditionnelle en 60% actions /40% obligations. Les backtests implémentés montrent que l'approche basée sur les trois signaux dans une stratégie de couverture dynamique actions/obligations/cash maximise le ratio de Sharpe Sharpe (1994) sur longue période, de janvier 2000 à février 2023. De plus, quelle que soit la période de détention du portefeuille considérée (fenêtres de un à dix ans glissantes) ou le régime monétaire/économique rencontré, les rendements et les ratios de Sharpe sont supérieurs à ceux du portefeuille 60/40 traditionnel, ce qui plaide en faveur de la nouvelle approche pour un investisseur à la recherche de rendements stables à travers le temps. L'utilité économique de l'investisseur dans les stratégies incorporant ces trois cycles s'avère maximale sur des fenêtres de un à dix ans glissantes, indépendamment de son profil d'aversion au risque.

1.2. Summary of the thesis works

This manuscript aims at connecting macroeconomic business cycle phases detection and asset allocation. Global economies, in particular the US one, have faced the most brutal recession in history through the Covid crisis. In the wake of this tremendous macroeconomic shock, business cycle phases identification poses significant hurdles for practitioners as traditional non-linear dynamic factor specifications are unable to deal with this extreme event correctly. This work proposes a new Markov-switching framework capable of dealing with this historic recession without hampering its capacity to detect shallower macroeconomic downturns. We reach this goal by taking into account specific volatility dynamics in the common factor synthesizing the unobserved underlying business cycle changes.

Timing recessions entry and exit points is essential for policy makers and investors who intend to monitor macroeconomic fluctuations at a high frequency basis. In that respect, this manuscript shows the benefits for a practitioner of adding financial prices as real-time assessors of economic fluctuations. We focus on a specific class of asset prices, corporate credit asset swaps spreads, which materializes a continuously revised default probabilities. The market assesses the ability of a given corporate bond issuer to pay back both interest expenses and the notional of a loan. Aggregating these probabilities through grade buckets ranging from speculative grade enterprises to high grade firms, covering a wide range of businesses for the US enables to capture the pervasiveness of business cycle comovement. This falls exactly in the definition given by Burns and Mitchell (1946):

> *"Business cycles are a type of fluctuation found in the aggregate economic activity of nations that organize their work mainly in business enterprises: a cycle consists of expansions occurring at about the same time in many economic activities, followed by similarly general recessions, contractions, and revivals which merge into the expansion phase of the next cycle."* (p. 3)

The corporate credit asset swap spreads and their underlying default probabilities can be viewed as a partial financial assessment of the aggregate economy dynamics. Partial because not all US businesses have an access to financial markets for funding (according to the Bank of International Settlements the non-financial corporate sector banking debt in the US stands at around 77% of the GDP whereas in Continental Europe, albeit some disparities, the corporate banking debt amounts to roughly 94.3%), a sufficient number of sizeable corporates allow us nonetheless to identify business cycle regimes in an efficient way. Being able to detect in a real-time fashion (e.g. on a weekly basis) economic downturns is most important to develop a flexible dynamic hedging investment strategies. Equity indices tend to react in tandem with negative shocks affecting the business cycle through a repricing of future revenues. This work bridges therefore the business cycles phases real-time assessment to hedging strategies reducing the weight to a risky asset proportionally to the probability of being in recession. This strategy improves the risk-adjusted returns for an investor.

Business cycle phases assessment is a prerequisite but this axis is not the only one an investor

monitors when it comes to multi-asset allocation. Some market stress could arise without any macroeconomic downturn or deceleration. Volatile capital markets tend to produce severe drawdowns during panic sell-offs triggered by rumors, exogenous news or market structures themselves. Market sentiment is thus vital and one should integrate it within an asset allocation strategy in order to mitigate portfolio exposures to risky asset fluctuations. Another factor an investor keeps track of in his/her allocation decision is the monetary policy stance. This stance plays a important role when defining discount factors and thus valuations. To that end, identifying the monetary policy stance the market currently expects can be of a great help when considering multi-asset strategies. The traditional, rule of thumb, 60% equities / 40% bonds portfolio which intends to maximise the risk-adjusted return through market phases shows its vulnerability when it comes to periods in which a restrictive monetary policy takes place or is expected by the market. This work will focus on deploying a market-based monetary policy stance assessor to hedge the 60% equities / 40% bonds portfolio with a disinvestment towards a risk-free asset (we will refer to it as "cash" throughout the rest of the manuscript, following the convention used in financial literature) whenever a hawkish monetary policy regime is identified. Combining a business cycle phase identifier, a monetary policy stance assessor together with a market sentiment allows an investor to get consistent risk-adjusted returns across several market downturns episodes.

1.2.1. Motivations

Dynamic factor models are widely used to summarize the sources of comovement across economic variables and have experienced several key evolutions since their first introduction (Bai and Ng (2008), Doz and Fuleky (2019), Barigozzi and Hallin (2023) among others propose an exhaustive coverage of the history and major developments in this field). Factor analysis was first introduced in psychology by Spearman (1904) who used an unobserved component to characterize individuals capacity to process and comprehend information. This framework was originally developed to handle random vectors independently distributed. However Geweke (1977) extended it to seize comovements among economic time series. This builds upon Burns and Mitchell (1946) definition of the business cycle being observable through expansion and recession phases in a broad set of individual economic series. Sargent and Sims (1977) and Stock and Watson (1989), in seminal works showed that a small set of common components could synthesize macroeconomic series joint behaviour. The resulting composite economic proxies have quickly been allowed to vary in phase with the business cycle. Business cycle regimes can indeed be cast in a Markov-switching framework. Kim (1994) and Diebold and Rudebusch (1996) were the first to incorporate Markov-switching into dynamic factor models. Diebold and Rudebusch (1996) defined a single factor summarizing the unobservable state of the economy. They allowed the factor parameters to be dependent on an latent two-state Markov-switching variable. Kim and Nelson (1998) proposed a Gibbs sampling framework to estimate the model parameters as well as the two latent variables. A first strand of the literature has focused on a frequentist approach in which an approximation proposed by Kim (1994) was used in the likelihood computation and the Kalman filter to avoid untractable M^T potential paths (with M the number of states of the Markov chain, T the number of observations).

Another method was put forward by Diebold and Rudebusch (1996). They introduced a two-step approach in which a coincident index is first built and the Hamilton model is estimated on it afterwards. Based on this intuition, Doz and Fuleky (2019) precise that one can use a two-step approach similar to Doz et al. (2011) in a linear framework. A linear dynamic factor model is first estimated by principal components on which a Markov-switching model can be estimated, in the spirit of Hamilton (1989), by maximum likelihood. Camacho et al. (2015) compare the two aforementioned approaches and point the accuracy of the one-step approach when it comes to small-scale datasets. Camacho et al. (2014) deploy a specification of the model taking into account ragged edge and mixed frequency data. We will, in the rest of the thesis manuscript, focus on the Bayesian estimation and will remain driven by our will to stick to small-scaled models (as in Stock and Watson (1989), Kim and Yoo (1995), Doz et al. (2020) or Leiva-Leon et al. (2020)). Chauvet and Piger (2008) show the ability of small-scaled Markov-switching dynamic factor model estimated with the Gibbs sampling approach to accurately detect the National Bureau of Economic Research (NBER) dated recessions.

The hurdle this manuscript tackles is the growing heterogeneity of the recession phases within a Markov-switching dynamic factor model framework. As pointed out by Leiva-Leon et al. (2020), taking a regime-wise constant intercept in the factor dynamic might trigger inaccurate shallower recession identification after the Great Financial Recession and the Covid Recession. The authors allow the intercept to be specific to each economic downturn episode by activating a within-recession random variable. Heterogeneous recessions could also be identified by the volatility associated to them. This was proposed first by Chauvet (1998) where a Markov chain is driving both the constant and the volatility. In a more recent attempt Doz et al. (2020) explore the possibility to take into account two independent Markov chains, one driving the constant term in the factor and the other the volatility hence yielding fours states: two low volatile expansions and recession regimes and two high volatile expansions and recessions phases. The parameters remain nonetheless constant in each regime. The Covid recession treatment remains a puzzling question. One could 'dummying out' data linked to this historic macroeconomic shock but these extreme values are not void of economic content as noted by Ng (2021). Focusing on linear VAR models, the author introduces Covid indicators to act as control variables and disentangle the pandemic and economic effects in the data. Carriero et al. (2022) propose a different approach, and specify a VAR with time-varying volatility to filter the extreme values through the volatility process. This is the intuition we will closely follow in the first chapter.

The timing of the recession occurrence is of a great interest for policy makers and market agents. Given the nature of the macroeconomic data characterized by lags and delays in their publication, it is hard to assess the current economic condition of a given economy. A proposal made by Furno and Giannone (2024) is to focus on Composite Index of Systemic Stress (CISS) together with early available survey data to infer in a timely manner the downturns episodes. They show that financial conditions, when added to macroeconomic indicators, increase the ability of a logit model to identify downturns. This is in line with Giannone et al. (2008) who show the marginal benefits

of financial prices to bring news and reduce uncertainty in a linear nowcasting framework. This research path motivates the second chapter when focusing on extracting weekly assessment of the business cycle phases.

Macroeconomic dynamics are crucial for an asset allocator who wants to tactically weigh his/her portfolio when a recession occurs or deploy hedging strategies against it. The literature indeed shows macroeconomic regimes determine financial returns distributions (Ang and Timmermann (2012)). Expected paths of future monetary policy rates or monetary policy regimes tend to impact asset prices variations (Rigobon and Sack (2004)). Improving portfolio returns can be achieved by adapting allocation through regimes identifications in conditional means, volatilities, and correlations within a capital asset pricing model (Ang and Bekaert (2004)). Accounting for business cycle phases into portfolio construction was first considered by Brocato and Steed (1998). Jensen and Mercer (2003) proposed to rather take into account monetary policy regimes in portfolio construction. On the other hand, Kollar and Schmieder (2019) advocate to consider connecting asset allocation to both business cycle phases and financial cycles in investment allocation. Kritzman et al. (2012) deploy a regime identification composed of growth, inflation and financial turbulences to build an adequate allocation strategy. More recently, Kim and Kwon (2023) present an investment framework for dynamic asset allocation strategies based on changes in the growth and inflation environments (implying a monetary policy reaction). In a similar vein, Bouyé and Teiletche (2024) show macro regime-based portfolios (overheating, "goldilock", stagflation, downturn) can outperform traditional asset-based portfolios. The literature cited above misses nonetheless the timing dimension of those regime in a real-time framework as most of the work is based on ex-post identification rather than "live" one. Those papers constitute the intuition we will follow in the third chapter: being able to track in real-time, market sentiment, business cycle phases as well as monetary policy stance and weigh asset allocation accordingly.

1.2.2. Main results

In the first chapter, a model extending the Markov-switching dynamic factor model literature by allowing the latent factor to have a continuous-path dynamic volatility process is introduced. A detailed MCMC Gibbs sampling algorithm is presented and the work shows the good performance of the new specification to identify turning points on simulated data. Additionally, the approach is confronted to misspecified data generating processes and artificial jumps to mimic exogenous shock such as the Covid recession and still manages to properly identify the underlying Markov-switching variable. We compare the performances of the new framework to text-book multi-frequential MS-DFM models on an in-sample turning point detection exercise. The model yields a precise, Covid-robust, dating of the NBER recessions whereas most alternative specifications hardly capture milder recessions. Moreover, a real-time exercise is carried out, showing the ability of the model to consistently capture the entry date into recession, as well as its readiness to detect new downturns (hard and shallower) in the future.

The second chapter of this thesis mitigates the delay in the identification of recessionary episodes due to hard economic data release schedules and shows the usefulness for investors willing to track the US business cycles phases closely to add corporate credit asset swap (ASW) spreads. More specifically, ASW spreads capture asynchronous macroeconomic data flows by continuously updating probabilities of default of given corporate bond issuers. We connect the sentiment in the credit market, measured by a broad grade buckets-based spreads contraction/widening, to the contemporaneous state of the economy in a real-time fashion by taking into account the comovement between ASW spreads and real economic variables usually used in small-scaled dynamic factor models. This work tracks on a weekly basis the occurrence of macroeconomic downturn episodes. It highlights the capacity of MS-DFMs incorporating both macroeconomic variables and ASW spreads to accurately identify recessions both in-sample and out-of-sample. These adverse economic episodes are known to trigger ample price variations in the equity markets as risk aversion gains investors. The chapter also shows that investors who want to build insurance-based strategies shall use the real-time downturn probabilities as an allocation rule between S&P500 and cash. Strategies based on the mixed data sample consistently outperforms a portfolio 100% invested on the S&P500 index as well as creates economic utility for the investor.

Investor seeking consistent returns across economic phases, both from a business cycle and monetary policy perspective, face challenging questions regarding portfolio construction. The third chapter introduces a novel approach to gauge the monetary policy regime through real interest rates dynamics using a Markov-switching dynamic factor model capturing the comovement of long-term maturities real yields. This model proves to be reliable in identifying monetary policy restriction signals both in-sample and out-of-sample using weekly market data. The work then extends Maheu et al. (2012) bull/bear specification into a dynamic factor model in order to capture a multivariate equity market sentiment allowing for bull corrections and bear rallies. This signal succeeds in capturing an underlying market sentiment across four major US equity indices. Finally the chapter combines the monetary policy stance signal with the market sentiment and a weekly real-time business cycle phase assessor within a long-only asset allocation framework. The benefit for an investor to take into account those three dimensions is paramount to weigh dynamically his/her portfolio. The regimes along those axes and their underlying market prices dynamics warrant allocations beyond the traditional fixed 60% equities /40% bonds split. The backtests implemented show that considering the three-signal approach in a dynamic equity/bond/cash hedging strategy maximizes the Sharpe ratio on a broad period from January 2000 to February 2023. Moreover, no matter the portfolio holding period considered (rolling 1 year to 10 year windows) or the monetary/economic regime faced, the returns and Sharpe ratios are higher than the 60% equities /40% bonds benchmark advocating this approach is reliable for an investor who seeks steady returns. The economic utility of the investor in strategies incorporating the three signals shows to be maximal on 1-year to 10-year rolling windows regardless of his/her risk aversion profile.

Chapter 2

Improving the robustness of Markov-switching dynamic factor models with time-varying volatility

Romain Aumond Julien Royer

Abstract: Tracking macroeconomic data at a high frequency is difficult as most time series are only available at a low frequency. Recently, the development of macroeconomic nowcasters to infer the current position of the economic cycle has attracted the attention of both academics and practitioners, with most of the central banks having developed statistical tools to track their economic situation. The specifications usually rely on a Markov-switching dynamic factor model with mixed-frequency data whose states allow for the identification of recession and expansion periods. However, such models are notoriously not robust to the occurrence of extreme shocks such as Covid-19. In this Chapter, we show how the addition of time-varying volatilities in the dynamics of the model alleviates the effect of extreme observations and renders the dating of recessions more robust. Both stochastic and conditional volatility models are considered and we adapt recent Bayesian estimation techniques to infer the competing models parameters. We illustrate the good behavior of our estimation procedure as well as the robustness of our proposed model to various misspecifications through simulations. Additionally, in a real data exercise, it is shown how, both in-sample and in an out-of-sample exercise, the inclusion of a dynamic volatility component is beneficial for the identification of phases of the US economy.

Keywords: Nowcasting; Bayesian Inference; Dynamic Factor Models; Markov Switching

2.1. Introduction

Dating economic recession and expansion periods is paramount for policy makers and asset managers. However, recessions are often identified after the publication of lagged low-frequency macroeconomic variables, resulting in an identification process that may be severely delayed. For example, the end of the Great Recession in June 2009 was announced by the National Bureau of Economic Research (NBER) more than a year later. In order to track the state of the economy in real-time and at a higher frequency, building upon nowcasting techniques popularized by Evans (2005), Giannone et al. (2008) and Bańbura et al. (2013), the use of Markov-switching dynamic factor models (MS-DFM) has recently gained popularity (Camacho et al. (2014, 2018); Doz et al. (2020)). Such models were initially introduced by Diebold and Rudebusch (1996) to capture the co-movements of multiple time series while allowing for the dynamic to be specific to different regimes. Chauvet and Piger (2008) and Hamilton (2011) emphasized the benefits of this specification to time economic recessions in the US.

The performance of these models has however been tremendously challenged by the occurrence of extreme values observed during the Covid-19 pandemic. Figure 2.1 provides a compelling and motivating example. Using the five variables recommended by the NBER and pursuant to Chauvet and Piger (2008), we fit a standard MS-DFM model to obtain the in-sample probability of the US economy being in a recession. Using a sample ranging from February 1947 to December 2019[1], we observe that the model is very accurate to date the recessions. This accuracy however sharply decreases after the introduction of Covid data in the sample. Indeed, the same model fitted on a sample from February 1947 to June 2023 fails to identify five recessions, only capturing very large shocks (the oil shock of 1973, the interest rates shock of 1980 and the Great Financial Crisis of 2008).

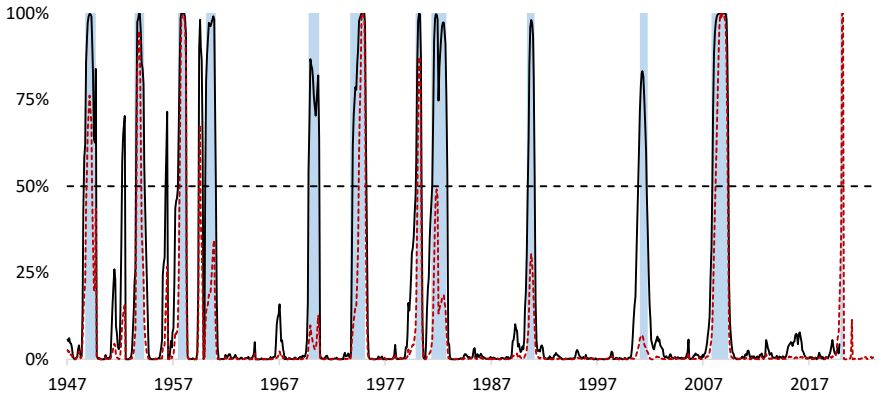

Figure 2.1: *Smoothed probability of being in a recession (Chauvet and Piger (2008)). The black line represents a sample from February 1947 to December 2019 while the red dashed line represents a sample from February 1947 to June 2023. Blue shades show the recessions as dated by the NBER.*

[1]Details about the data are presented in Section 4.

The treatment of Covid data when modeling macroeconomic phenomena has puzzled econometricians as well as practitioners. While simply 'dummying out' data linked to the pandemic shock may seem appealing, these extreme values are not void of economic content as noted by Ng (2021). Focusing on linear VAR models, the author introduces Covid indicators to act as control variables and disentangle the pandemic and economic effects in the data. Carriero et al. (2022) propose a different approach, and specify a VAR with time-varying volatility to filter the extreme values through the volatility process. The benefits of including dynamic volatility components in VAR models are well documented in the literature (see for example Clark (2011); Clark and Ravazzolo (2015); Chan and Eisenstat (2018)) and have influenced models with latent variables, Antolin-Diaz et al. (2017) introducing a linear DFM with stochastic volatility, as well as Markov-switching models (see for example Eo and Kim (2016)). To the best of our knowledge, the development of MS-DFM with time-varying volatility has been limited and mostly focused around dynamic but piecewise-constant volatility processes as presented in Doz et al. (2020).

In this Chapter, we introduce new MS-DFM specifications to allow for continuous dynamic volatility processes. In particular, we will consider two well-known competing models: conditional volatility, where the dynamic variance is a measurable function of the past observations, and stochastic volatility processes, where the volatility is a random variable not directly linked to the σ-field of the data. We will show that, both in-sample and out-of-sample, models with dynamic volatilities outperform standard MS-DFM model in which homoskedasticity is assumed, in particular when large shocks occur. The remainder of the Chapter is organized as follows. Section 2 presents the general form of the model and discusses its Bayesian inference. Section 3 presents Monte Carlo experiments, illustrating the good-behavior of our estimation procedure. Additionally, a careful attention is dedicated to show the ability of our proposed model to remain robust even under misspecification and jumps in the simulated data generating process. Section 4 presents an application on real data, emphasizing the out-performance of our model for timing US recessions when Covid-data are considered in-sample. Section 5 provides an out-of-sample exercise where we compare the ability to date recessions in a real-time nowcasting exercise. Section 6 concludes. Technical details about the Bayesian estimation are relegated to the appendix.

2.2. Markov-Switching Dynamic Factor Models with continuous time-varying volatility

The modelling of potentially large systems of economic time series via a small number of latent factors has been a workhorse of the economic literature. Initially introduced by Diebold and Rudebusch (1996), MS-DFM aim at capturing both the co-movements of multiple macroeconomic data - possibly sampled at different frequencies - and the changes in time series dynamics induced by latent regimes usually linked to the business cycle, in the spirit of Hamilton (1989). Chauvet (1998) and Kim and Nelson (1998) were the first to propose estimation procedures, the former considering a frequentist approach and the latter a Bayesian approach. Recently, the inclusion of

time-varying volatility has proved useful in modeling linear DFM (Antolin-Diaz et al. (2017)) as well as Markov-Switching models where no factor structure is assumed (Eo and Kim (2016)). The aim of our specification is to bridge the gap between the latter and the MS-DFM literature.

2.2.1. Model specification

Let $\boldsymbol{y}_t$ a vector of q quarterly and m monthly observable time series and let $\boldsymbol{f}_t$ a set of k latent common factors. We have the standard DFM given by

$$\boldsymbol{y}_t = \boldsymbol{\Lambda} \boldsymbol{f}_t + \boldsymbol{u}_t, \tag{2.1}$$

where $\boldsymbol{\Lambda}$ denotes the loadings matrix, $\boldsymbol{u}_t$ is orthogonal to $\boldsymbol{f}_t$ and for all $j = 1, \ldots, m+q$

$$\psi_j(L) u_{j,t} = e_{j,t}, \quad e_{j,t} \sim \mathcal{N}(0, \sigma^2_{e,j}), \tag{2.2}$$

and the set of factors follows

$$\boldsymbol{f}_t = \boldsymbol{\mu}_{S_t} + \boldsymbol{\Phi} \boldsymbol{f}_{t-1} + \boldsymbol{\Sigma}_{\boldsymbol{t}}^{1/2} \boldsymbol{\eta}_t \tag{2.3}$$

where $\boldsymbol{\eta_t}$ is iid $(0, \boldsymbol{I}_k)$ and S_t is an independent first order Markov chain.

In most applications, a two-state ($S_t = 0$ or 1) regime-switching model is considered with a unique factor ($k = 1$) capturing the co-movements of the economic time series. For the sake of simplicity, in the remainder of the Chapter we will focus on this simplified form. We thus have

$$\begin{aligned} \boldsymbol{f}_t = &\quad f_t = \mu_{S_t} + \phi f_{t-1} + \varepsilon_t \\ \varepsilon_t = &\quad \sigma_t \eta_t \end{aligned} \tag{2.4}$$

with $\mu_{S_t} = \mu_1 S_t + \mu_0 (1 - S_t)$.

Among the most famous specifications, Kim and Nelson (1998) assume a constant volatility for the factor residual ($\sigma_t = \sigma$). The inclusion of a dynamic volatility component was first proposed by Chauvet (1998) by letting the constant volatility switch with the latent regimes, yielding $\sigma_t = \sigma_{S_t}$. More recently, Doz et al. (2020) extend this model by letting the volatility process be influenced by an additional two-state first-order Markov chain V_t, independent from S_t, yielding $\sigma_t = \sigma_{V_t}$. It is noteworthy that, while time-varying, the proposed volatility processes are piecewise-constant which might be difficult to justify empirically. Alternatively, we consider models where the volatility is time-varying but not piecewise constant. In particular, we introduce well-known competitors: conditional volatility models and stochastic volatility (SV) models. In the former, the volatility is a measurable function with regard to the σ-field $\mathcal{F}_t$ generated by $\{f_u, t < u\}$. The simplest form of this model was introduced by Engle (1982) through the ARCH(1) equation

$$\sigma_t^2 = \omega + \alpha \varepsilon_{t-1}^2 \tag{2.5}$$

which was extended by Bollerslev (1986) to yield the famous GARCH(1,1) model

$$\sigma_t^2 = \omega + \alpha\varepsilon_{t-1}^2 + \beta\sigma_{t-1}^2 \tag{2.6}$$

where ω, α and β are positive parameters to estimate with $0 < \alpha + \beta < 1$. On the contrary, stochastic volatility models do not assume that volatility is a function of the past but a random variable (in particular $\sigma_t^2 \neq \mathbb{E}[\varepsilon_t^2 \mid \mathcal{F}_t]$). The standard SV model is given by

$$\sigma_t^2 = e^{h_t}, \quad h_t = \mu_h + \phi_h(h_{t-1} - \mu_h) + \varepsilon_{h,t}, \quad \varepsilon_{h,t} \sim \mathcal{N}(0, \omega_h^2). \tag{2.7}$$

where the log-volatility h_t follows a stationary AR(1) process with μ_h, $|\phi_h| < 1$ and ω_h being parameters to estimate. Tracking real-time economic conditions require to integrate time series measured at different frequencies, such as quarterly GDP and monthly employment data. Following Mariano and Murasawa (2003), the model is therefore specified at a monthly frequency where the observed quarterly data $\boldsymbol{y}_t^{(q)}$ can be related to unobserved synthetic monthly data $\boldsymbol{y}_t^{(m)}$

$$\boldsymbol{y}_t^{(q)} = \frac{1}{3}\boldsymbol{y}_t^{(m)} + \frac{2}{3}\boldsymbol{y}_{t-1}^{(m)} + \boldsymbol{y}_{t-2}^{(m)} + \frac{2}{3}\boldsymbol{y}_{t-3}^{(m)} + \frac{1}{3}\boldsymbol{y}_{t-4}^{(m)}. \tag{2.8}$$

Substituting quarterly series in (2.1) with the synthetic higher-frequency data in (2.8) allows us to obtain a dynamic factor model at a monthly frequency where missing data can be inferred from our Bayesian estimation procedure.

2.2.2. Bayesian estimation

It is useful to rewrite the MS-DFM model defined by equations (2.1)-(2.2)-(2.4) into a state-space equation. For any $j = 1, \ldots, m+q$, let us denote $\boldsymbol{\psi}_j = (\psi_{j,1}, \ldots, \psi_{j,l})'$ the coefficients of the lag polynomial $\psi_j(L)$ assumed of order l and $\boldsymbol{\Psi} = (\boldsymbol{\psi}_1', \ldots, \boldsymbol{\psi}_m')'$. Additionally, let $\boldsymbol{H}$ the $(m+q) \times (ml + 5 + 5q)$ matrix such that

$$\boldsymbol{H} = \begin{bmatrix} \lambda_1\boldsymbol{h}_q & \boldsymbol{h}_q & \ldots & 0 & 0 & \ldots & 0 \\ \vdots & \vdots & \ddots & \vdots & \vdots & \ddots & \vdots \\ \lambda_q\boldsymbol{h}_q & 0 & \ldots & \boldsymbol{h}_q & 0 & \ldots & 0 \\ \lambda_{q+1}\boldsymbol{h}_m^5 & 0 & \ldots & 0 & \boldsymbol{h}_m^l & \ldots & 0 \\ \vdots & \vdots & \ddots & \vdots & \vdots & \ddots & \vdots \\ \lambda_{q+m}\boldsymbol{h}_m^5 & 0 & \ldots & 0 & 0 & \ldots & \boldsymbol{h}_m^l \end{bmatrix}$$

where $\boldsymbol{h}_q = \begin{bmatrix} \frac{1}{3} & \frac{2}{3} & 1 & \frac{2}{3} & \frac{1}{3} \end{bmatrix}$, $\boldsymbol{h}_m^5 = \begin{bmatrix} 1 & 0 & 0 & 0 & 0 \end{bmatrix}$, $\boldsymbol{h}_m^l = \begin{bmatrix} 1 & 0 & \ldots & 0 \end{bmatrix}$.
$\boldsymbol{h}_m^l$ is a $1 \times l$ vector with the only first element equal to one. We define the lag vectors $\boldsymbol{L^4} =$

$(1, L, \ldots, L^4)$. The vector of unobserved variables $\boldsymbol{z}_t$ is given by

$$\boldsymbol{z}_t = (\boldsymbol{L^4} f_t, \boldsymbol{L^4} u_{1,t}, \ldots, \boldsymbol{L^4} u_{q,t}, (1, L, \ldots, L^{l-1}) u_{q+1,t}, \ldots, (1, L, \ldots, L^{l-1}) u_{m+q,t})'.$$

We can rewrite the factor model into a state-space equation as follows

$$\begin{array}{lll} \boldsymbol{y}_t = & \boldsymbol{H}\boldsymbol{z}_t + \boldsymbol{\varsigma}_t & \boldsymbol{\varsigma}_t \sim \mathcal{N}(0, \boldsymbol{R}) \\ \boldsymbol{z}_t = & \boldsymbol{\delta}_{S_t} + \boldsymbol{\Xi}\boldsymbol{z}_{t-1} + \boldsymbol{\zeta}_t & \boldsymbol{\zeta}_t \sim \mathcal{N}(0, \boldsymbol{Q}_t) \end{array} \tag{2.9}$$

with $\boldsymbol{\delta}_{S_t} = (\mu_{S_t}, 0, \ldots, 0)'$, $\text{diag}(\boldsymbol{Q}_t) = (\sigma_t^2 \boldsymbol{h}_m^5, \sigma_{e,1}^2 \boldsymbol{h}_m^5, \ldots, \sigma_{e,q}^2 \boldsymbol{h}_m^5, \sigma_{e,q+1}^2 \boldsymbol{h}_m^l, \ldots \sigma_{e,m+q}^2 \boldsymbol{h}_m^l)$ where $\boldsymbol{\Xi}$ is a $ml + 5 + 5q$ square block diagonal matrix given by

$$\boldsymbol{\Xi} = \begin{bmatrix} \boldsymbol{\phi} & & & \\ & \boldsymbol{\Xi}_1 & & \\ & & \ddots & \\ & & & \boldsymbol{\Xi}_{m+q} \end{bmatrix} \quad \text{where} \quad \boldsymbol{\phi} = \begin{bmatrix} \phi & 0 & 0 & 0 & 0 \\ 1 & 0 & 0 & 0 & 0 \\ 0 & 1 & 0 & 0 & 0 \\ 0 & 0 & 1 & 0 & 0 \\ 0 & 0 & 0 & 1 & 0 \end{bmatrix}$$

such that, for $j_q = 1, \ldots, q$ and $j_m = q+1, \ldots, m+q$, $\boldsymbol{\Xi}_{j_q}$ is a 5×5 matrix and $\boldsymbol{\Xi}_{j_m}$ a $l \times l$ matrix given by

$$\boldsymbol{\Xi}_{j_q} = \begin{bmatrix} 0 & 0 & 0 & 0 & 0 \\ 1 & 0 & 0 & 0 & 0 \\ 0 & 1 & 0 & 0 & 0 \\ 0 & 0 & 1 & 0 & 0 \\ 0 & 0 & 0 & 1 & 0 \end{bmatrix} \quad \text{and} \quad \boldsymbol{\Xi}_{j_m} = \begin{bmatrix} \psi_{j_m,1} & \psi_{j_m,2} & \ldots & \psi_{j_m,l-1} & \psi_{j_m,l} \\ 1 & 0 & \ldots & 0 & 0 \\ 0 & 1 & \ldots & 0 & 0 \\ \vdots & \vdots & \ddots & \vdots & \vdots \\ 0 & 0 & \ldots & 1 & 0 \end{bmatrix}.$$

Additionally, we follow Leiva-Leon et al. (2020) and restrict the individual components of the quarterly observations to be white noises.

Denoting the transition probabilities

$$q = \mathbb{P}(S_t = 0 | S_{t-1} = 0) \quad \text{and} \quad p = \mathbb{P}(S_t = 1 | S_{t-1} = 1),$$

the vector of parameters to estimate is given by

$$\boldsymbol{\vartheta} = (p, q, \boldsymbol{\Psi}', \sigma_{e,1}, \ldots, \sigma_{e,m}, \boldsymbol{\Lambda}', \mu_0, \mu_1, \phi, \boldsymbol{\theta}^{(.)'})'$$

where $\boldsymbol{\theta}^{(.)}$ is the vector of parameters driving the dynamic volatility equation σ_t

$$\boldsymbol{\theta}^{(\text{ARCH})} = (\omega, \alpha), \quad \boldsymbol{\theta}^{(\text{GARCH})} = (\omega, \alpha, \beta), \quad \text{and} \quad \boldsymbol{\theta}^{(\text{SV})} = (\mu_h, \phi_h, \omega_h).$$

Let us denote $\boldsymbol{z}^{(T)} = \{\boldsymbol{z}_1, \ldots, \boldsymbol{z}_T\}$ the unobserved state vector in equation (2.9), $\boldsymbol{y}^{(T)} = \{\boldsymbol{y}_1, \ldots, \boldsymbol{y}_T\}$

the observed data, and $S^{(T)} = \{S_1, \ldots, S_T\}$ the unobserved Markov Chain. The model is estimated using a Markov Chain Monte Carlo (MCMC) Gibbs sampling algorithm in the spirit of Kim and Nelson (1999) and Bai and Wang (2015) where conditional draws of the state vector, the Markov Chain, and the parameters vector $\boldsymbol{\vartheta}$ are obtained sequentially. In particular, we adapt the Metropolis Hastings procedure presented in Chan and Grant (2016) and Chan (2023) to sample stochastic and conditional volatilities. Details on the priors and a complete description of our sampling algorithm are presented in Appendices 2.7.1 and 2.7.2 but the main steps can be summarized as follows:

1. We generate conditional draws of the state vector from $p(\boldsymbol{z}^{(T)}|\boldsymbol{y}^{(T)}, S^{(T)}, \boldsymbol{\vartheta})$ using the forward-filtering backward-smoothing algorithm of Carter and Kohn (1994).

2. We generate conditional draws of the Markov chain from $p(S^{(T)}|\boldsymbol{y}^{(T)}, \boldsymbol{z}^{(T)}, \boldsymbol{\vartheta})$ based on the Hamilton filter (Hamilton (1989)).

3. We generate conditional draws for the parameters vector from $p(\boldsymbol{\vartheta}|\boldsymbol{y}^{(T)}, \boldsymbol{z}^{(T)}, S^{(T)})$ by sequentially drawing in the conditional distribution of components of $\boldsymbol{\vartheta}$ as follows:

   - We obtain conditional draws for p and q following Albert and Chib (1993).
   - We obtain conditional draws for $(\boldsymbol{\Psi}', \sigma_{e,1}, \ldots, \sigma_{e,m}, \boldsymbol{\Lambda}')$ from usual priors in the literature (see for example Bai and Wang (2015)).
   - To obtain conditional draws for $(\mu_0, \mu_1, \phi, \boldsymbol{\theta}^{(.)'})$, we build upon the Metropolis Hastings algorithm presented in Chan and Grant (2016). In particular, in the case of stochastic volatility, we use the precision sampler of Chan and Jeliazkov (2009) for efficiency gains.

2.3. Monte Carlo experiments

In order to assess the performance of our estimation procedure as well as the robustness of our model to potential misspecifications, we conduct some Monte Carlo experiments.

In all cases, we model a five-variable system, with one quarterly data and four monthly data, driven by a single latent regime-switching factor. On all simulations, we use our MCMC procedure to fit five competing MS-DFM models as described by (2.1)-(2.2)-(2.4): a standard model with constant volatility (simply denoted MS-DFM), a model where the factor volatility follows an ARCH(1) dynamic (denoted MS-DFM-ARCH), a model where the factor volatility follows a GARCH(1,1) dynamic (denoted MS-DFM-GARCH), a model where the factor volatility is stochastic with dynamic (2.7) (denoted MS-DFM-SV), and a model where the factor volatility is piece-wise constant and driven by an additional Markov- chain independent of S_t as presented by Doz et al. (2020) (denoted 2MS-DFM). All estimation results are obtained from 1600 draws of the Gibbs sampler.

To conduct our experiments, we first simulate a two-state first order Markov chain with $p = q = 0.97$ and $T = 1000$. From the obtained Markov chain, we simulate f_t under different specifications (that we will develop in the reminder of this section), which yields the four monthly variables and the quarterly variable from (2.8). In particular, we use $\beta_1 = \cdots = \beta_5 = 0.1$ and an AR(1) structure

for the $u_{j,t}$ sequence with $\psi_j = 0.7$ and $\sigma_{e,j} = 1$ for all j.

We first simulate the factor assuming the true data generating process (DGP) follows the standard MS-DFM with constant volatility of Kim and Nelson (1998). In particular, we set $\mu_0 = -2$, $\mu_1 = 2$, $\phi = 0,7$ and $\varepsilon_t \sim \mathcal{N}(0,1)$. Figure 2.2 presents the in-sample probability of being in regime 1 when fitting a standard MS-DFM (dotted red line) and a MS-DFM-GARCH (plain black line). Shaded areas correspond to the simulated regimes sequence. In this case, the standard MS-DFM model is apt at identifying regime switches and performs very well in-sample. Interestingly, although misspecified, the MS-DFM-GARCH also appears to be well behaved even if the true DGP has constant volatility.

We then repeat the same experience, with the exact same setting, but proceed to shock the innovation sequence by forcing ε_{460} to take an extreme value ($\varepsilon_{460} = -35$). This shock will act as a jump, impacting the factor conditional mean through the AR(1) process. Figure 2.3 presents the in-sample probabilities when a shock occurs at time $t = 460$. The occurrence of an extreme value clearly derails the standard MS-DFM, failing at identifying most of the regime switches in-sample and reminding us of the deterioration of the performance of this model to date NBER recessions after the Covid-19 pandemic as emphasized by Figure 2.1. The in-sample probabilities derived from a MS-DFM-GARCH contrast sharply. The model is able to identify most regime switches even in the presence of an extreme shock, emphasizing the gain in robustness brought by the inclusion of a time-varying volatility process.

To rank the performance of the competing models, we consider two standard metrics based on the errors between the simulated state sequence $S_{0,t}$ (assumed observed) and the filtered probability of being in regime 1 at time t ($S_t = 1$). More precisely, we consider the Quadratic Probability Score (QPS) given by

$$\frac{1}{T}\sum_{t=1}^{T}(S_{0,t} - p(S_t = 1|\mathcal{F}_{t-1}))^2 \tag{2.10}$$

and the False Probability Score (QPS) given by

$$\frac{1}{T}\sum_{t=1}^{T}(S_{0,t} - 1_{p(S_t=1|\mathcal{F}_{t-1})>0.5})^2. \tag{2.11}$$

Table 2.1 presents FPS and QPS metrics for our five competing models in the two presented cases (no jump and one jump), as well as an additional case where two shocks of lower intensities occur ($\varepsilon_{460} = -30$ and $\varepsilon_{800} = -20$). Although misspecified, the four competing time-varying volatility models appear well suited both without shocks and in the presence of extreme values.

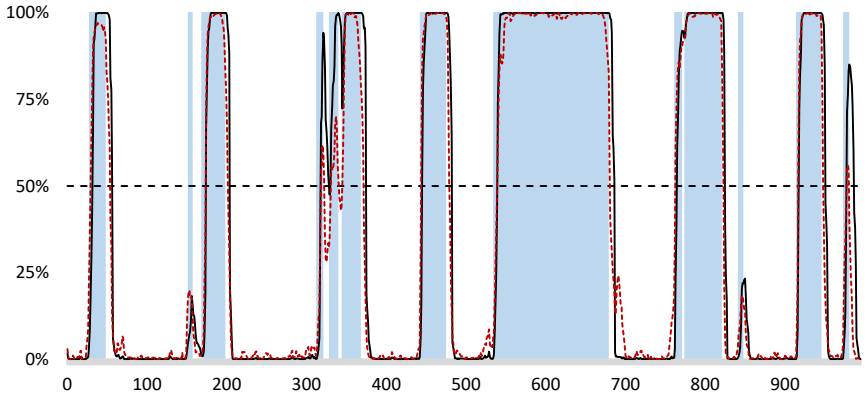

Figure 2.2: *Simulated recession regimes and smoothed recession probabilities from the MS-DFM model (in red) and MS-DFM-GARCH model (in black) when the DGP is a MS-DFM model*

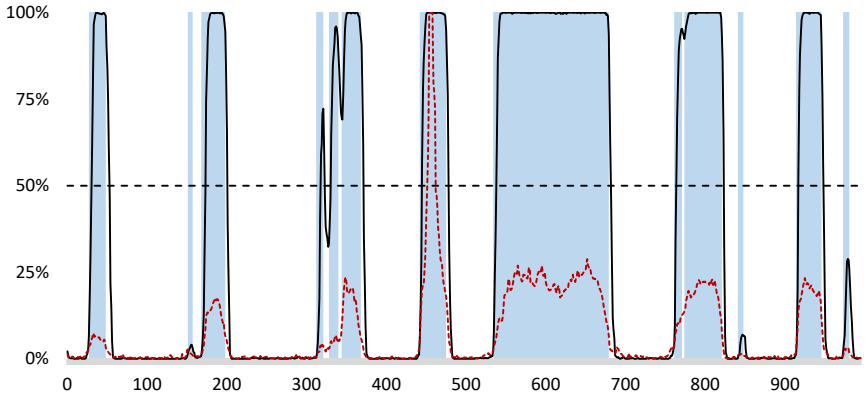

Figure 2.3: *Simulated recession regimes and smoothed recession probabilities from the MS-DFM model (in red) and MS-DFM-GARCH model (in black) when the DGP is a MS-DFM model but a large jump occurs at* $t = 460$

Models	**No jump**		**One jump**		**Two jumps**	
	FPS	QPS	FPS	QPS	FPS	QPS
MS-DFM	0.071	0.053	0.362	0.252	0.354	0.329
MS-DFM-ARCH	0.090	0.072	0.072	0.053	0.073	0.053
MS-DFM-GARCH	0.114	0.093	0.079	0.059	0.072	0.054
MS-DFM-SV	0.079	0.055	0.072	0.054	0.084	0.059
2MS-DFM	0.075	0.055	0.081	0.055	0.082	0.060

Table 2.1: *Simulated regime dating under jumps and misspecifications when the true DGP is a standard MS-DFM*

We then simulate the factor assuming the true (DGP) follows the standard MS-DFM-GARCH with dynamic volatility following (2.6). In particular, we let $\mu_0 = -2$, $\mu_1 = 2$, $\phi = 0.7$ and set $\omega = 1$, $\alpha = \beta = 0.4$ with $\eta_t \sim \mathcal{N}(0,1)$. Figure 2.4 presents the in-sample probability of being in regime 1 when fitting a standard MS-DFM (dotted red line) and a MS-DFM-GARCH (plain black line). Surprisingly, spuriously assuming constancy of the volatility process does not appear to penalize

the inference of the regimes as the MS-DFM proves able to accurately detect regime switches. This relative irrelevance of heteroskedasticity on the Bayesian estimation of such MS-DFM models may explain the only recent attention to MS-DFM with dynamic volatility. The behavior of the MS-DFM-GARCH on this exercise illustrate the good performance of our Bayesian estimation procedure detailed in Appendices 2.7.1 and 2.7.2.

We again repeat the experience and shock the innovation sequence with the same amplitude as the previous simulation. This extreme value will, this time, impact both the factor conditional mean through the AR(1) process and the conditional volatility through the GARCH process. Figure 2.5 presents the in-sample probabilities when a shock occurs at time $t = 460$. The occurrence of an extreme value once again strongly deteriorates the performance of the standard MS-DFM, while the in-sample probabilities derived from a MS-DFM-GARCH remain relatively unchanged.

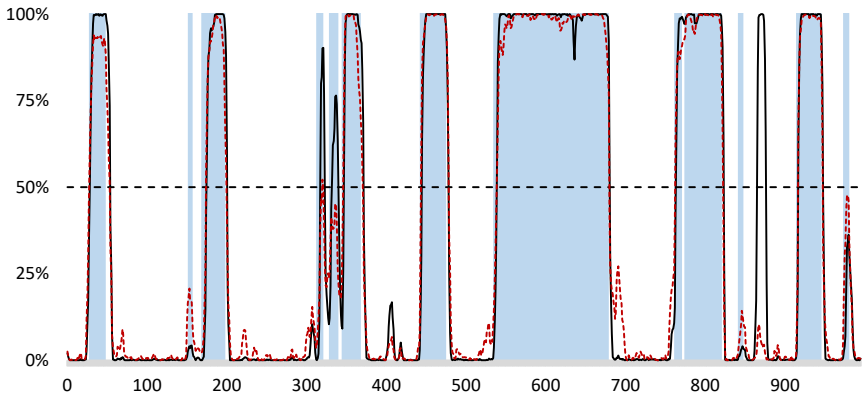

Figure 2.4: *Simulated recession regimes and smoothed recession probabilities from the MS-DFM model (in red) and MS-DFM-GARCH model (in black) when the DGP is a MS-DFM-GARCH model*

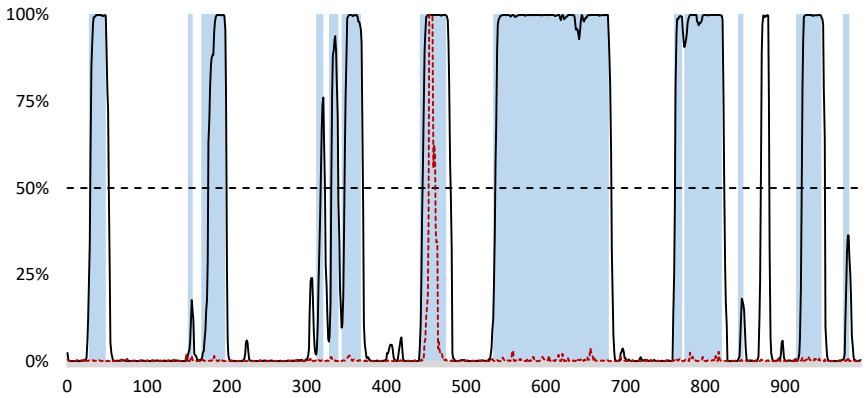

Figure 2.5: *Simulated recession regimes and smoothed recession probabilities from the MS-DFM model (in red) and MS-DFM-GARCH model (in black) when the DGP is a MS-DFM-GARCH model but a large jump occurs at* $t = 460$

Models	No jump		One jump		Two jumps	
	FPS	QPS	FPS	QPS	FPS	QPS
MS-DFM	0.074	0.050	0.364	0.359	0.357	0.348
MS-DFM-ARCH	0.084	0.063	0.086	0.065	0.085	0.068
MS-DFM-GARCH	0.087	0.072	0.097	0.077	0.082	0.062
MS-DFM-SV	0.078	0.055	0.075	0.059	0.102	0.072
2MS-DFM	0.069	0.050	0.092	0.067	0.095	0.067

Table 2.2: *Simulated regime dating under jumps and misspecifications when the true DGP is a MS-DFM-GARCH*

Results in Table 2.2 confirm the previous findings and emphasize the robustness to extreme values stemming from the inclusion of time-varying volatility. Interestingly, in this case, although better than the standard MS-DFM, the MS-DFM-ARCH and the 2MS-DFM of Doz et al. (2020) appear less apt than the MS-DFM-GARCH to identify regime switches. This could be due to the slow decay of the volatility path after the shocks, induced by the GARCH(1,1) equation, that is incompatible with short memory feature of the ARCH(1) model and the piecewise-constant nature of the volatility in the 2MS-DFM. The MS-DFM-SV and MS-DFM-GARCH specifications appear difficult to discriminate in this simulation exercise.

2.4. A Covid-robust timing of US recessions

The main application of MS-DFM is the timing of recession and expansion periods underlying economic data. Tracking these recurring cycles is paramount for policy makers and asset managers, but Covid-data have tremendously complicated the identification process as emphasized by Figure 2.1. In a recent exercise, Doz et al. (2020) show that the inclusion of time-varying volatility improves the detection of recessions in the US. However, their sample stops before the occurrence of the Covid-19 pandemic. Simulations presented in the previous section yield promising results on the ability of MS-DFM models, when extended with continuous volatility processes, to be robust to extreme values. In this section, we propose to confront this assumption to a real-data exercise.

Following the NBER Business Cycle Dating Committee recommendations, we consider a five-variable system, as presented in Table 2.3. The US quarterly GDP is obtained from the ALFRED database while the four monthly series are extracted from the FRED-MD database, both maintained by the Federal Reserve Bank of St Louis (see McCracken and Ng (2016)). All series are seasonally adjusted. The sample ranges from January 1947 to June 2023.

Data	Frequency	Start date	Transformation
Real GDP	Quarterly	Q1 1947	Diff Log
Industrial production	Monthly	Jan. 1947	Diff Log
Real personal income excluding transfer payments	Monthly	Jan. 1959	Diff Log
Real manufacturing trade and sales	Monthly	Jan. 1959	Diff Log
Non-agricultural civilian employment	Monthly	Jan. 1948	Diff Log

Table 2.3: *Data description*

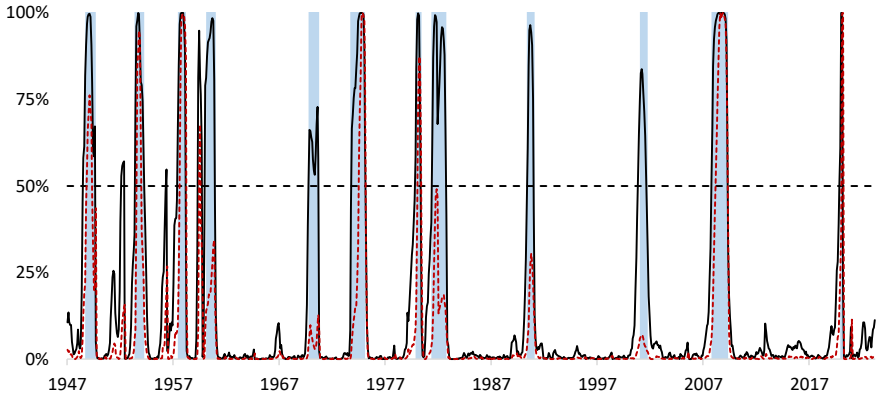

Figure 2.6: *Smoothed recession probability based on the MS-DFM-GARCH model*

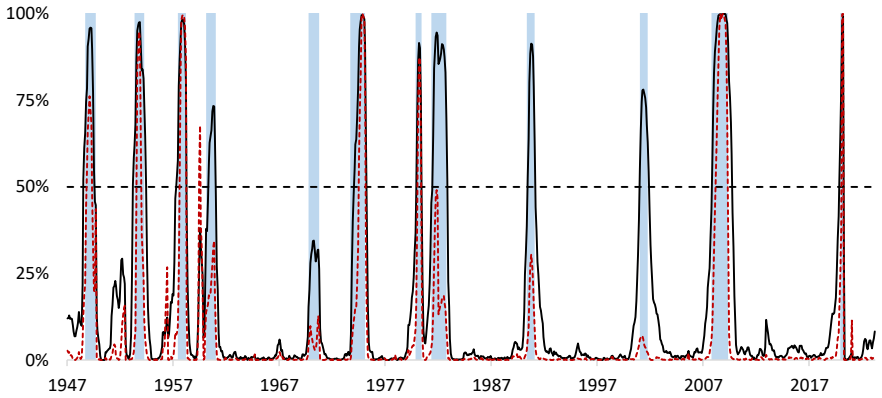

Figure 2.7: *Smoothed recession probability based on the MS-DFM-SV model*

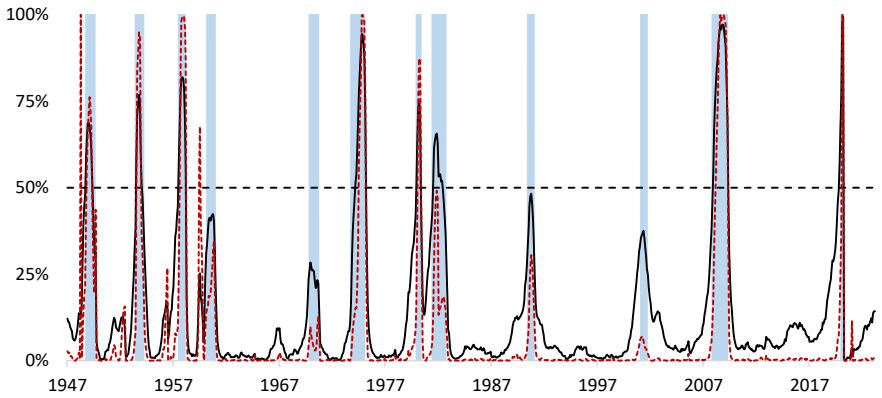

Figure 2.8: *Smoothed recession probability based on the 2MS-DFM model*

Similarly to Kim and Nelson (1998), Chauvet and Piger (2008) and Doz et al. (2020), we assume a single-factor structure driven by a two-state Markov chain corresponding to recessions ($S_t = 1$) and expansion periods ($S_t = 0$). On our data, we fit five competing models as presented in the previous section. In addition, we also include constrained specifications where the autoregressive term in

the latent factor dynamic is constrained to 0 ($\phi = 0$ in (2.4)). Figures 2.6, 2.7 and 2.8 present the smoothed recession probabilities for the unconstrained MS-DFM-GARCH, MS-DFM-SV and 2MS-DFM respectively (black lines). It is remarkable that the inclusion of time-varying volatility proves very effective for a Covid-robust timing of US recessions. However, the 2MS-DFM, clearly underperforms the MS-DFM-GARCH and MS-DFM-SV in-sample, emphasizing the need for a continuous volatility process. The MS-DFM-SV, although outperforming the standard MS-DFM, fails at identifying the shallow early-1970s recession.

To quantify the performance of the competing models, we evaluate the QPS and FPS by replacing $S_{0,t}$ in (2.10) and (2.11) with the recessions regimes as provided by the NBER. Results are reported in Table 2.4. In addition, we report the Portmanteau test statistics of Li and Mak (1994), an extended version of the standard goodness-of-fit test for conditional volatility models. Interestingly, the MS-DFM-GARCH is the only unconstrained specification to pass this test of at all considered lags. All other models reject the goodness-of-fit hypothesis, which emphasizes the heteroskedasticity of the latent factor, often neglected in the literature. Moreover, volatility exhibits some persistence, the short-memory feature of volatility induced by the ARCH(1) equation yielding autocorrelated squared residuals. It is noteworthy that the constrained MS-DFM-GARCH with $\phi = 0$ both present the smallest FPS and QPS and does not reject the goodness-of-fit test.

Models	**QPS**	**FPS**	**Portmanteau test**		
			$q_{\max} = 3$	$q_{\max} = 5$	$q_{\max} = 10$
MS-DFM	0.045	0.045	129.2	129.2	130.8
MS-DFM ($\phi = 0$)	0.054	0.052	49.7	49.8	50.8
MS-DFM-ARCH	0.031	0.019	169.1	169.6	170.6
MS-DFM-ARCH ($\phi = 0$)	0.035	0.041	28.0	28.8	30.1
MS-DFM-GARCH	0.022	0.026	**3.7**	**3.8**	**4.0**
MS-DFM-GARCH ($\phi = 0$)	0.019	0.026	**6.5**	**6.8**	**7.1**
MS-DFM-SV	0.041	0.041	17.8	20.5	21.6
MS-DFM-SV ($\phi = 0$)	0.036	0.033	19.8	22.5	23.0
2MS-DFM	0.041	0.048	88.2	90.2	91.9
2MS-DFM ($\phi = 0$)	0.059	0.067	52.4	53.4	53.6
		threshold	7.81	11.07	18.31

Table 2.4: *Empirical results on US recessions dating; Li and Mak (1994) Portmanteau test on factor residuals*

2.5. Real-time assessment: nowcasting US recessions

We proceed to a real-time downturn assessment of the five competing models. The monthly seasonally adjusted macroeconomic aggregates building up our information sample come from the FRED-MD database provided by the Federal Reserve Bank of St Louis McCracken and Ng (2016). We carry the exercise on vintages available from January 2001 onwards. In the FRED-MD database, for a given month M, industrial production and non farm payroll employment are displayed up until month M-1, real personal income excluding transfer payments up until month M-1 or M-2, and real manufacturing and trade sales up until month M-2 or M-3. We also use real

seasonally adjusted quarterly GDP vintages from the ALFRED database. The first estimate of a quarterly GDP figure for a given quarter is usually available at the end of the first month following the reference period. It is then revised up to two times with the third estimate available at the end of the following quarter. We run the competing models on a monthly basis from January 2000 to June 2023 adding the new information available this given month (it means the only data available in March 2009 is employment and industrial production reports from February 2009). To fit best the day to day monitoring of macroeconomic conditions by practitioners we attribute the probability extracted from a given month data vintage to this month as the macroeconomic information availability is known to be lagging and asynchronous. The models filtered probabilities associated to downturns from the competing models are reported in Figure 2.9.

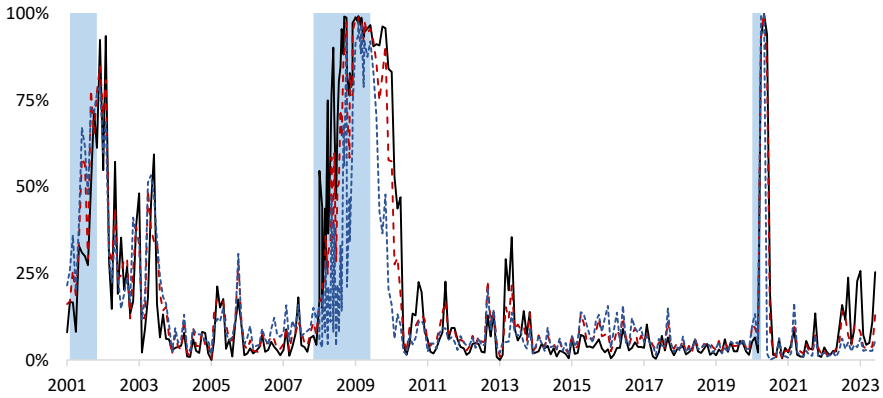

Figure 2.9: *Real-time probabilities of being in a recession. The black line represents the MS-DFM-GARCH probabilities, the red line displays the MS-DFM-SV probabilities. The blue line represents the Constant variance model probabilities. Blue shades show the recessions as dated by the NBER.*

Given the fact that both amplitude and heterogeneity of downturn episodes have been increasing over the three recession episodes available in our vintages, a constant-volatility model seems to be performing well in capturing the entry date and the exit date of the downturns. This fact is depicted in the QPS and FPS identification measures reported in the first columns of Table 2.4. However, one could argue that this good performance of the standard MS-DFM model on this out-of-sample exercise is misleading, as the real-time datasets were not polluted by abnormal episodes. Indeed, Covid-data may have deteriorated the ability of the MD-DFM to identify softer low growth regimes. Because no recession has occurred in the recent post-Covid era, it is difficult to outperform standard MS-DFM in nowcasting the US economy from 2001 to 2023. In order to assess the benefits of our model, we thus propose to simulate the real-time occurrence of a crisis. Focusing on a GFC-type crisis and a dotcom-type crisis, we investigate the ability of the competing models to capture, in a timely manner, the entry in these of recessions, should they repeat after the shock produced by the Covid crisis. Therefore, two datasets are built. We first extend the observation sample from July 2023 by adding an expanding information sample composed of the observations from January 2008 up until May 2009 — the *artificial* GFC. A second observation sample is composed of data observed up until July 2023 to which we add observations from March

to November 2001 — the *artificial* dotcom bubble. Figures 2.10a and 2.10b focus on the real GFC crisis and the *artificial* GFC as well as the corresponding filtered probabilities of being in a recession regime in real-time. Figures 2.10c and 2.10d focus on the dotcom crisis.

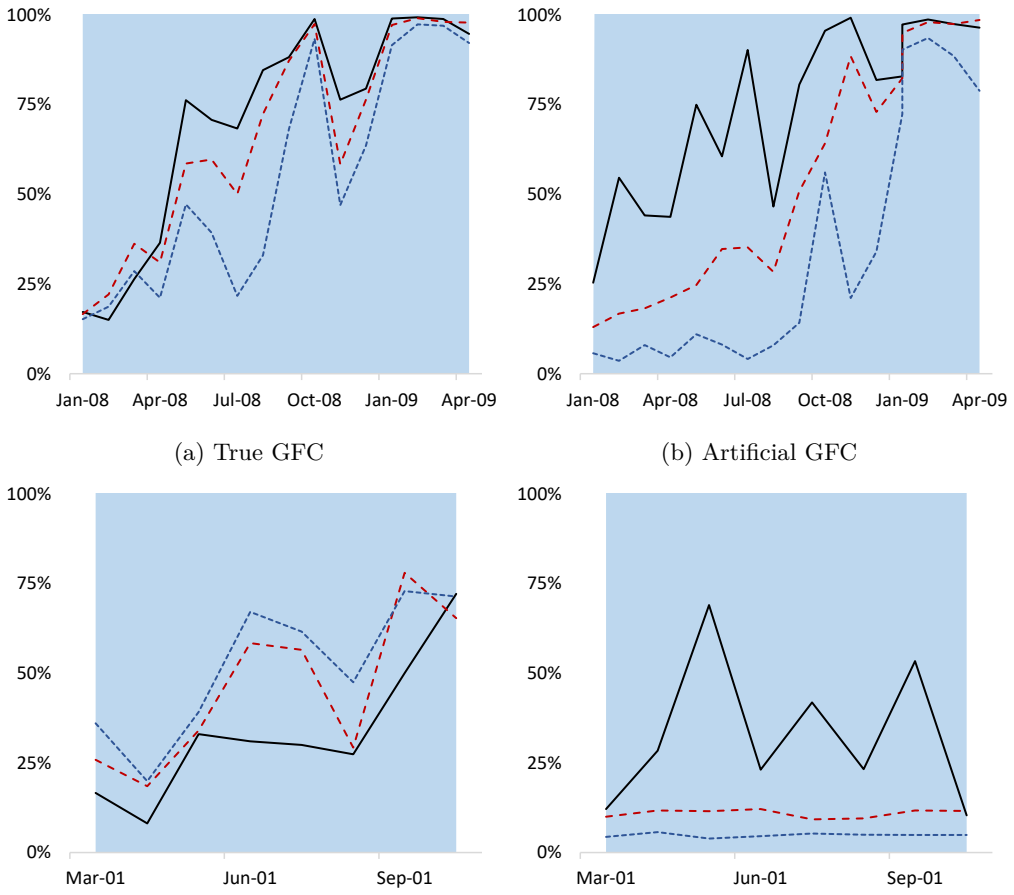

(a) True GFC

(b) Artificial GFC

(c) True dotcom recession

(d) Artificial dotcom recession

Figure 2.10: *Real-time probabilities of being in a recession obtained from a MS-DFM-GARCH (black line), MS-DFM-SV (red dashed line) and standard MS-DFM (blue dotted line). Blue shades show the GFC recession as dated by the NBER.*

In both cases, extended MS-DFM with dynamic volatility do not seem to outperform the standard MS-DFM when the crisis occur prior to the Covid-19 shock. However, when the crisis repeat after the Covid-induced recession of 2020, the MS-DFM-GARCH is clearly outperforming its competitors at timing the artificially created recessions, as emphasized in the last columns of Table 2.5. This feature is a further evidence to the observations brought by Camacho et al. (2018) and Leiva-Leon et al. (2020) regarding the weakness of constant-variance model to identify in a timely fashion the occurrence of a downturn episode. The results defer from the above-mentioned papers to the extent that the exit of the recession episode as given by the real-time filtered probabilities intervenes around 6 months after the official dating given by the NBER.

Models	All sample		True GFC		True .com		*Art. GFC*		*Art. .com*	
	FPS	**QPS**	**FPS**	**QPS**	**FPS**	**QPS**	**FPS**	**QPS**	**FPS**	**QPS**
MS-DFM-ARCH	0.11	0.08	0.50	0.30	0.88	0.53	*0.47*	*0.31*	*1.00*	*0.78*
MS-DFM-GARCH	0.12	0.09	**0.28**	**0.20**	0.88	0.48	***0.18***	***0.09***	***0.75***	***0.49***
MS-DFM-SV	**0.10**	0.08	**0.28**	0.22	0.50	0.34	*0.41*	*0.26*	*1.00*	*0.79*
MS-DFM	0.10	**0.07**	0.56	0.31	**0.50**	**0.26**	*0.65*	*0.54*	*1.00*	*0.91*
2MS-DFM	**0.10**	0.08	0.44	0.23	0.50	0.31	*0.59*	*0.39*	*1.00*	*0.81*

Table 2.5: *Performance of the competing models on the whole out-of-sample exercise, the GFC and dotcom recessions, and their artificial counterparts. Bold numbers display the minimum statistics while italic indicate the artificially created samples.*

2.6. Conclusion

Coping with the Covid shock in macroeconomic aggregates is a new challenge for econometricians and practitioners. Given the increasing heterogeneity of downturn phases - and the amplitude of the last recessionary episode - this challenge is even more essential for dating business cycles. In this Chapter, we introduce a novel Markov-switching dynamic factor model that proves highly robust to extreme shocks. This model extends the existing literature by allowing the latent factor to have a continuous-path dynamic volatility process. We present a detailed MCMC Gibbs sampling algorithm and show its good performance on simulated data. Additionally, we establish the robustness of this framework in its capacity to properly identify regimes under misspecified data generating processes and artificial jumps through Monte Carlo experiments. We compare the performances of the new framework to text-book multi-frequency MS-DFM models on an in-sample turning point detection exercise. In particular, our model yields a precise, Covid-robust, dating of the NBER recessions. Finally, a real-time exercise is carried out, showing the ability of our model to consistently capture the entry date into recession, as well as its readiness to detect new downturns in the future. The addition of alternative data, supposed to be contemporaneous with the business cycle and observable at a higher frequency (such as market prices) could however improve the timing of recessions ends. We leave this problem for future research.

2.7. Appendix

2.7.1. Priors

This section describes the priors used for the distributions of the parameter vector $\boldsymbol{\vartheta}$.
λ_1 is set to one for identification purposes. For all $j = 2, \ldots, m+q$, we use the following prior to sample λ_j the j-th element of the factor loading matrix $\boldsymbol{\Lambda}$ in (2.1)

$$\lambda_j \sim \mathcal{N}(a_j, A_j) \tag{2.12}$$

where hyperparameters are set to $a_j = 0$ and $A_j = 0.1$. To sample the parameters linked to the residuals $u_{j,t}$ in (2.2), we use the following priors, for $l = 1, 2$,

$$\begin{aligned} \psi_{j,l} \sim &\quad \mathcal{N}(\pi, \Pi) \quad \pi = 0, \Pi = 0.1 \\ \sigma^2_{e,j} \sim &\quad IG(\nu_i, Z_i) \quad \nu_i = 10, Z_i = 2 \end{aligned} \tag{2.13}$$

where IG denotes the inverse-gamma distribution. Additionally, independent beta distributions can be used as conjugate prior for each transition probability

$$\pi(q, p) \propto q^{u_{00}}(1-q)^{u_{01}} p^{u_{11}}(1-p)^{u_{10}} \tag{2.14}$$

As in Doz et al. (2020), we put an informative prior and set $u_{00} = 470, u_{01} = 9, u_{10} = 9, u_{11} = 90$ in order to take into account the relative persistence of each of the regimes as observed on macroeconomic data. The prior for the Markov-switching intercept in equation (2.4) is given by :

$$\boldsymbol{\mu} = (\mu_0, \mu_1)' \sim \mathcal{N}(\alpha^*, A^*) \tag{2.15}$$

with $\alpha^* = (4, -2)'$ and $A^* = \text{diag}(0.02, 0.02)$. We acknowledge that, in the spirit of Leiva-Leon et al. (2020), relatively tight priors are used for identification purposes. The informativeness brought by the first moment is indeed needed to discriminate between the regimes over the parameters space. The prior for the autoregressive parameter ϕ in equation (2.4) is given by

$$\phi \sim \mathcal{N}(\alpha, A) \tag{2.16}$$

where $\alpha = 0$, $A = 0.1$. In the case of a MS-DFM-ARCH, we use the following prior for the vector $\boldsymbol{\theta}^{(\text{ARCH})} = (\omega, \alpha)$

$$\log \boldsymbol{\theta}^{(\text{ARCH})} \sim \mathcal{N}(\theta_0^{(\text{ARCH})}, V_\theta) \mathbb{1}(\alpha < 1).$$

$\boldsymbol{\theta}^{(\text{ARCH})}$ thus follows a truncated log-normal distribution with the stationarity restriction that $\alpha < 1$. We set the hyperparameters to $\theta_0^{(\text{ARCH})} = \log(1, 0.5)$ and $V_\theta = \text{diag}(1, 1)$. In the case of MS-DFM-GARCH, we use the following prior for the vector $\boldsymbol{\theta}^{(\text{GARCH})} = (\omega, \alpha, \beta)$

$$\log \boldsymbol{\theta}^{(\text{GARCH})} \sim \mathcal{N}(\theta_0^{(\text{GARCH})}, V_\theta) \mathbb{1}(\alpha + \beta < 1).$$

Similarly to the ARCH(1) specification, $\boldsymbol{\theta}^{(\text{GARCH})}$ follows a truncated log-normal distribution with the adapted stationarity restriction $\alpha + \beta < 1$. Hyperparameters are set to $\theta_0^{(\text{GARCH})} = \log(1, 0.5, 0.4)$ and $V_\theta = \text{diag}(1, 1, 1)$. Note that in both cases, the priors are relatively non-informative. Finally, in the MS-DFM-SV, we use the following prior for the vector $\boldsymbol{\theta}^{(\text{SV})} = (\mu_h, \phi_h, \omega_h)$

$$\mu_h \sim \mathcal{N}(\mu_{h0}, V_{\mu_h}) \quad \phi_h \sim \mathcal{N}(\phi_{h0}, V_{\phi_h}) \quad \omega_h \sim IG(\nu_h, S_h)$$

where $\mu_{h0} = 1$, $V_{\mu_h} = 50$, $\phi_{h0} = 0.9$, $V_{\phi_h} = 1$, $\nu_h = 1$, and $S_h = 1$. These priors are intended to make the stochastic volatility process exhibits persistence in a similar fashion as the conditional variance in the GARCH framework.

2.7.2. Bayesian Estimation

Let $\boldsymbol{z}^{(T)} = \{\boldsymbol{z}_1, ..., \boldsymbol{z}_T\}$ the unobserved state, $\boldsymbol{y}^{(T)} = \{\boldsymbol{y}_1, ..., \boldsymbol{y}_T\}$ the observed data and $S^{(T)} = \{S_1, ..., S_T\}$ the first order Markov-Chain. We describe the Gibbs sampler steps based on Kim and Nelson (1999) and follow their notations. The Gibbs sampler consists of iterating between the three following steps sequentially.

2.7.2.1. Generation of the state vector

The joint distribution of $\boldsymbol{z}^{(T)}$, given $\boldsymbol{y}^{(T)}$, $S^{(T)}$ and $\boldsymbol{\vartheta}$ can be defined as

$$p(\boldsymbol{z}^{(T)} \mid \boldsymbol{y}^{(T)}, S^{(T)}, \boldsymbol{\vartheta}) = p(\boldsymbol{z}_T \mid \boldsymbol{y}^{(T)}, S^{(T)}, \boldsymbol{\vartheta}) \prod_{t=1}^{T-1} p(\boldsymbol{z}_t \mid \boldsymbol{y}^{(t)}, S^{(t)}, \boldsymbol{\vartheta}, \boldsymbol{z}_{t+1})$$

which boils down to generating $\boldsymbol{z}_t$ for $t = T, T-1, ..., 1$ from

$$\begin{aligned} &\boldsymbol{z}_T \mid \boldsymbol{y}^{(T)}, S^{(T)}, \boldsymbol{\vartheta} \sim \mathcal{N}(\boldsymbol{z}_{T|T}, \boldsymbol{V}_{T|T}) \\ &\boldsymbol{z}_t \mid \boldsymbol{y}^{(t)}, S^{(t)}, \boldsymbol{z}_{t+1}, \boldsymbol{\vartheta} \sim \mathcal{N}(\boldsymbol{z}_{t|t,\boldsymbol{z}_{t+1}}, \boldsymbol{V}_{t|t,\boldsymbol{z}_{t+1}}) \end{aligned} \tag{2.17}$$

where $\boldsymbol{z}_{t|t} = E(\boldsymbol{z}_t \mid \boldsymbol{y}^{(t)})$ and $\boldsymbol{V}_{t|t} = Var(\boldsymbol{z}_t \mid \boldsymbol{y}^{(t)})$ for $t = 1, ..., T$. In equation (2.17), $\boldsymbol{z}_T \mid \boldsymbol{y}^{(T)}, S^{(T)}, \boldsymbol{\vartheta}$ can be generated using the Multi-move Gibbs sampling introduced by Carter and Kohn (1994) as follows

1. We use the Kalman filter to obtain $\boldsymbol{z}_{t|t}$ and $\boldsymbol{V}_{t|t}$ for $t = 1, ..., T$. The last iteration of the filter gives $\boldsymbol{z}_{T|T}$ and $\boldsymbol{V}_{T|T}$ which are then used to generate $\boldsymbol{z}_T$.

2. For $t = T-1, T-2, ..., 1$, $\boldsymbol{z}_{t|t}$ and $\boldsymbol{V}_{t|t}$, $\boldsymbol{z}_{t+1}$ can be considered as an incremental vector of observations in the system. The distribution $p(\boldsymbol{z}_t \mid \boldsymbol{y}^{(T)}, S^{(t)}, \boldsymbol{\vartheta}, \boldsymbol{z}_{t+1})$ is then deduced from the Kalman smoother. From equation (2.9), updating equation are then given by

$$\begin{aligned} \boldsymbol{z}_{t|t,\boldsymbol{z}_{t+1}} &= \boldsymbol{z}_{t|t} + \boldsymbol{V}_{t|t}\boldsymbol{\Xi}\tilde{\boldsymbol{\varsigma}}_t / R_t \\ \boldsymbol{V}_{t|t,\boldsymbol{z}_{t+1}} &= \boldsymbol{V}_{t|t} - \boldsymbol{V}_{t|t}\boldsymbol{\Xi}'\boldsymbol{\Xi}\boldsymbol{V}'_{t|t} / R_t \end{aligned}$$

   where $\tilde{\boldsymbol{\varsigma}}_t = \boldsymbol{z}_{t+1} - \boldsymbol{\delta}_{S_{t+1}} - \boldsymbol{\Xi}\boldsymbol{z}_{t|t}$ and $R_t = \boldsymbol{\Xi}\boldsymbol{V}_{t|t}\boldsymbol{\Xi}' + \sigma^2_{t+1}$.

2.7.2.2. Generation of the Markov Chain

Once $\boldsymbol{z}^{(T)}$ has been simulated, given $\boldsymbol{\vartheta}$, the Markov Chain $S^{(T)}$ can be generated from the following distribution

$$\begin{aligned} p(S^{(T)} \mid \boldsymbol{y}^{(T)}, \boldsymbol{z}^{(T)}, \boldsymbol{\vartheta}) &= p(S_T \mid \boldsymbol{y}^{(T)}, \boldsymbol{z}^{(T)}, \boldsymbol{\vartheta}) \prod_{t=1}^{T-1} p(S_t \mid \boldsymbol{y}^{(t)}, \boldsymbol{z}^{(t)}, S_{t+1}, \boldsymbol{\vartheta}) \\ &= p(S_T \mid \boldsymbol{z}^{(T)}, \boldsymbol{\vartheta}) \prod_{t=1}^{T-1} p(S_t \mid \boldsymbol{z}^{(t)}, S_{t+1}, \boldsymbol{\vartheta}) \end{aligned}$$

as the distribution of $S^{(T)}$ is orthogonal to $\boldsymbol{y}^{(T)}$ given $\boldsymbol{z}^{(T)}$. We can thus obtain conditional draws for $S^{(T)}$ as follows

1. We use the Hamilton (1989) filter on (2.3) to generate $p(S_t \mid \boldsymbol{z}^{(t)}, \boldsymbol{\vartheta})$ for $t = 1, 2, ..., T$ and save them. The last iteration gives $p(S_T \mid \boldsymbol{z}^{(T)}, \boldsymbol{\vartheta})$ from which we get S_T.

2. To draw S_t given $\boldsymbol{z}^{(T)}$ and S_{t+1}, for $t = T-1, T-2, ..., 1$ the following result is used

$$p(S_t \mid \boldsymbol{z}^{(t)}, S_{t+1}, \boldsymbol{\vartheta}) = \frac{p(S_{t+1} \mid S_t) p(S_t \mid \boldsymbol{z}^{(t)}, \boldsymbol{\vartheta})}{p(S_{t+1} \mid \boldsymbol{z}^{(t)}, \boldsymbol{\vartheta})} \propto p(S_{t+1} \mid S_t) p(S_t \mid Z^{(t)}, \boldsymbol{\vartheta})$$

   where $p(S_{t+1} \mid S_t)$ is the transition probability in $\boldsymbol{\vartheta}$ and $p(S_t \mid \boldsymbol{z}^{(t)}, \boldsymbol{\vartheta})$ is obtained form the values saved in the previous step.

3. The last step consist of drawing from

$$Pr(S_t = 1 \mid \boldsymbol{z}^{(t)}, S_{t+1}, \boldsymbol{\vartheta}) = \frac{p(S_{t+1} \mid S_t = 1) p(S_t = 1 \mid \boldsymbol{z}^{(t)}, \boldsymbol{\vartheta})}{\sum_{j=0}^{1} p(S_{t+1} \mid S_t = j) p(S_t = j \mid \boldsymbol{z}^{(t)}, \boldsymbol{\vartheta})}$$

   where S_t is drawn from a uniform distribution $S_t \sim \mathcal{U}(0, 1)$. If the generated number is smaller than $Pr(S_t = 1 \mid S_{t+1}, \boldsymbol{z}^{(t)}, \boldsymbol{\vartheta})$, $S_t = 1$, otherwise $S_t = 0$.

2.7.2.3. Generation of the parameters vector

We now turn to the generation of draws for the vector of parameters. To do so, we will sequentially draw components of the $\boldsymbol{\vartheta}$ vector as follows.

We obtain conditional draws for the transition probabilities p and q following Albert and Chib (1993). In particular, given $S^{(T)}$ and the initial state, we denote the transition from the state $S_{t-1} = i$ to $S_t = j$ by n_{ij}, the log-likelihood is given by

$$L(q, p) = q^{n_{00}} (1-q)^{n_{01}} p^{n_{11}} (1-p)^{n_{10}}.$$

By combining the likelihood function and the conjugate priors presented in the previous section, from equation (2.14), we get the conditional distributions of (p, q) as the product of the independent

beta distributions from which we generate p and q as

$$\begin{aligned} q \mid S^{(T)} &\sim \text{Beta}(u_{00} + n_{00}, u_{01} + n_{01}) \\ p \mid S^{(T)} &\sim \text{Beta}(u_{11} + n_{11}, u_{10} + n_{10}). \end{aligned}$$

Given $\boldsymbol{y}^{(T)}$ and $f^{(T)}$, we can rewrite equation-by-equation equation (2.1) with

$$y^*_{j,t} = \lambda_j f^*_{j,t} + e_{j,t}$$

for $j = 2, \ldots, m+q$, where $y^*_{j,t}$ and $f^*_{j,t}$ are the j-the respective components of

$$\begin{aligned} \boldsymbol{y}^*_t = &\quad \boldsymbol{y}_t - \bar{\boldsymbol{\psi}}_1 \circ \boldsymbol{y}_{t-1} + \bar{\boldsymbol{\psi}}_2 \circ \boldsymbol{y}_{t-2} \\ \boldsymbol{f}^*_t = &\quad \boldsymbol{e}_m f_t - \bar{\boldsymbol{\psi}}_1 f_{t-1} + \bar{\boldsymbol{\psi}}_2 f_{t-2} \end{aligned} \tag{2.18}$$

with $\boldsymbol{e}_m$ denoting a vector of 1 of length m qnd $\bar{\boldsymbol{\psi}}_l = (\psi_{1,l}, \ldots, \psi_{m,l})$, $l = 1, \ldots, L$; $L = 2$ being the order of the AR specification in equation (2.2). From (2.12) and (2.18), we obtain conditional draws for λ_j from the posterior distribution

$$\mathcal{N}\left[\left(A_j^{-1} + \sigma_{e,j}^{-2} f_j^{*(T)'} f_j^{*(T)}\right)^{-1} \left(A_j a_j + \sigma_{e,j}^{-2} f_j^{*(T)'} y_j^{*(T)}\right), \left(A_j^{-1} + \sigma_{e,j}^{-2} f_j^{*(T)'} f_j^{*(T)}\right)^{-1}\right].$$

Given $\boldsymbol{y}^{(T)}$ and $f^{(T)}$, from (2.1) we can measure $\boldsymbol{u}^{(T)}$ and from equation (2.2) and the prior distribution (2.13), for all $j = 1, \ldots, m$, we can draw $\boldsymbol{\psi}_j$ from the posterior distribution

$$\mathcal{N}\left[\left(\boldsymbol{\Pi}_j^{-1} + \sigma_{e,j}^{-2} \boldsymbol{w}_j^{(T)'} \boldsymbol{w}_j^{(T)}\right)^{-1} \left(\boldsymbol{\Pi}_j^{-1} \boldsymbol{\pi}_j + \sigma_{e,j}^{-2} \boldsymbol{w}_j^{(T)'} u_j^{(T)}\right), \left(\boldsymbol{\Pi}_j^{-1} + \sigma_{e,j}^{-2} \boldsymbol{w}_j^{(T)'} \boldsymbol{w}_j^{(T)})^{-1}\right)\right]$$

where $\boldsymbol{w}_{j,t} = (u_{j,t-1}, u_{j,t-2})'$. Similarly, from the generated $\boldsymbol{\psi}_j$ and from (2.13), we can draw $\sigma^2_{e,j}$ from the posterior distribution

$$IG\left(\nu_j + \frac{T}{2}, Z_j + \frac{\left(u_j^{(T)} - \boldsymbol{\psi}_j' \boldsymbol{w}_j^{(T)}\right)' \left(u_j^{(T)} - \boldsymbol{\psi}_j' \boldsymbol{w}_j^{(T)}\right)}{2}\right).$$

Finally, we turn to the generation of $(\mu_0, \mu_1, \phi, \boldsymbol{\theta}^{(.)'})$. As the Gibbs sampling methods differ between conditional and stochastic volatility, we will detail our algorithm for the different models, starting with the latter.

For the MS-DFM-SV, we draw the individual parameters in $(\mu_0, \mu_1, \phi, \boldsymbol{\theta}^{(SV)'})$ sequentially. Rewriting equation (2.4), we have

$$\frac{f_t - \phi f_{t-1}}{\sigma_t} = \frac{\mu_0(1 - S_t) + \mu_1 S_t}{\sigma_t} + \eta_t$$

Let us denote G^*_t the left-hand side of the above equation and Let us denote G^*_t the left-hand side

of the above equation and

$$Q^{*(T)} = \begin{bmatrix} 1 - S^{(T)} & S^{(T)} \end{bmatrix}$$

From the prior distribution (2.15), $\boldsymbol{\mu}$ can be drawn from the posterior distribution

$$\boldsymbol{\mu} \sim \mathcal{N}((A^{*-1} + Q^{*(T)\prime}Q^{*(T)})^{-1}(A^{*-1}\alpha + Q^{*(T)\prime}G^{*(T)}), (A^{*-1} + Q^{*(T)\prime}Q^{*(T)})^{-1}),$$

and only draws verifying the condition $\mu_0 > \mu_1$ are kept. Rewriting again equation (2.4) yields

$$\frac{f_t - \mu_0(1 - S_t) - \mu_1 S_t}{\sigma_t} = \phi \frac{f_{t-1}}{\sigma_t} + \eta_t.$$

Denoting $\tilde{G}_t$ the left-hand side of the above equation and $\tilde{Q}_t$ the right-hand side, from (2.16) ϕ can be drawn from the following posterior distribution

$$\phi \sim \mathcal{N}((A^{-1} + \tilde{Q}'\tilde{Q})^{-1}(A^{-1}\alpha + \tilde{Q}'\tilde{G}), (A^{-1} + \tilde{Q}'\tilde{Q})^{-1}).$$

Only draws satisfying the stationarity condition $|\phi| < 1$ are kept. We then jointly sample the log-volatility from the conditional density

$$p(\boldsymbol{h}^{(T)} \mid \boldsymbol{z}^{(T)}, S^{(T)}, \mu_0, \mu_1, \phi, \boldsymbol{\theta}^{(SV)'})$$

based on the acceptance-rejection Metropolis Hastings algorithm described in Chan (2017) using the precision sampler of Chan and Jeliazkov (2009). To that end, we compute the mode of $p(\boldsymbol{h}^{(T)} \mid \boldsymbol{z}^{(T)}, S^{(T)}, \mu_0, \mu_1, \phi, \boldsymbol{\theta}^{(SV)'})$ and the Hessian of the log-density evaluated at this mode denoted $\hat{h}$ and K_h. We then use $\mathcal{N}(\hat{h}, K_h^{-1})$ as a proposal distribution in the acceptance-rejection Metropolis Hastings step from which we can directly sample $\boldsymbol{h}^{(T)}$.

For the MS-DFM-GARCH, we draw the parameters from the three full conditional distributions $p(\boldsymbol{\mu} \mid \boldsymbol{z}^{(T)}, S^{(T)}, \phi, \boldsymbol{\theta}^{(\text{GARCH})})$, $p(\phi \mid \boldsymbol{z}^{(T)}, S^{(T)}, \boldsymbol{\theta}^{(\text{GARCH})})$ and $p(\boldsymbol{\theta}^{(\text{GARCH})} \mid \boldsymbol{z}^{(T)}, S^{(T)}, \phi)$ sequentially. Since μ_{S_t} and ϕ appear in the conditional variance equation, those distributions are non-standard, as noted by Chan and Grant (2016), and Metropolis Hastings algorithms are required. To sample ϕ we use a Gaussian proposal with mean $\bar{\phi}$ and variance V_ϕ given by

$$\begin{aligned} \bar{\phi} = &\quad (A^{-1} + \tilde{Q}'\tilde{Q})^{-1}(A^{-1}\alpha + \tilde{Q}'\tilde{G}) \\ V_\phi = &\quad (A^{-1} + \tilde{Q}'\tilde{Q})^{-1}. \end{aligned}$$

Only draws satisfying the stationarity condition $|\phi| < 1$ are kept. To sample $\boldsymbol{\mu}$, we use a multivariate Gaussian proposal

$$\mathcal{N}\left[(A^{*-1} + Q^{*(T)\prime}Q^{*(T)})^{-1}(A^{*-1}\alpha + Q^{*(T)\prime}G^{*(T)}), (A^{*-1} + Q^{*(T)\prime}Q^{*(T)})^{-1}\right]$$

and only keep draws verifying $\mu_0 > \mu_1$. Finally to sample $\boldsymbol{\theta}^{(\text{GARCH})}$, we use a Gaussian proposal centered at the mode of $p(\boldsymbol{\theta}^{(\text{GARCH})} \mid \boldsymbol{z}^{(T)}, S_t, \phi)$ with covariance matrix set to be the outer product of the scores.

2.7.2.4. GARCH model parameters posteriors

Table 2.6: *MS-DFM-GARCH model parameters posteriors*

Variables	Parameters	Mean	Std
GDP	λ	1	0
IP	λ	0.49	0.24
RS	λ	0.50	0.02
PI	λ	0.24	0.01
E	λ	0.26	0.01
GDP	ψ_1	0.00	0.08
IP	ψ_1	0.31	0.05
RS	ψ_1	-0.45	0.04
PI	ψ_1	-0.08	0.04
E	ψ_1	-0.13	0.04
GDP	ψ_2	0.00	0.08
IP	ψ_2	0.04	0.04
RS	ψ_2	-0.22	0.04
PI	ψ_2	0.02	0.04
E	ψ_2	0.05	0.04
GDP	σ_e^2	0.28	0.09
IP	σ_e^2	0.38	0.04
RS	σ_e^2	0.69	0.05
PI	σ_e^2	0.27	0.02
E	σ_e^2	0.23	0.02
Factor			
	μ_1	-1.05	0.01
	μ_0	1.11	0.01
	ϕ	-0.30	0.04
	ω	2.01	0.38
	α	0.46	0.06
	β	0.22	0.07
	q	0.98	0.01
	p	0.90	0.02

Chapter 3

Asset swap spreads as business cycle phases assessors: when real-time tracking of macroeconomic fluctuations is useful in asset allocation

Abstract: Asynchronous and lagging macroeconomic information in nowcasting models are challenging for both practitioners and policy makers. Timing the entry and the exit of macroeconomic downturns is nonetheless of greatest importance. Adding asset swap spreads to the information sample to mitigate the usual macroeconomic data-related caveats can be helpful. This work sheds light on the capability of this weekly market information to correctly assess the business cycle phases. We build upon the existing literature of Markov-Switching Dynamic Factor Models with dynamic volatility in the factor auto-regressive behavior. This approach demonstrates the benefits of using this information flow to infer business cycle phases and implement macro-based allocation strategies. Using asset swap spreads as a proxy for market sentiment regarding current macroeconomic conditions enhances the detection of turning points and improves the risk-adjusted return of allocation strategies that seek business cycle downturn hedging signals.

Keywords: *Nowcasting; Bayesian Estimation; Dynamic Factor; Non-linearity*

3.1. Introduction

Real-time assessment of the state of the business economy has become an overarching question in the past decade for policy makers and market participants. In the wake of the Great Financial Crisis and the more recent Covid Pandemic, heterogeneity of the contractionary episodes in terms of duration and amplitude has triggered hurdles for practitioners to identify econominc turning points in a timely fashion. This work intends to show the credit market asset swap spreads capability to improve economic downturns identification. Those spreads are interpreted as a compensation of the Asset Swap (ASW) buyer for taking credit risk (O'Kane (2000)). A key advantage of this information sample is the daily availability of the market prices which in turn, enables to bypass the caveats related to the nowcasting literature; namely the asynchronicity in the publication of lagged economic data. Ideed, the first hard macro-data available for a given month **M** in the US is the job report published by the Bureau of Labor statistics the first friday of the following month. When looking at GDP, the first estimate of the figure is available one month after the reference quarter period. The Chapter's bedrock is to consider the default pricing capacity of the credit market as a relevant real-time assessor of the real economy booms and busts. We thus rely on the market efficiency hypothesis through the financial accelerator mechanism highlighted by Bernanke and Gertler (1989) and Kiyotaki and Moore (1997): a negative shock to business economy triggers an immediate alteration in corporate balance sheets and a decline in expected revenues. This deterioration hampers investment capabilities and ultimately output. This development is embodied in the widening of the spreads : among the rate buckets of corporate asset swaps, a broad -sometimes distorted- repricing of default probabilities occurs. If this tension in the credit market arises the information can be valuable in the economic turning point detection process. We develop a market-based real-time indicator of US activity which tracks the changes alongside the business cycle phases and captures the asymmetry and heterogeneity of the contractionary episodes. These market prices bring additional and valuable information to the usual macroeconomic datasets composed of lagged hard data.

One can observe a non-linear pattern in the co-movement of risks re-pricing through securities spreads grade buckets. We embed this non-linear behavior into an econometric framework allowing for regime switching in the dynamics of an unobserved factor, in a Markov Switching Dynamic Factor Model (MS-DFM). This class of models in the nowcasting literature unifies two properties of the business cycle dynamics observed by Burns and Mitchell (1946) : a co-movement diffused across several economic aggregates and asymmetries along the regime phases. These properties are also observed in the ASW markets. MS-DFMs are based on the seminal work of Diebold and Rudebusch (1996) that bridged contributions of Stock and Watson (1991) who developed a linear coincident indicator summarizing the co-movement of several aggregate time series and Hamilton (1989) in identifying regimes in a given time-series model through a Markov-Chain specification. Kim and Yoo (1995) further expanded the specification in a multivariate case and alternative specifications were used by Chauvet (1998) and Kim and Nelson (1998). We build upon the first Chapter of this manuscript by using a MS-DFM specification including a time-varying volatility in

the common factor dynamic which follows a autoregressive conditional heteroskedastic (ARCH) or a generalized autoregressive conditional heteroskedastic (GARCH) process. It aims at capturing the broader heterogeneity in the amplitude of the shocks affecting the cycle. This works is thus related to the recent developments of treating time-varying volatility in dynamic factor models in order to overcome the Covid shock in the data. One can mention the work of Marcellino et al. (2016) and Antolin-Diaz et al. (2023) who develop time-varying volatility in MIDAS and linear dynamic factor models in a linear framework respectively. This econometric structure allows us to track the business cycle and to infer in a timely fashion the occurrence of the adverse shocks.

This Chapter builds upon a vast strand of literature using asset prices variations as predictors of economic activity[1]. Nonetheless it differs from the above cited literature in its objective : we are not interested into projecting economic dynamics to a short or medium term horizon (Gilchrist et al. (2009), De Santis (2016)). This exercise rather undertakes an assessment on a high frequency basis of the current economic conditions as being "filtered" by the credit markets. This approach is more in line with Chauvet and Senyuz (2016) who use the information content of US Bond market to produce an assessment of real economy downturns. More recently, Furno and Giannone (2024) have undertaken a similar work looking at financial conditions and monthly economic surveys embedded in Purchasing Managers' Indices (PMI) to develop a robust framework of activity monthly nowcast. The interactions between the credit market sentiment and the real economy and the leading relationship between the both (López-Salido et al. (2016)) is however out of scope. A considerable literature depicts the fact that spreads do not only reflect a contemporaneous state of the economy but also a hedge against adverse economic scenario (Driessen (2005), Philippon (2009), De Santis (2016)). A complementary work by De Santis (2018) also provides a measure of excess bond premia and therefore fragmentation for the Euro Zone. This work refers to the co-movement across a broad range of asset swap spreads as a coherent real-time macroeconomic risk repricing. This repricing occurs when the expected contractionary macroeconomic episode becomes the core market concern. The co-movement also falls into Burns and Mitchell (1946) definition of pervasiveness characterizing the business cycle : nations organizing their work mainly in business enterprises face expansions in many economic activities but also recessions. We capture the co-movement by the exhaustive coverage of asset swap spreads synthetic indices we use from sectors depicted in Appendix 3.10.1. This broad scope of sectors and firms can be represented in credit grade buckets from high-grades to speculative-grades credit ratings which enables to seize, beyond the rating buckets subject to specific stresses, a repricing of credit risk signalling macroeconomic vulnerability in real-time.

This work exhibits the usefulness of incorporating this highly valuable credit data by comparing specifications taking both the real monthly economic data and the ASW spreads or taking the hard macroeconomic data only. Considering both macroeconomic and financial data in the information set does not hamper in-sample recession identification and proves to be highly reliable

[1] Among others Fama (1981), Harvey (1988), Hamilton and Kim (2002), Stock and Watson (2003), more precisely upon corporate credit spreads as in the vein of Gilchrist et al. (2009) and Faust et al. (2011)

in out-of-sample exercises. This work also bridges this macroeconomic turning point real-time identification to allocation strategy in which the high frequency signals of macroeconomic downturn is used to weigh a cash (risk-free) allocation allowing to modulate an exposure to a risky asset. Indeed, previous studies have emphasized the critical role of business cycle phases for investors to take in portfolio construction. We can mention here the work introduced by Brocato and Steed (1998) who deploy portfolio optimization à la Markowitz (1952) conditional on business cycle phases. van Vliet and Blitz (2011) propose a dynamic strategic asset allocation across the economic cycle. de Longis and Ellis (2023) deploy a tactical asset allocation across recovery, expansion, slowdown, and contraction. Those applications fail nonetheless to identify business cycle phases in a real-time fashion. This is the main contribution of this Chapter. The application demonstrates the need to incorporate ASW spreads to the information sample in order to be able to follow in a timely manner coincident macroeconomic dynamics and deploy a robust hedging strategy.

The Chapter is organized as follows. Section 3.2 justifies the use of assets swap spreads as real-time business cycle assessors. Section 3.3 describes the data used. Section 3.4 covers the MS-DFMs specifications used. Section 3.5 present the Gibbs sampler algorithm implemented to estimate the models. Section 3.7 analyses the real-time weekly backtests implemented. Section 3.8 gauges the usefulness of the signals extracted through the backtest of allocation strategies using the signals developped. Section 3.9 concludes.

3.2. Asset swap spreads, a rational gauge of real economy developments

Asset swaps belong to the class of over-the-counter (OTC) contracts. This is a synthetic floating-rate note which enables the investor (*asset swapper*) to exchange a fixed-coupon bond against a floating rate (SOFR + ASW spread). The investor takes exposure to credit risk without bearing the interest movements risk related to it (i.e. the duration risk). As a matter of fact if the bond issuer defaults, *the asset swapper* gets the recovery value but needs to honour the swap contract without the side funding of the bond coupon -if the position is not closed at mark-to-market value. ASW spreads can be interpreted as default risk compensations and are defined as the difference between the floating rate and the SOFR rate. They are derived from the bond yield, prices and the forward SOFR rate as follows solving for S^{ASW} taking notations from De Santis (2016):

$$(100 - P) + \sum_{m=1}^{M} C z_{t_m} = \sum_{m=1}^{M} (L_{t_{m-1},t_m} + S^{ASW}) z_{t_m} \qquad m = 1, 2, ..., M \tag{3.1}$$

where $100-P$ is the asset value to get the full price of par, P is the full market price of the bond, M the residual maturity of the bond, C the annual bond coupon, z_{t_m} the discount factor, L_{t_{m-1},t_m} is the forward SOFR rate between the two cash flow dates t_{m-1}, t_m and S^{ASW} the asset swap spread.

The pricing of the ASW spreads captures asynchronous and multi-frequential macroeconomic data flows materialized by a continuously updated probability of default. As De Santis (2016) stresses it out, *"the ASW spreads are primarily driven by the credit quality of the issuer"* and are also *"less confounded by tax and various market micro-structure effects, because the bond is not sold and investment banks' business model rotate around swap contracts"*. De Santis (2016) shows that ASW spreads are highly correlated with yield spreads, the spreads between the yield to maturity of a bond and a risk free rate of same remaining maturity. They are moreover homogeneous across countries and over time. However, during stressed periods, liquidity premia in the ASW market is lower than the bond market one, making the ASW spread less sensitive to those periods compared to yield spreads. The basis of this Chapter is to consider one major feature of credit risk pricing associated to the ASW spread, as highlighted by Aussenegg et al. (2016), i.e. the negative relationship between the spread and the enterprise value which in turns depends, from a macroeconomic point of view and on synthetic indices, on the business cycle phases as perceived by market participants. Finally, one could have thought of asset backed credit default swaps data for instance, but those swaps do not display sufficient history of data (starting back in 2005). ASW spreads display thus a broader history, making the backtest exercise more relevant.

3.3. Data Used

We use in our analysis for the US seven asset swap synthetic spreads splitted in grade buckets illustrated in Figure 3.1 as well as four coincident monthly macroeconomic variables in Figure 3.2. The data commonly used by the NBER to date recessions constitute our information sample: industrial production (dIP), real manufacturing and trade sales (dRS), real personal income excluding transfer payments (dPI) and non farm payroll employment (dE). Following Camacho et al. (2015) we decide to keep the information sample as small as possible in terms of number of time series. Shaded areas correspond to periods of recessions as defined by the NBER. Those periods correspond to the time span between the peak to the trough along the business cyle phases.

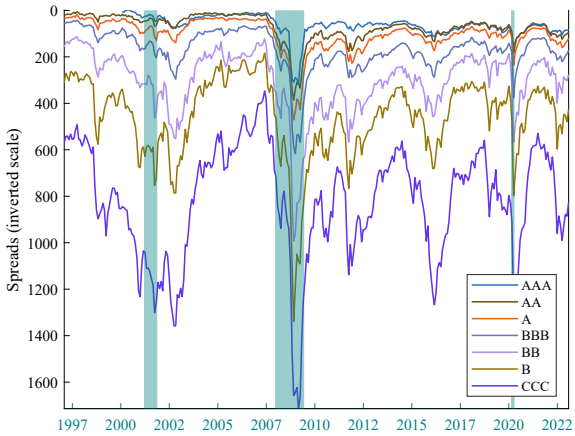

Figure 3.1: *Asset swap spreads*

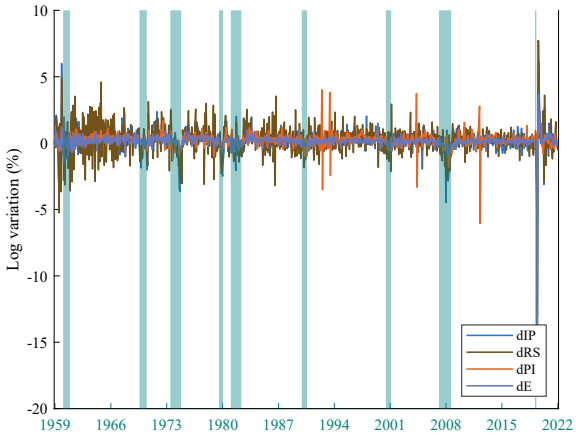

Figure 3.2: *Macro variables*

The four US monthly seasonally adjusted macroeconomic variables we use (what we we will hereafter call hard data) stem from the FRED-MD database developed and updated by the Federal Reserve Bank of St Louis (McCracken and Ng (2016)). Monthly vintages are available from August 1999 onwards. In the FRED-MD database, for a vintage of month M, industrial production and non farm payroll employment are displayed up until month M-1, real personal income excluding transfer payments up until month M-1 or M-2, and real manufacturing and trade sales up until month M-2 or M-3. ASW spreads are available all working days of a year and can be considered as the market assessment of the current economic situation.

In this Chapter we focus on the contemporaneous relationships between ASW spreads and real economic activity data which are usually observed with a delay. There is at least one month lag between the first available macroeconomic data for a given monthly reference period. These data are moreover published in an asynchronous fashion. Practitioners who want to get a hint on the actual state of the economy have to wait at least one week to get new informational content on the reference period. This time span is costly when developping allocation strategies based on high frequency macroeconomic signal extraction. We use the ASW spreads to "bridge" the sentiment in the credit market, measured by a broad grade-based spread contraction/widening, to the contemporaneous state of the economy in a real-time fashion. We achieve the later by taking into account the co-movement between ASW spreads and real economic variables. Our framework aims at identifying business cycle regime in real-time rather than predicting real activity in the sense of Gilchrist and E.Zakrajšek (2012) [2]. We therefore ignore the information from credit markets not attributable to current economic conditions. To that extent we diverge from the two-factor approach developed by Leiva-León et al. (2022) intending to provide a real-time gauge of a "sentiment" in credit markets, above and beyond that attributable to contemporaneous economic conditions which can cause strong asymmetric and nonlinear effects on economic activity.

3.4. Model

First introduced by Diebold and Rudebusch (1996) based on the seminal work of Hamilton (1989), Markov-switching dynamic factor models (MS-DFM) derived in their multivariate form by Kim and Yoo (1995) and afterwards used by Chauvet (1998) were initially applied to a set of U.S. real activity indicators at a monthly frequency. Their aim was to summarize this information into a single index subject to regime changes, showing its ability to identify turning points in a timely fashion. This class of models manages indeed two characteristics of economic cycles defined by Burns and Mitchell (1946) : a comovement across economic series and the regime-specific nature of economic dynamics navigating through expansions and recessions. The common factor embeds the information relative to economic growth. Its dynamics defined as a Markov-chain process enable to seize the two-regime nature of the economic cycle. Chauvet and Piger (2008) highlight that Markov-switching dynamic factor models beat other non-parametric approaches in identifying

[2] The authors do allow in their regression the possibility of forecasting at a zero-horizon falling into our nowcasting framework.

U.S. recessions as dated by the NBER. Building on the work of Hamilton (1989), earlier MS-DFMs specifications were characterized by a MS-constant applying uniformly across all expansion and recession periods. We compare two competitive MS-DFM specifications using an information sample composed only of hard macroeconomic data or both hard macroeconomic and ASW spreads data to show the added value of more timely available information. Camacho et al. (2018) highlighted the ability of this class of models to handle asynchronous data releases, which is a key aspect of the real-time analysis we want to dig into. We compare two specifications proposed in the first Chapter of this manuscript where a unique Markov process drives the constant in the state-space transition equation of the unobserved component synthesizing the co-movement of the observable variables. We allow the volatility of the factor to be dynamic, absorbing heterogeneous macroeconomic shocks without impairing its regime detection ability. We nonetheless remain in a uni-frequential framework.

Let $\boldsymbol{y}_t$ a vector of m monthly observable time series and let f_t a latent common factor. We have the standard DFM given by :

$$\boldsymbol{y}_t = \boldsymbol{\Lambda} f_t + \boldsymbol{u}_t, \tag{3.2}$$

where $\boldsymbol{\Lambda}$ denotes the loadings matrix, $\boldsymbol{u}_t$ is orthogonal to f_t and for all $j = 1, \ldots, m$

$$\psi_j(L) u_{j,t} = e_{j,t}, \quad e_{j,t} \sim \mathcal{N}(0, \sigma^2_{e,j}), \tag{3.3}$$

let us denote $\boldsymbol{\psi}_j = (\psi_{j,1}, \ldots, \psi_{j,l})'$ the coefficients of the lag polynomial $\psi_j(L)$ of order $l = 1$ and the set of factor follows

$$\begin{aligned} f_t &= \mu_{S_t} + \phi f_{t-1} + \varepsilon_t \\ \varepsilon_t &= \sigma_t \eta_t \end{aligned} \tag{3.4}$$

where η_t is iid $(0, 1)$ and S_t is an independent first order Markov chain. A two-state ($S_t = 0$ or 1) regime-switching model is considered with $\mu_{S_t} = \mu_1 S_t + \mu_0(1 - S_t)$. $S_t = 1$ is the recessionary episode and $\mu_1 < \mu_0$. Based on the first Chapter of this manuscript we consider after two conditional volatility models for σ_t. The ARCH(1) version

$$\sigma^2_t = \omega + \alpha \varepsilon^2_{t-1} \tag{3.5}$$

where $\omega > 0$, $0 < \alpha < 1$ and a GARCH(1,1)

$$\sigma^2_t = \omega + \alpha \varepsilon^2_{t-1} + \beta \sigma^2_{t-1} \tag{3.6}$$

where $\omega > 0$, $0 < \alpha + \beta < 1$

3.5. Gibbs sampling

The general model from (3.2) to (3.4) can be cast in state space form :

$$\begin{aligned} \boldsymbol{y}_t &= \boldsymbol{H}\boldsymbol{z}_t + \boldsymbol{\varsigma}_t & \boldsymbol{\varsigma}_t &\sim \mathcal{N}(0, \boldsymbol{R}) \\ \boldsymbol{z}_t &= \boldsymbol{\delta}_{S_t} + \boldsymbol{\Xi}\boldsymbol{z}_{t-1} + \boldsymbol{\zeta}_t & \boldsymbol{\zeta}_t &\sim \mathcal{N}(0, \boldsymbol{Q}_t) \end{aligned} \tag{3.7}$$

$\boldsymbol{H}$ the $(m) \times (ml+1)$ matrix, $\boldsymbol{\Xi}$ the $(ml+1) \times (ml+1)$ matrix, and $\boldsymbol{\Xi}_{j=1\dots m}$ the $l \times l$ matrix such that

$$\boldsymbol{H} = \begin{bmatrix} \lambda_1 & \boldsymbol{h}^l & \dots & 0 \\ \vdots & \vdots & \ddots & \vdots \\ \lambda_m & 0 & \dots & \boldsymbol{h}^l \end{bmatrix} \quad \boldsymbol{\Xi} = \begin{bmatrix} \boldsymbol{\phi} & & & \\ & \boldsymbol{\Xi}_1 & & \\ & & \ddots & \\ & & & \boldsymbol{\Xi}_m \end{bmatrix}$$

$$\text{with} \quad \boldsymbol{\Xi}_{j=1\dots m} = \begin{bmatrix} \psi_{j,1} & \psi_{j,2} & \dots & \psi_{j,l-1} & \psi_{j,l} \\ 1 & 0 & \dots & 0 & 0 \\ 0 & 1 & \dots & 0 & 0 \\ \vdots & \vdots & \ddots & \vdots & \vdots \\ 0 & 0 & \dots & 1 & 0 \end{bmatrix}.$$

$\lambda_1 = 1$ for identification purpose. $\boldsymbol{h}^l$ is a $1 \times l$ vector with the only first element equal to one. $\boldsymbol{\delta}_{S_t} = (\mu_{S_t}, 0, \dots, 0)'$, $\text{diag}(\boldsymbol{Q}_t) = (\sigma_t^2, \sigma_{e,1}^2 \boldsymbol{h}^l, \dots \sigma_{e,m}^2 \boldsymbol{h}^l)$. The vector $(ml+1)$ of unobserved variables $\boldsymbol{z}_t$ is given by

$$\boldsymbol{z}_t = (f_t, (1, L, \dots, L^{l-1})u_{1,t}, \dots, (1, L, \dots, L^{l-1})u_{m,t})'.$$

Defining the transition probabilities

$$q = \mathbb{P}(S_t = 0 | S_{t-1} = 0) \quad \text{and} \quad p = \mathbb{P}(S_t = 1 | S_{t-1} = 1),$$

the vector of parameters to be estimated is characterized as follows

$$\boldsymbol{\vartheta} = (p, q, \boldsymbol{\Psi}', \sigma_{e,1}, \dots, \sigma_{e,m}, \boldsymbol{\Lambda}', \mu_0, \mu_1, \phi, \boldsymbol{\theta}^{(.)'})'$$

where $\boldsymbol{\theta}^{(.)}$ is the vector of parameters driving the dynamic volatility equation σ_t

$$\boldsymbol{\theta}^{(\text{ARCH})} = (\omega, \alpha), \quad \boldsymbol{\theta}^{(\text{GARCH})} = (\omega, \alpha, \beta).$$

We denote $\boldsymbol{z}^{(T)} = \{\boldsymbol{z}_1, \dots, \boldsymbol{z}_T\}$ the unobserved state vector in equation (3.7), $\boldsymbol{y}^{(T)} = \{\boldsymbol{y}_1, \dots, \boldsymbol{y}_T\}$ the monthly observed data, and $S^{(T)} = \{S_1, \dots, S_T\}$ the unobserved Markov Chain. The model is estimated using a Markov Chain Monte Carlo (MCMC) Gibbs sampling algorithm in the spirit of Kim and Nelson (1999) and Bai and Wang (2015) where conditional draws of the state vector,

the Markov Chain, and the parameters vector $\boldsymbol{\vartheta}$ are obtained sequentially. In particular, we adapt the Metropolis Hastings procedure presented in Chan (2023) to sample the conditional volatilities. Details on the priors and a complete description of the sampling algorithm are presented in Appendices 3.10.2 and 3.10.3. The general form of the algorithm can be summarized as follows:

1. We generate conditional draws of the state vector from $p(\boldsymbol{z}^{(T)}|\boldsymbol{y}^{(T)}, S^{(T)}, \boldsymbol{\vartheta})$ using the forward-filtering backward-smoothing algorithm of Carter and Kohn (1994).

2. We generate conditional draws of the Markov chain from $p(S^{(T)}|\boldsymbol{y}^{(T)}, \boldsymbol{z}^{(T)}, \boldsymbol{\vartheta})$ based on the Hamilton filter (Hamilton (1989)).

3. We generate conditional draws for the parameters vector from $p(\boldsymbol{\vartheta}|\boldsymbol{y}^{(T)}, \boldsymbol{z}^{(T)}, S^{(T)})$ by sequentially drawing in the conditional distribution of components of $\boldsymbol{\vartheta}$ as follows:

   - We obtain conditional draws for p and q following Albert and Chib (1993).
   - We obtain conditional draws for $(\boldsymbol{\Psi}', \sigma_{e,1}, \ldots, \sigma_{e,m}, \boldsymbol{\Lambda}')$ from usual priors in the literature (see for example Bai and Wang (2015)).
   - To obtain conditional draws for $(\mu_0, \mu_1, \phi, \boldsymbol{\theta}^{(.)'})$, we build upon the Metropolis Hastings algorithm presented in Chan and Grant (2016).

3.6. In-sample probabilities

We first estimate the models on the monthly datasets based either solely on the hard macroeconomic data sample or on the dataset composed of both seven ASW spreads grade buckets and macroeconomic hard data. The time spans from January 1959 to February 2023 for monthly macroeconomic data. The ASW spreads are available from 1997 onwards. We compare the probabilities of being in recession with regards to shaded NBER dated recessions in Figure 3.3.

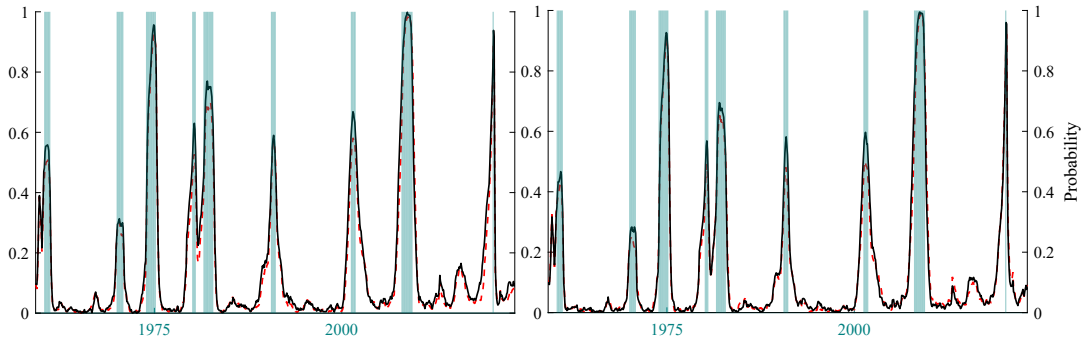

Figure 3.3: *In-sample smoothed probabilities to be in a contraction regime from the ARCH extension (left hand side) and GARCH extension (right hand side). Red dashed line : macro variables used only. Black line: macro and financial data used*

At first sight adding the ASW spreads to the hard data sample does not hamper nor improve

the identification of turning points. Regime identification is less pronounced than using a multi-frequential framework as shown by Camacho et al. (2018) but we still recover eight out of nine recessionary episodes. We will show in the following section that the gain of adding the asset swap spreads to the hard data sample arises when assessing in real-time the macroeconomic downturn episodes.

3.7. Real-time assessments of downturns

We perform a weekly real-time backtest of the models compared on the basis of an information sample either composed of macroeconomic data only or hard and spread data combined together. To achieve this exercise we use the rules of weekly publication of Table 3.1 in a given month for the data described in Section 3.3.

Table 3.1: *Usual weekly publication schedule of US data in a given month of 5 weeks*

Reference M	**M-1**	**M-2 or 3**	**M-1 or 2**	**M-1**
	IP	**RS**	**PI**	**E**
1st week				x
2nd week	x			x
3rd week	x			x
4th week	x	x	x	x
5th week	x	x	x	x

For a given month in the United States, only employment data for the reference period M-1 are available at the end of the first week of the following month M. One can easily get a hint of the added value for a practitioner to get valuable market information up until the moment he runs his turning point nowcast. We measure the performance of adding ASW spread data to our information sample using the quadratic probability score (QPS) and the False Probability Score (FPS). We show below the benefit of adding ASW spreads as business cycle real-time assessors. The main drawback of the information sample used is the availability of the data. Indeed, asset swap spreads indices are available since 1997 in the US. However, adding this valuable information in a timely fashion due the ever-growing interactions between wall and main street economics shall be taken into account. The QPS is defined as follows:

$$QPS = \frac{1}{T}\sum_{t=1}^{T}(S_t - P(S_t = 1 \mid I_t))^2 \tag{3.8}$$

With S_t the recession dummy provided by the NBER business cycle dating committee. As the carried out backtest is implemented on a weekly basis to match the practitioner usual usage of nowcasting tools we make the hypothesis that the recession start at the first week of the month of the recession dating. This hypothesis might underestimate the ability of the ASW market to correctly track economic downturns. $P(S_t = 1 \mid I_t)$ is the filtered probability inferred by the model regarding the occurrence of the regime switch to a contractionnary episode given an information

sample available I_t. The FPS is given by :

$$FPS = \frac{1}{T}\sum_{t=1}^{T}(S_t - I_{P(S_t=1|I_t)>0.5})^2 \tag{3.9}$$

We compare the two models defined in Section 3.4 on two data information samples. The backtest is ran, for comparison from 7th of January 2000 to the 24th February 2023. Results of the real-time exercise are reported in Table 3.2. The weekly backtest displays the ability of spread data to accurately assess the downturns episodes when added to the hard data information sample. This confers a highly valuable information regarding the state in which the economy currently is. This also confirms our intuition on linkages between macroeconomic and ASW spreads. Regarding the model specifications, adding a dynamic variance to the common factor proves to be effective in discriminating between states of the economy. The ARCH extension is the specification which performs best across the FPS and QPS performance metrics.

	M & F		M	
Models	QPS	FPS	QPS	FPS
MS-DFM-GARCH	**0.053**	**0.060**	0.093	0.133
MS-DFM-ARCH	**0.052**	**0.046**	0.094	0.127

Table 3.2: *Identification statistics. Bold figures display the minimal values. M&F refers to the model using both asset swap spreads and macro variables whereas M refers to the model using only macro variables.*

Moreover, looking at the filtered probabilities in Figures 3.4 and 3.5, we can see the ability of the new information sample to catch in a very simultaneous way the downturn signals. This fact is also highlighted in Appendix 3.10.5 during the selected downturn episodes composed of the Great Financial Crisis and the Covid recession. The interesting pattern of the filtered probabilities from the models based on the both samples combined is their ability to capture the occurrence of the downturn signal before the models only based on the hard data sample. They also display the capacity to react more quickly to the end of the recessions. This timing ability is of a great help in asset allocation strategies described in the following section.

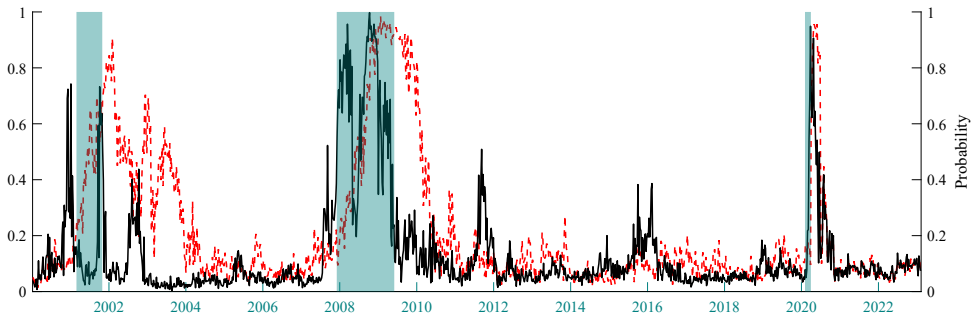

Figure 3.4: *Out-of-sample probabilities of being in a downturn episode with the ARCH specification. The dashed red line is the probability from macroeconomic variables only whereas the black solid line is the probability from macro variables and asset swap spreads.*

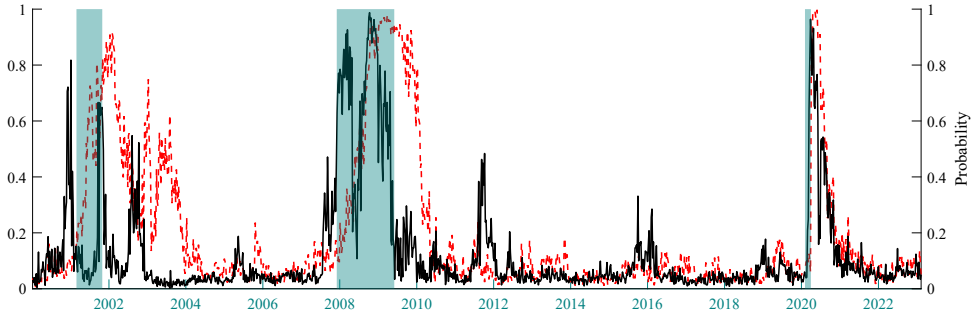

Figure 3.5: *Out-of-sample probabilities of being in a downturn episode with the GARCH specification. The dashed red line is the probability from macroeconomic variables only whereas the black solid line is the probability from macro variables and asset swap spreads.*

3.8. Asset allocation strategies based on signals extracted

One of a the well-known features of financial markets is to follow closely the developments of the business cycles as phenomena such as fly-to-quality reactions and forward looking valuations tend to impose a specific temporality in the market sentiment about real economy phases. A vast strand of literature has focused on the links between real business conditions and stock price variations, among others McQueen and Roley (1993) and more recently Kroencke (2022), Heinlein and Lepori (2022). Markets usually react in a contemporaneous manner to the downturn, forward earnings for equity markets being revised and investors looking for more secure assets. This bridges to fundamental valuation as exposed by Shiller et al. (1981) and Campbell and Shiller (1988) discounted dividends models. The markets display an interesting behavior when it comes to the recovery phases. In the past major economic downturns one can observe the a rebound in the risky assets classes before the end of main street downturn. This fact is depicted in Figure 3.6. The expectation component in the equity valuation plays a major role as market participants revise gradually the future earnings and dividends around the recession exit date .

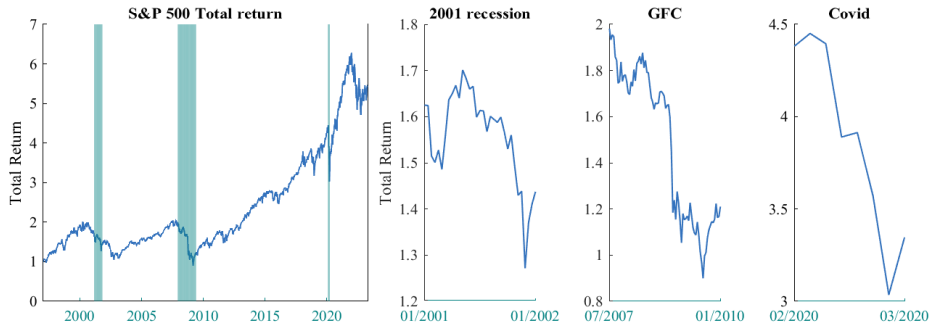

Figure 3.6: *S&P 500 Cumulative Total Return and selected economic downturns*

We use the filtered weekly macro signals obtained in Section 3.7 to gauge the benefits of using asset swap spreads as real-time business cycle phase assessor in asset allocation. We develop and backtest a strategy based on two securities, a risky one, the equity indices S&P 500 for the US and

3M deposit rate as risk-free asset in Dollar. We define the weight of the asset *equity* and *cash* at the end of a given week t as follows:

$$w_t^{equity} = 1 - P(S_t = 1 \mid I_t) \quad w_t^{cash} = P(S_t = 1 \mid I_t) \tag{3.10}$$

The bigger the probability of recession the lower the exposure to the risky asset. The underlying intuition is based on Figure 3.7. We show the total return of the equity indices and the cash holding from January 2000 onwards as well as a hypothetical strategy built upon the recession dates produced by the NBER. Whenever a recession occurs, the weight of the risky asset in the portfolio is set to 0 and the weight of cash is set to 1. This is a typical insurance-based allocation where the investor discards his/her exposition to the risky asset. This strategy is considered hypothetical as the NBER dating committee produces ex-post recession dates (determinations can take between 4 and 21 months). The practitioner does not observe in real-time the downturn dated. Avoiding the recession-induced drawdown and being able to catch-up the recovery phase is key for market performances as highlighted by the Figure 3.7. We thus track the macroeconomic environment by the use of our recession signals from the two competitive models implemented on the two different types of datasets. We compare the performances of the strategies through annualised returns and Sharpe ratios[3] (Sharpe (1994)) we want to maximize, annualised volatility and annualised maximum drawdown we seek to reduce. The exercise is also augmented by the same descriptive statistics computed on weekly rolling windows ranging from 1 to 10 years portfolio holding periods to mitigate the entry point impact in the backtest exercise. The end of week prices used are the Friday ones as the impact of the economic news releases embedded in the Employment Situation Summary produced by the BLS is fully incorporated in the prices of ASW spreads and S&P 500. The allocation rule defined in (3.10) defines a dynamic allocation rule rebalancing the portfolio at the end of each week. We assume in our backtest exercise transaction costs of 2 basis points for the risky asset and none for the risk-free securities. Finally, the backtest is carried out on a weekly basis from 7th January 2000 to 24th February 2023.

Figure 3.7: *Total return of the securities used in the allocation strategy*

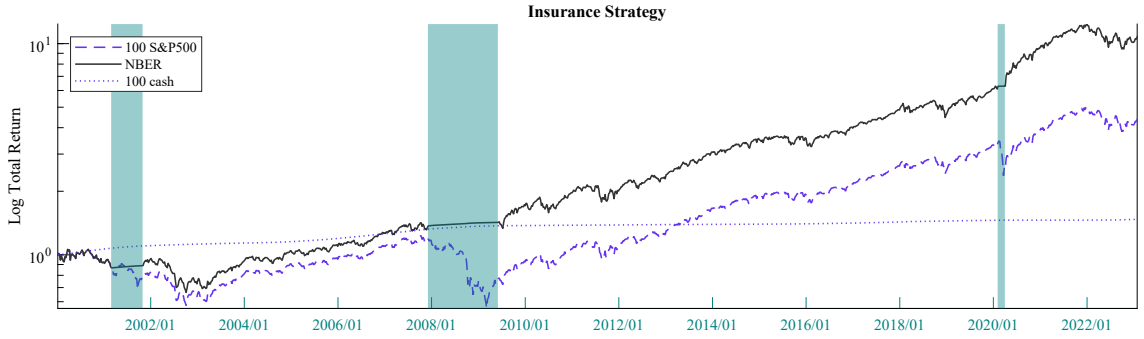

[3]The Sharpe ratio is defined in our case as the difference between the return of the strategy and the risk-free asset return divided by the volatility of the strategy

We denote $\boldsymbol{w_t} = [w_t^{equity}, w_t^{cash}]$ and the return of each asset $\boldsymbol{r_t} = [r_t^{equity}, r_t^{cash}]$. The weekly total return of a specific asset a, is given by $r_t^a = (P_t^a/P_{t-1})^a - 1$, P_t^a being the price of asset a at time t. The strategy s return at time t, $r_{t,s}$ is given by $\boldsymbol{w_{t-1}r_t'}$. Results of the backtest exercises are reported in Table 3.3. We compare the allocation strategies to three benchmarks : the hypothetical NBER categorical allocation, the constant holding of 100% of equity and 100% holding of cash. The reported statistics shed light on the capability of the datasets composed of both hard data and ASW spreads (M & F) to perform very well in terms of risk-adjusted return maximization either on a annualised basis or on portfolio holding rolling windows from one to ten years. This is true compared to datasets incorporating only macro data (M) Secondly, the strategies beat their benchmarks of holding 100% of the risky asset both from return perspective and volatility minimization. The NBER remains the best strategy but given only as theoretical benchmark as we do not observe the recession in real-time. Log cumulative returns are depicted in Figure 3.8. On 23 years of weekly backtest, the hard macro data and ASW spread specifications are the best, the ARCH extension being slightly the best.

Table 3.3: *Performances of Portfolios*

	M & F ARCH	M ARCH	**M & F GARCH**	M GARCH	100 S&P500	NBER	100 Cash
Ann. Return	**7.3%**	6.4%	**6.9%**	6.1%	6.5%	10.7%	1.7%
Ann. Vol	**15.0%**	14.2%	**14.7%**	14.3%	18.1%	14.6%	
Ann. Sharpe	**0.37**	0.33	**0.36**	0.31	0.26	0.61	
Ann. Max DD	**46.7%**	38.3%	**48.1%**	40.4%	54.7%	37.5%	
1 Year Av. Return	**8.8%**	7.5%	**8.4%**	7.2%	8.3%	12.2%	1.6%
1 Year Av. Volatility	**13.9%**	12.9%	**13.6%**	12.9%	16.3%	13.2%	
1 Year Av. Sharpe	**0.52**	0.46	**0.50**	0.44	0.42	0.81	
1 Year Av. Max DD	**12.0%**	11.0%	**11.7%**	11.2%	14.3%	9.8%	
2 Year Av. Return	**8.9%**	7.7%	**8.6%**	7.6%	8.1%	12.3%	1.6%
2 Year Av. Volatility	**13.8%**	12.9%	**13.5%**	13.1%	16.5%	13.3%	
2 Year Av. Sharpe	**0.53**	0.47	**0.52**	0.46	0.39	0.81	
2 Year Av. Max DD	**16.1%**	14.9%	**15.7%**	15.2%	20.2%	12.8%	
5 Year Av. Return	**9.4%**	8.3%	**9.2%**	8.3%	7.5%	11.1%	1.7%
5 Year Av. Volatility	**13.6%**	12.3%	**13.1%**	12.5%	16.6%	13.0%	
5 Year Av. Sharpe	**0.57**	0.53	**0.57**	0.52	0.35	0.72	
5 Year Av. Max DD	**23.1%**	18.2%	**22.0%**	18.6%	31.4%	16.8%	
10 Year Av. Return	**9.7%**	7.7%	**9.4%**	7.8%	7.0%	11.5%	1.7%
10 Year Av. Volatility	**14.2%**	12.5%	**13.5%**	12.8%	18.1%	13.3%	
10 Year Av. Sharpe	**0.56**	0.48	**0.57**	0.48	0.29	0.74	
10 Year Av. Max DD	**31.7%**	22.5%	**28.9%**	22.7%	49.9%	20.9%	

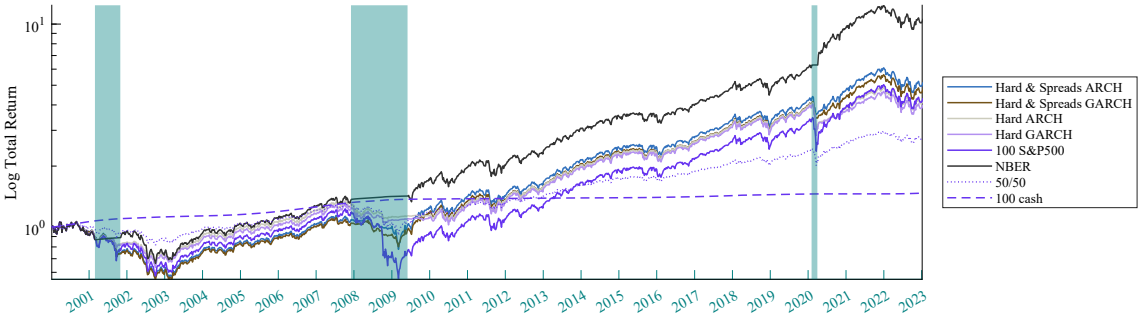

Figure 3.8: *Total return of the competitive strategies based on defined information sample and models specifications*

Taking into account the economic regime specification is of high interest for practitioners. We observe nonetheless the lag associated with the economic downturn detection using only macroeconomic vintaged data on a weekly basis. This fact is depicted in the Figures 3.4 and 3.5. The strategies integrating spread data to the macro information set tend to be more reactive during contraction episodes. It allows for a timely rebalancing towards the risky asset at the very end of recessionary episode as the ASW market already prices in the exit of the downturn episode. This is shown by the Figures 3.14 and 3.15 during the Great Financial Crisis and the Covid recession. We focus on calendar years returns during recessions in Table 3.4. The strategy based on signals incorporating ASW spreads and hard macro data (M & F) are the ones enabling to limit average drawdown compared to the strategies incorporating macro data only (M). Moreover the specification combining the datasets beat the 100% holding S&P500 providing a robust hedging solution. Worth to be noted is the capacity of the ARCH-extension to beat on average the 100% cash holding strategy. NBER is once again put as theoretical benchmark as this is the allocation rule our competing strategies are supposed to mimic.

Table 3.4: *Yearly returns during macroeconomic downturns years*

	2001	2008	2009	2020	Average
M & F ARCH	**-18.4%**	**-9.2%**	**26.5%**	**10.8%**	**2.4%**
M ARCH	-9.7%	-12.7%	2.4%	-3.2%	-5.8%
M & F GARCH	**-19.5%**	**-12.7%**	**29.2%**	**8.4%**	**1.4%**
M GARCH	-10.6%	-12.6%	3.5%	-4.3%	-6.0%
100% S&P500	-10.7%	-39.0%	31.5%	16.1%	-0.5%
NBER	2.7%	3.0%	21.3%	53.8%	20.2%
100% cash	3.7%	3.0%	0.7%	0.2%	1.9%

We focus on calendar years returns during expansion periods in Table 3.5. On average combining macro and financial data (M & F) does not hamper yearly returns significantly compared to holding a constant 100% weight in the risky asset. The GARCH extension even yield similar returns with regards to the benchmarks. This validates the idea that the insurance premium is very low during macroeconomic expansions periods.

Table 3.5: *Yearly returns during years of macroeconomic expansion*

	2000	2002	2003	2004	2005	2006	2007	2010	2011	2012
M & F ARCH	-4.3%	-22.6%	26.4%	12.0%	4.6%	15.3%	4.8%	12.4%	0.4%	13.1%
M ARCH	-4.7%	-23.1%	26.5%	11.9%	4.4%	15.4%	3.6%	12.6%	1.3%	12.8%
M & F GARCH	-6.4%	-14.3%	23.5%	12.1%	4.2%	15.1%	5.9%	12.8%	3.2%	13.8%
M GARCH	-6.8%	-16.1%	23.9%	11.9%	3.9%	15.3%	5.8%	12.9%	3.2%	13.5%
100 S&P500	-7.4%	-23.0%	26.8%	12.1%	4.8%	15.5%	6.1%	13.4%	2.1%	13.8%
NBER	-7.4%	-23.0%	26.8%	12.1%	4.8%	15.5%	8.1%	13.4%	2.1%	13.8%
100 cash	6.5%	1.7%	1.1%	1.5%	3.5%	5.1%	5.3%	0.4%	0.3%	0.4%

	2013	2014	2015	2016	2017	2018	2019	2021	2022	Average
M & F ARCH	33.0%	15.4%	0.2%	10.1%	21.2%	-4.7%	31.2%	29.1%	-18.6%	**9.4%**
M ARCH	33.2%	15.3%	0.1%	9.7%	21.3%	-5.1%	31.0%	29.2%	-18.3%	9.3%
M & F GARCH	31.7%	15.2%	0.7%	10.2%	20.8%	-5.2%	31.2%	27.1%	-17.0%	**9.7%**
M GARCH	32.2%	15.3%	0.5%	10.3%	20.8%	-5.1%	31.3%	25.1%	-17.4%	9.5%
100 S&P500	33.4%	15.4%	0.8%	10.6%	21.4%	-5.1%	32.3%	29.3%	-17.8%	9.7%
NBER	33.4%	15.4%	0.8%	10.6%	21.4%	-5.1%	32.3%	29.3%	-17.8%	9.8%
100 cash	0.2%	0.2%	0.4%	0.8%	1.2%	1.0%	0.7%	0.0%	0.8%	1.6%

Given that first moments of the statistics depicted in Table 3.3 for the rolling window holding periods are auto-correlated, we now focus on empirical cumulative Sharpe Ratios and Returns distributions. The cumulative distributions of the Sharpe ratios are plotted in Figure 3.9 whereas returns cumulative distributions are displayed in Appendix 3.11. The 10 year rolling holding period portfolio shows the strategies embedding ASW spreads and macro data yields significantly higher Sharpe ratios as the cumulative distribution curves are below the competing specifications and benchmarks on the whole support. For the 5Y rolling holding period, only 12% of the distribution is below the competing strategies and 5% below the 100% equity portfolio Sharpe ratios. Looking at the 1 to 2 year holding periods the curves are more alike. Regarding the returns cumulative distributions presented in Figure 3.16, the same conclusion holds: on 5 to 10 year rolling holding periods, the specification incorporating financial and macro data yield better returns on a vast majority of the support. Short-term holding periods are more similar in the pattern behaviour. This brings us to consider Fleming et al. (2003) approach in order to measure the economic utility for an investor to detain a given portfolio. This economic utility has ties with the mean-variance and the quadratic utility frameworks. The realized weekly utility generated by a strategy s is given by :

$$U(r_{t,s}) = W_0 \left((1 + r_t^f + r_{t,s}) - \frac{\gamma}{2(1+\gamma)} (1 + r_t^f + r_{t,s})^2 \right) \tag{3.11}$$

W_0 is the initial wealth invested, r_t^f the 3-month deposit return, $r_{t,s}$ the portfolio return and γ a constant aversion parameter. We quantify the value of a strategy compared to another one by defining a constant Δ which equalizes :

$$\sum_{t=1}^{T} U(r_{t,s1}) = \sum_{t=1}^{T} U(r_{t,s2} - \Delta)$$

The constant Δ is defined as the maximum performance fee an investor would accept to pay for

switching from strategy $s1$ to $s2$ under the hypothesis that he is indifferent between both. The strategy $s2$ is more valuable for the investor when the Δ is high. Table 3.6 and Table 3.7 display the Δs associated to 1 year and 2 year rolling holding portfolios. The tables depict the maximum fee an investor would agree to pay for switching from the strategies at a given aversion coefficient γ in columns towards the strategy in line, namely from strategies incorporating only hard macro data (M) or benchmarks of holding 100% equity or 100% cash to strategies incorporating both ASW spreads data and hard macro data (M&F). Table 3.6 shows that no matter the aversion coefficient γ, an investor is willing to switch from competing specifications only based on hard macro data or the 100% equity portfolio towards macro and ASW spreads combined, and more specifically on the M&F ARCH extension. An investor with a low aversion profile $\gamma = 1$ will also be eager to switch from cash to the alternative strategies. Nevertheless, an investor with a high aversion profile will always prefer cash with regards to other strategies. Table 3.7, for a 2-year rolling holding period displays exactly the same conclusion.

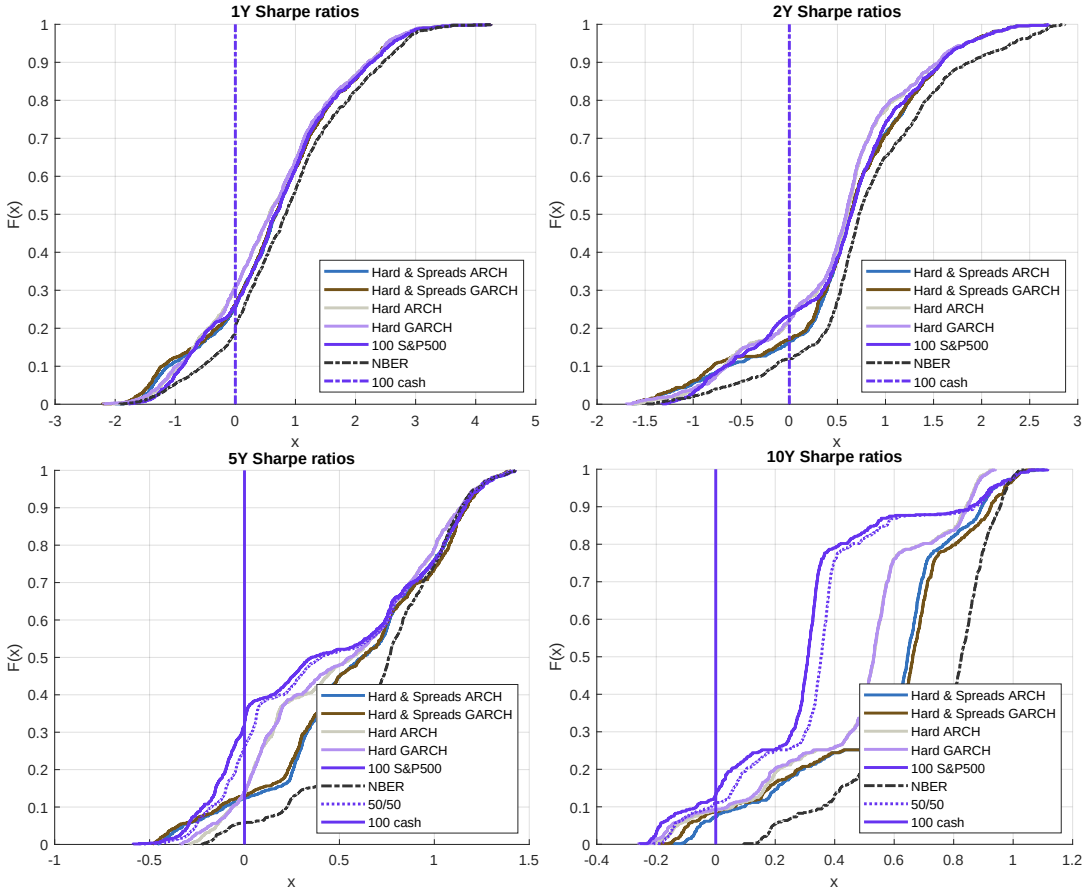

Figure 3.9: *Cumulative distribution functions of rolling window Sharpe from 1Y to 10Y holding horizons*

Table 3.6: *1 Year rolling* Δs

	M ARCH		M GARCH		S&P		Cash	
γ	1	10	1	10	1	10	1	10
M&F ARCH	1.18%	0.23%	1.39%	0.50%	1.09%	6.93%	7.36%	-2.03%
M&F GARCH	0.82%	0.36%	1.02%	1.02%	0.74%	7.19%	7.01%	-1.87%

Table 3.7: *2 Year rolling* Δs

	M ARCH		M GARCH		S&P		Cash	
γ	1	10	1	10	1	10	1	10
M&F ARCH	1.05%	0.02%	1.18%	0.29%	1.15%	6.79%	7.35%	-1.87%
M&F GARCH	0.71%	0.22%	0.84%	0.84%	0.80%	7.05%	7.01%	-1.66%

3.9. Conclusion

Tracking business cycle phases in a real time fashion usually induces difficulties for practitioners who want to develop suitable asset allocation strategies. Macroeconomic data are indeed characterised by lags and asynchronous releases which make a real-time tracking of downturn episodes challenging. The asymmetry and heterogeneity of adverse economic phases advocate for the use of non-linear models to properly identify them. Markov Switching Dynamic Factor models (MS-DFM) have shown to be a convenient class of models to handle the latter features. To mitigate the delay in the identification of recessionary episodes due to hard macro data release schedules this work shows the usefulness for investors willing to track the US business cycles phases closely to add asset swap (ASW) spreads. More specifically, ASW spreads pricing capture asynchronous macroeconomic data flows by continuously updating probabilities of default. We narrow the sentiment in the credit market, measured by a broad grade buckets-based spreads contraction/widening, to the contemporaneous state of the economy in a real-time fashion. To fulfill this bridging exercise we take into account the co-movement between ASW spreads and real economic variables used in the literature. We thus track on a weekly basis the occurrence of macroeconomic downturn episodes. This work sheds light on the capacity of MS-DFMs incorporating both macroeconomic variables and ASW spreads to accurately identify recessions both in-sample and out-of-sample. These adverse economic episodes usually trigger ample price variations in the equity markets as risk aversion gains investors. We put forward the need for investors who want to build insurance-based strategies to use the real-time downturn probabilities as an allocation rule between S&P500 and cash. This Chapter further shows that implementing strategies based on the new data sample specification consistently outperforms a 100% S&P500 portfolio as well as creates economic utility for the investor.

3.10. Appendix

3.10.1. Sectoral coverage of ICE BofA Indices

Sectors	Financial Services	Insurance	Automotive
Subsectors	Banking	Life Insurance	Auto Loans
	Brokerage	Monoline Insurance	Auto Parts & Equipment
	Cons/Comm/Lease Financing	Multi-Line Insurance	Automakers
	Investments & Misc Financial Services	P&C	

Sectors	Consumer Goods	Energy	Healthcare
Subsectors	Beverage	Energy - Exploration & Production	Health Services
	Food - Wholesale	Integrated Energy	Medical Products
	Personal & Household Products	Oil Field Equipment & Services	Pharmaceuticals
	Tobacco	Oil Refining & Marketing	

Sectors	Basic Industry	Capital Goods	Leisure
Subsectors	Building & Construction	Aerospace/Defense	Gaming
	Building Materials	Diversified Capital Goods	Hotels
	Chemicals	Machinery	Recreation & Travel
	Forestry/Paper	Packaging	
	Metals/Mining Excluding Steel		
	Steel Producers/Products		

Sectors	Media	Real Estate	Retail
Subsectors	Advertising	RealEstate Dev & Mgt	Food & Drug Retailers
	Cable & Satellite TV	REITs	Restaurants
	Media - Diversified		Specialty Retail
	Media Content		

Sectors	Telecommunications	Services	Technology & Electronics
Subsectors	Telecom - Satellite	Environmental	Electronics
	Telecom - Wireless	Support-Services	Software/Services
	Telecom - Wireline Integrated & Services		Tech Hardware & Equipment

Sectors	Transportation	Utilities
Subsectors	Air Transportation	Electric-Distr/Trans
	Rail	Electric-Generation
	Transport Infrastructure/Services	Electric-Integrated
	Trucking & Delivery	Non-Electric Utilities

3.10.2. Priors

This section describes the priors used for the distributions of the parameter vector $\boldsymbol{\vartheta}$.
λ_1 is set to one for identification purposes. For all $j = 2, \ldots, m$, we use the following prior to sample λ_j the j-th element of the factor loading matrix $\boldsymbol{\Lambda}$ in (3.2)

$$\lambda_j \sim \mathcal{N}(a_j, A_j) \tag{3.12}$$

where hyperparameters are set to $a_j = 0$ and $A_j = 0.1$. To sample the parameters linked to the residuals $u_{j,t}$ in (3.3), we use the following priors, for $l = 1, 2$,

$$\begin{array}{rll} \psi_{j,l} \sim & \mathcal{N}(\pi, \Pi) & \pi = 0, \Pi = 0.1 \\ \sigma^2_{e,j} \sim & IG(\nu_i, Z_i) & \nu_i = 2, Z_i = 1 \end{array} \tag{3.13}$$

where IG denotes the inverse-gamma distribution. Additionally, independent beta distributions can be used as conjugate prior for each transition probability

$$\pi(q, p) \propto q^{u_{00}}(1-q)^{u_{01}} p^{u_{11}}(1-p)^{u_{10}} \tag{3.14}$$

As in Doz et al. (2020), we put an informative prior and set $u_{00} = 470, u_{01} = 9, u_{10} = 9, u_{11} = 90$ in order to take into account the relative persistence of each of the regimes as observed on macroeconomic data. The prior for the Markov-switching intercept in equation (3.4) is given by :

$$\boldsymbol{\mu} = (\mu_0, \mu_1)' \sim \mathcal{N}(\alpha^*, A^*) \tag{3.15}$$

with $\alpha^* = (.3, -.3)'$ and $A^* = \text{diag}(0.04, 0.04)$. We acknowledge that, in the spirit of Leiva-Leon et al. (2020), relatively tight priors are used for identification purposes. The informativeness brought by the first moment is indeed needed to discriminate between the regimes over the parameters space. The prior for the autoregressive parameter ϕ in equation (3.4) is given by

$$\phi \sim \mathcal{N}(\alpha, A) \tag{3.16}$$

where $\alpha = 0$, $A = 0.1$. In the case of a MS-DFM-ARCH, we use the following prior for the vector $\boldsymbol{\theta}^{(\text{ARCH})} = (\omega, \alpha)$

$$\log \boldsymbol{\theta}^{(\text{ARCH})} \sim \mathcal{N}(\theta_0^{(\text{ARCH})}, V_\theta) \mathbb{1}(\alpha < 1)$$

$\boldsymbol{\theta}^{(\text{ARCH})}$ thus follows a truncated log-normal distribution with the stationarity restriction that $\alpha < 1$. We set the hyperparameters to $\theta_0^{(\text{ARCH})} = \log(1, 0.5)$ and $V_\theta = \text{diag}(1, 1)$. In the case of MS-DFM-GARCH, we use the following prior for the vector $\boldsymbol{\theta}^{(\text{GARCH})} = (\omega, \alpha, \beta)$

$$\log \boldsymbol{\theta}^{(\text{GARCH})} \sim \mathcal{N}(\theta_0^{(\text{GARCH})}, V_\theta) \mathbb{1}(\alpha + \beta < 1)$$

Similarly to the ARCH(1) specification, $\boldsymbol{\theta}^{(\text{GARCH})}$ follows a truncated log-normal distribution with the adapted stationarity restriction $\alpha + \beta < 1$. Hyperparameters are set to $\theta_0^{(\text{GARCH})} = \log(1, 0.5, 0.4)$ and $V_\theta = \text{diag}(1, 1, 1)$. Note that in both cases, the priors are relatively non-informative.

3.10.3. Bayesian Estimation

Let $\boldsymbol{z}^{(T)} = \{\boldsymbol{z}_1, ..., \boldsymbol{z}_T\}$ the unobserved state, $\boldsymbol{y}^{(T)} = \{\boldsymbol{y}_1, ..., \boldsymbol{y}_T\}$ the observed data and $S^{(T)} = \{S_1, ..., S_T\}$ the first order Markov-Chain. We describe the Gibbs sampler steps based on Kim and Nelson (1999) and follow their notations. The Gibbs sampler consists of iterating between the three following steps sequentially.

3.10.4. Generation of the state vector

The joint distribution of $\boldsymbol{z}^{(T)}$, given $\boldsymbol{y}^{(T)}$, $S^{(T)}$ and $\boldsymbol{\vartheta}^{(.)}$ can be defined as

$$p(\boldsymbol{z}^{(T)} \mid \boldsymbol{y}^{(T)}, S^{(T)}, \boldsymbol{\vartheta}^{(.)}) = p(\boldsymbol{z}_T \mid \boldsymbol{y}^{(T)}, S^{(T)}, \boldsymbol{\vartheta}^{(.)}) \prod_{t=1}^{T-1} p(\boldsymbol{z}_t \mid \boldsymbol{y}^{(t)}, S^{(t)}, \boldsymbol{\vartheta}^{(.)}, \boldsymbol{z}_{t+1})$$

which boils down to generating $\boldsymbol{z}_t$ for $t = T, T-1, ..., 1$ from

$$\begin{aligned} &\boldsymbol{z}_T \mid \boldsymbol{y}^{(T)}, S^{(T)}, \boldsymbol{\vartheta}^{(.)} \sim \mathcal{N}(\boldsymbol{z}_{T|T}, \boldsymbol{V}_{T|T}) \\ &\boldsymbol{z}_t \mid \boldsymbol{y}^{(t)}, S^{(t)}, \boldsymbol{z}_{t+1}, \boldsymbol{\vartheta}^{(.)} \sim \mathcal{N}(\boldsymbol{z}_{t|t,\boldsymbol{z}_{t+1}}, \boldsymbol{V}_{t|t,\boldsymbol{z}_{t+1}}) \end{aligned} \tag{3.17}$$

where $\boldsymbol{z}_{t|t} = E(\boldsymbol{z}_t \mid \boldsymbol{y}^{(t)})$ and $\boldsymbol{V}_{t|t} = Var(\boldsymbol{z}_t \mid \boldsymbol{y}^{(t)})$ for $t = 1, ..., T$. In equation (3.17), $\boldsymbol{z}_T \mid \boldsymbol{y}^{(T)}, S^{(T)}, \boldsymbol{\vartheta}^{(.)}$ can be generated using the Multi-move Gibbs sampling introduced by Carter and Kohn (1994) as follows

1. We use the Kalman filter to obtain $\boldsymbol{z}_{t|t}$ and $\boldsymbol{V}_{t|t}$ for $t = 1, ..., T$. The last iteration of the filter gives $\boldsymbol{z}_{T|T}$ and $\boldsymbol{V}_{T|T}$ which are then used to generate $\boldsymbol{z}_T$.

2. For $t = T-1, T-2, ..., 1$, $\boldsymbol{z}_{t|t}$ and $\boldsymbol{V}_{t|t}$, $\boldsymbol{z}_{t+1}$ can be considered as an incremental vector of observations in the system. The distribution $p(\boldsymbol{z}_t \mid \boldsymbol{y}^{(T)}, S^{(t)}, \boldsymbol{\vartheta}^{(.)}, \boldsymbol{z}_{t+1})$ is then deduced from the Kalman smoother. From equation (3.7), updating equation are then given by

$$\begin{aligned} \boldsymbol{z}_{t|t,\boldsymbol{z}_{t+1}} &= \boldsymbol{z}_{t|t} + \boldsymbol{V}_{t|t}\boldsymbol{\Xi}\tilde{\boldsymbol{\zeta}}_t / R_t \\ \boldsymbol{V}_{t|t,\boldsymbol{z}_{t+1}} &= \boldsymbol{V}_{t|t} - \boldsymbol{V}_{t|t}\boldsymbol{\Xi}'\boldsymbol{\Xi}\boldsymbol{V}'_{t|t} / R_t \end{aligned}$$

   where $\tilde{\boldsymbol{\zeta}}_t = \boldsymbol{z}_{t+1} - \boldsymbol{\delta}_{S_{t+1}} - \boldsymbol{\Xi}\boldsymbol{z}_{t|t}$ and $R_t = \boldsymbol{\Xi}\boldsymbol{V}_{t|t}\boldsymbol{\Xi}' + \sigma^2_{t+1}$.

3.10.4.1. Generation of the Markov Chain

Once $\boldsymbol{z}^{(T)}$ has been simulated, given $\boldsymbol{\vartheta}^{(.)}$, the Markov Chain $S^{(T)}$ can be generated from the following distribution

$$\begin{aligned} p(S^{(T)} \mid \boldsymbol{y}^{(T)}, \boldsymbol{z}^{(T)}, \boldsymbol{\vartheta}^{(.)}) &= p(S_T \mid \boldsymbol{y}^{(T)}, \boldsymbol{z}^{(T)}, \boldsymbol{\vartheta}^{(.)}) \prod_{t=1}^{T-1} p(S_t \mid \boldsymbol{y}^{(t)}, \boldsymbol{z}^{(t)}, S_{t+1}, \boldsymbol{\vartheta}^{(.)}) \\ &= p(S_T \mid \boldsymbol{z}^{(T)}, \boldsymbol{\vartheta}^{(.)}) \prod_{t=1}^{T-1} p(S_t \mid \boldsymbol{z}^{(t)}, S_{t+1}, \boldsymbol{\vartheta}^{(.)}) \end{aligned}$$

as the distribution of $S^{(T)}$ is orthogonal to $\boldsymbol{y}^{(T)}$ given $\boldsymbol{z}^{(T)}$. We can thus obtain conditional draws for $S^{(T)}$ as follows

1. We use the Hamilton (1989) filter on (3.4) to generate $p(S_t \mid \boldsymbol{z}^{(t)}, \boldsymbol{\vartheta}^{(.)})$ for $t = 1, 2, ..., T$ and save them. The last iteration gives $p(S_T \mid \boldsymbol{z}^{(T)}, \boldsymbol{\vartheta}^{(.)})$ from which we get S_T.

2. To draw S_t given $\boldsymbol{z}^{(T)}$ and S_{t+1}, for $t = T-1, T-2, ..., 1$ the following result is used

$$p(S_t \mid \boldsymbol{z}^{(t)}, S_{t+1}, \boldsymbol{\vartheta}^{(.)}) = \frac{p(S_{t+1} \mid S_t) p(S_t \mid \boldsymbol{z}^{(t)}, \boldsymbol{\vartheta}^{(.)})}{p(S_{t+1} \mid \boldsymbol{z}^{(t)}, \boldsymbol{\vartheta}^{(.)})} \propto p(S_{t+1} \mid S_t) p(S_t \mid Z^{(t)}, \boldsymbol{\vartheta}^{(.)})$$

   where $p(S_{t+1} \mid S_t)$ is the transition probability in $\boldsymbol{\vartheta}^{(.)}$ and $p(S_t \mid \boldsymbol{z}^{(t)}, \boldsymbol{\vartheta}^{(.)})$ is obtained form the values saved in the previous step.

3. The last step consists in drawing from

$$Pr(S_t = 1 \mid \boldsymbol{z}^{(t)}, S_{t+1}, \boldsymbol{\vartheta}^{(.)}) = \frac{p(S_{t+1} \mid S_t = 1) p(S_t = 1 \mid \boldsymbol{z}^{(t)}, \boldsymbol{\vartheta}^{(.)})}{\sum_{j=0}^{1} p(S_{t+1} \mid S_t = j) p(S_t = j \mid \boldsymbol{z}^{(t)}, \boldsymbol{\vartheta}^{(.)})}$$

   where S_t is drawn from a uniform distribution $S_t \sim \mathcal{U}(0, 1)$. If the generated number is smaller than $Pr(S_t = 1 \mid S_{t+1}, \boldsymbol{z}^{(t)}, \boldsymbol{\vartheta}^{(.)})$, $S_t = 1$, otherwise $S_t = 0$.

3.10.4.2. Generation of the parameters vector

We now turn to the generation of draws for the vector of parameters. To do so, we will sequentially draw components of the $\boldsymbol{\vartheta}$ vector as follows.
We obtain conditional draws for the transition probabilities p and q following Albert and Chib (1993). In particular, given $S^{(T)}$ and the initial state, we denote the sum of transitions from the state $S_{t-1} = i$ to $S_t = j$ by n_{ij}, the log-likelihood is given by

$$L(q, p) = q^{n_{00}} (1-q)^{n_{01}} p^{n_{11}} (1-p)^{n_{10}}.$$

By combining the likelihood function and the conjugate priors presented in the previous section, from equation (3.14), we get the conditional distributions of (p, q) as the product of the independent beta distributions from which we generate p and q as

$$\begin{aligned} q \mid S^{(T)} &\sim \text{Beta}(u_{00} + n_{00}, u_{01} + n_{01}) \\ p \mid S^{(T)} &\sim \text{Beta}(u_{11} + n_{11}, u_{10} + n_{10}). \end{aligned}$$

Given $\boldsymbol{y}^{(T)}$ and $f^{(T)}$, we can rewrite equation-by-equation equation (3.2) with

$$y_{j,t}^* = \lambda_j f_{j,t}^* + e_{j,t}$$

for $j = 2, \ldots, m$, where $y_{j,t}^*$ and $f_{j,t}^*$ are the j-the respective components of

$$\begin{aligned} \boldsymbol{y}_t^* = &\quad \boldsymbol{y}_t - \bar{\boldsymbol{\psi}}_1 \circ \boldsymbol{y}_{t-1} \\ \boldsymbol{f}_t^* = &\quad \boldsymbol{e}_m f_t - \bar{\boldsymbol{\psi}}_1 f_{t-1} \end{aligned} \tag{3.18}$$

with $\boldsymbol{e}_m$ denoting a vector of 1 of length m qnd $\bar{\boldsymbol{\psi}}_l = (\psi_{1,l}, \ldots, \psi_{m,l})$, $l = 1$ being the order of the AR specification in equation (3.3). From (3.12) and (3.18), we obtain conditional draws for λ_j from the posterior distribution

$$\mathcal{N}\left[\left(A_j^{-1} + \sigma_{e,j}^{-2} f_j^{*(T)'} f_j^{*(T)}\right)^{-1} \left(A_j a_j + \sigma_{e,j}^{-2} f_j^{*(T)'} y_j^{*(T)}\right), \left(A_j^{-1} + \sigma_{e,j}^{-2} f_j^{*(T)'} f_j^{*(T)}\right)^{-1}\right].$$

Given $\boldsymbol{y}^{(T)}$ and $f^{(T)}$, from (3.2) we can measure $\boldsymbol{u}^{(T)}$ and from equation (3.3) and the prior distribution (3.13), for all $j = 1, \ldots, m$, we can draw $\boldsymbol{\psi}_j$ from the posterior distribution

$$\mathcal{N}\left[\left(\boldsymbol{\Pi}_j^{-1} + \sigma_{e,j}^{-2} \boldsymbol{w}_j^{(T)'} \boldsymbol{w}_j^{(T)}\right)^{-1} \left(\boldsymbol{\Pi}_j^{-1} \boldsymbol{\pi}_j + \sigma_{e,j}^{-2} \boldsymbol{w}_j^{(T)'} u_j^{(T)}\right), \left(\boldsymbol{\Pi}_j^{-1} + \sigma_{e,j}^{-2} \boldsymbol{w}_j^{(T)'} \boldsymbol{w}_j^{(T)})^{-1}\right)\right]$$

where $\boldsymbol{w}_{j,t} = (u_{j,t-1}, u_{j,t-2})'$. Similarly, from the generated $\boldsymbol{\psi}_j$ and from (3.13), we can draw $\sigma_{e,j}^2$ from the posterior distribution

$$IG\left(\nu_j + \frac{T}{2}, Z_j + \frac{\left(u_j^{(T)} - \boldsymbol{\psi}_j' \boldsymbol{w}_j^{(T)}\right)' \left(u_j^{(T)} - \boldsymbol{\psi}_j' \boldsymbol{w}_j^{(T)}\right)}{2}\right).$$

Finally, we turn to the generation of $(\mu_0, \mu_1, \phi, \boldsymbol{\theta}^{(.)'})$. The parameters are drawn from the three full conditional distributions $p(\boldsymbol{\mu} \mid \boldsymbol{z}^{(T)}, S^{(T)}, \phi, \boldsymbol{\theta}^{(.)})$, $p(\phi \mid \boldsymbol{z}^{(T)}, S^{(T)}, \boldsymbol{\theta}^{(.)})$ and $p(\boldsymbol{\theta}^{(.)} \mid \boldsymbol{z}^{(T)}, S^{(T)}, \phi)$ sequentially. Since μ_{S_t} and ϕ appear in the conditional variance equation, those distributions are non-standard, as noted by Chan and Grant (2016), and Metropolis Hastings algorithms are required. Rewriting equation (3.4), we have

$$\frac{f_t - \phi f_{t-1}}{\sigma_t} = \frac{\mu_0(1 - S_t) + \mu_1 S_t}{\sigma_t} + \eta_t$$

Let us denote G_t^* the left-hand side of the above equation and Let us denote G_t^* the left-hand side of the above equation and

$$Q^{*(T)} = \begin{bmatrix} 1 - S^{(T)} & S^{(T)} \end{bmatrix}$$

From the prior distribution (3.15), to sample $\boldsymbol{\mu}$, we use a multivariate Gaussian proposal :

$$\mathcal{N}\left[(A^{*-1} + Q^{*(T)\prime} Q^{*(T)})^{-1} (A^{*-1}\alpha + Q^{*(T)\prime} G^{*(T)}), (A^{*-1} + Q^{*(T)\prime} Q^{*(T)})^{-1}\right]$$

and only keep draws verifying $\mu_0 > \mu_1$. Rewriting again equation (3.4) yields

$$\frac{f_t - \mu_0(1 - S_t) - \mu_1 S_t}{\sigma_t} = \phi \frac{f_{t-1}}{\sigma_t} + \eta_t.$$

Denoting $\tilde{G}_t$ the left-hand side of the above equation and $\tilde{Q}_t$ the right-hand side. To sample ϕ we use a Gaussian proposal with mean $\bar{\phi}$ and variance V_ϕ given by

$$\begin{aligned} \bar{\phi} = &\quad (A^{-1} + \tilde{Q}'\tilde{Q})^{-1}(A^{-1}\alpha + \tilde{Q}'\tilde{G}) \\ V_\phi = &\quad (A^{-1} + \tilde{Q}'\tilde{Q})^{-1}. \end{aligned}$$

Only draws satisfying the stationarity condition $|\phi| < 1$ are kept. Finally to sample $\boldsymbol{\theta}^{(.)}$, we use a Gaussian proposal centered at the mode of $p(\boldsymbol{\theta}^{(.)} \mid \boldsymbol{z}^{(T)}, S_t, \phi)$ with covariance matrix set to be the outer product of the scores.

3.10.4.3. Posterior distributions of the parameters

Table 3.8: *ARCH MS-DFM model parameters with macro data only*

Variables	Parameters	Mean	Std
IP	λ	1	0
RS	λ	1.86	0.70
PI	λ	1.57	0.59
E	λ	1.91	0.72
IP	ψ	0.24	0.06
RS	ψ	-0.35	0.04
PI	ψ	-0.12	0.04
E	ψ	-0.01	0.06
IP	σ_e^2	0.54	0.17
RS	σ_e^2	0.47	0.05
PI	σ_e^2	0.68	0.04
E	σ_e^2	0.49	0.07
Factor			
	μ_1	-0.25	0.10
	μ_0	0.01	0.02
	ϕ	0.02	0.04
	ω	0.22	0.34
	α	0.59	0.09
	q	0.99	0.01
	p	0.91	0.02

Table 3.9: *GARCH MS-DFM model parameters with macro data only*

Variables	Parameters	Mean	Std
IP	λ	1	0
RS	λ	2.66	0.23
PI	λ	2.20	0.17
E	λ	2.68	0.21
IP	ψ	0.27	0.04
RS	ψ	-0.33	0.04
PI	ψ	-0.10	0.04
E	ψ	0.00	0.05
IP	σ_e^2	0.70	0.04
RS	σ_e^2	0.50	0.05
PI	σ_e^2	0.70	0.05
E	σ_e^2	0.53	0.08
Factor			
	μ_1	-0.20	0.04
	μ_0	0.00	0.01
	ϕ	0.01	0.03
	ω	0.01	0.00
	α	0.39	0.07
	β	0.16	0.10
	q	0.99	0.01
	p	0.91	0.03

Table 3.10: *ARCH MS-DFM model parameters with macro and spreads data*

Variables	Parameters	Mean	Std
IP	λ	1	0
RS	λ	1.17	0.60
PI	λ	1.52	0.55
E	λ	1.85	0.67
AAA	λ	0.01	0.14
AA	λ	-0.22	0.17
A	λ	-0.23	0.16
BBB	λ	-0.28	0.17
BB	λ	-0.19	0.17
B	λ	-0.10	0.16
CCC	λ	0.08	0.16
IP	ψ	0.24	0.06
RS	ψ	-0.33	0.04
PI	ψ	-0.13	0.04
E	ψ	-0.01	0.06
AAA	ψ	0.29	0.06
AA	ψ	0.26	0.05
A	ψ	0.29	0.06
BBB	ψ	0.29	0.06
BB	ψ	0.15	0.06
B	ψ	0.16	0.06
CCC	ψ	0.25	0.06
IP	σ_e^2	0.53	0.15
RS	σ_e^2	0.49	0.05
PI	$\sigma_e v$	0.67	0.04
E	σ_e^2	0.47	0.07
AAA	σ_e^2	0.91	0.08
AA	σ_e^2	0.93	0.07
A	σ_e^2	0.92	0.08
BBB	σ_e^2	0.92	0.08
BB	σ_e^2	0.98	0.08
B	σ_e^2	0.98	0.08
CCC	σ_e^2	0.94	0.08
Factor			
	μ_1	-0.23	0.10
	μ_0	0.01	0.02
	ϕ	0.02	0.04
	ω	0.27	0.37
	α	0.60	0.06
	q	0.98	0.01
	p	0.91	0.03

Table 3.11: *GARCH MS-DFM model parameters with macro and spreads data*

Variables	Parameters	Mean	Std
IP	λ	1	0
RS	λ	2.48	0.26
PI	λ	2.12	0.20
E	λ	2.56	0.24
AAA	λ	0.05	0.19
AA	λ	-0.23	0.22
A	λ	-0.23	0.23
BBB	λ	-0.29	0.23
BB	λ	-0.17	0.24
B	λ	-0.07	0.23
CCC	λ	0.18	0.22
IP	ψ	0.27	0.04
RS	ψ	-0.33	0.04
PI	ψ	-0.11	0.04
E	ψ	0.01	0.05
AAA	ψ	0.29	0.05
AA	ψ	0.25	0.05
A	ψ	0.27	0.06
BBB	ψ	0.27	0.06
BB	ψ	0.14	0.06
B	ψ	0.15	0.06
CCC	ψ	0.24	0.06
IP	σ_e^2	0.68	0.05
RS	σ_e^2	0.50	0.05
PI	σ_e^2	0.69	0.05
E	σ_e^2	0.52	0.08
AAA	σ_e^2	0.91	0.08
AA	σ_e^2	0.94	0.08
A	σ_e^2	0.93	0.08
BBB	σ_e^2	0.94	0.08
BB	σ_e^2	0.98	0.08
B	σ_e^2	0.98	0.08
CCC	σ_e^2	0.93	0.08
Factor			
	μ_1	-0.19	0.04
	μ_0	0.01	0.01
	ϕ	0.03	0.04
	ω	0.02	0.00
	α	0.46	0.10
	β	0.17	0.06
	q	0.99	0.01
	p	0.91	0.02

3.10.5. Specific downturn episodes week by week filtered probabilities

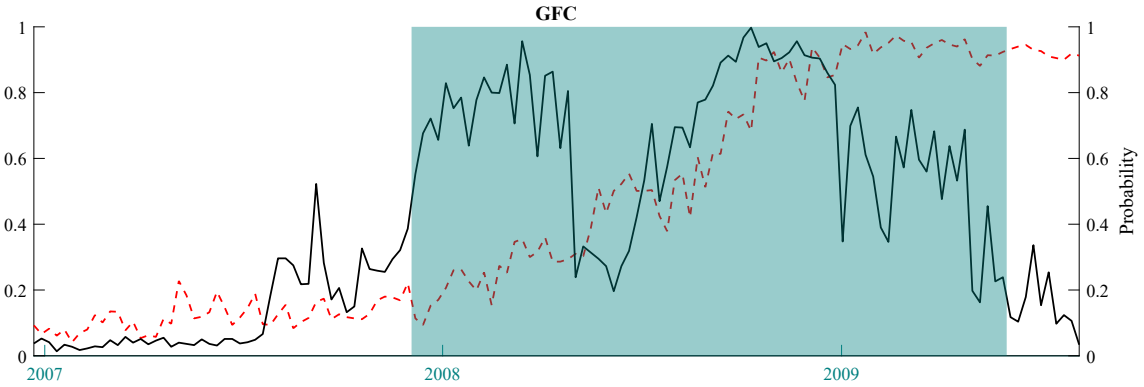

Figure 3.10: *Out-of-sample probabilities of being in a downturn episode with the ARCH specification. The dashed red line is the probability from macroeconomic variables only whereas the black solid line is the probability from macro variables and asset swap spreads.*

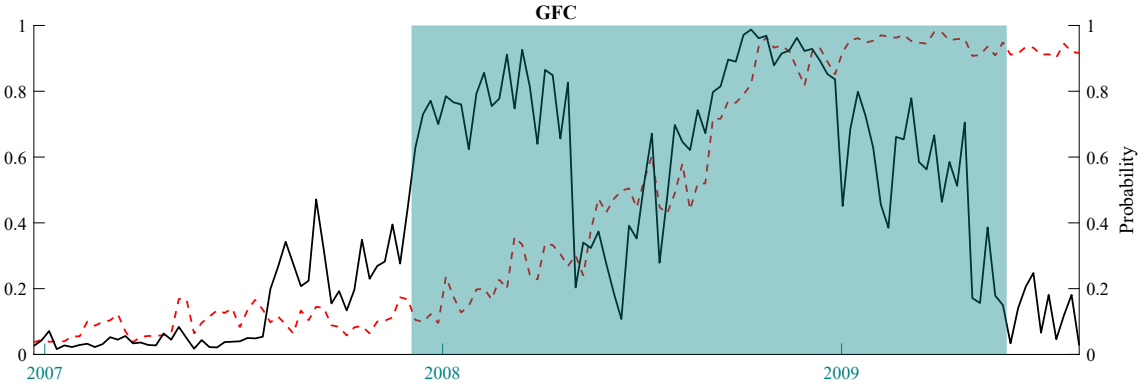

Figure 3.11: *Out-of-sample probabilities of being in a downturn episode with the GARCH specification. The dashed red line is the probability from macroeconomic variables only whereas the black solid line is the probability from macro variables and asset swap spreads.*

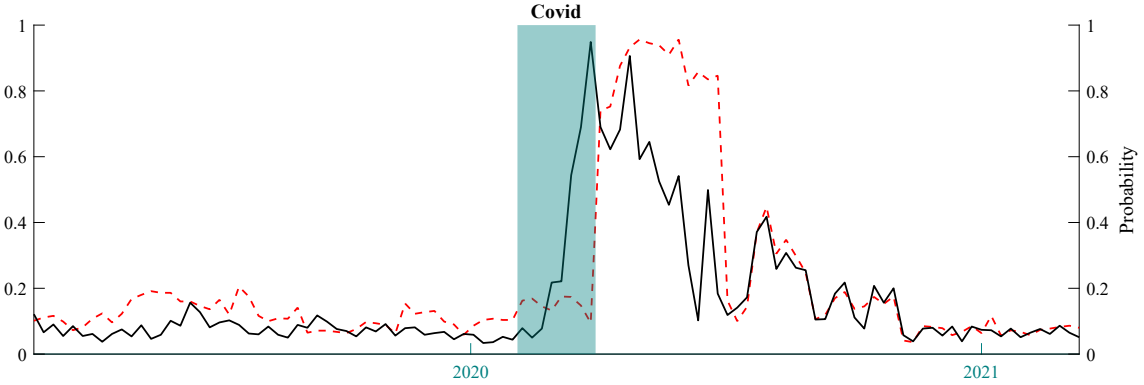

Figure 3.12: *Out-of-sample probabilities of being in a downturn episode with the ARCH specification. The dashed red line is the probability from macroeconomic variables only whereas the black solid line is the probability from macro variables and asset swap spreads.*

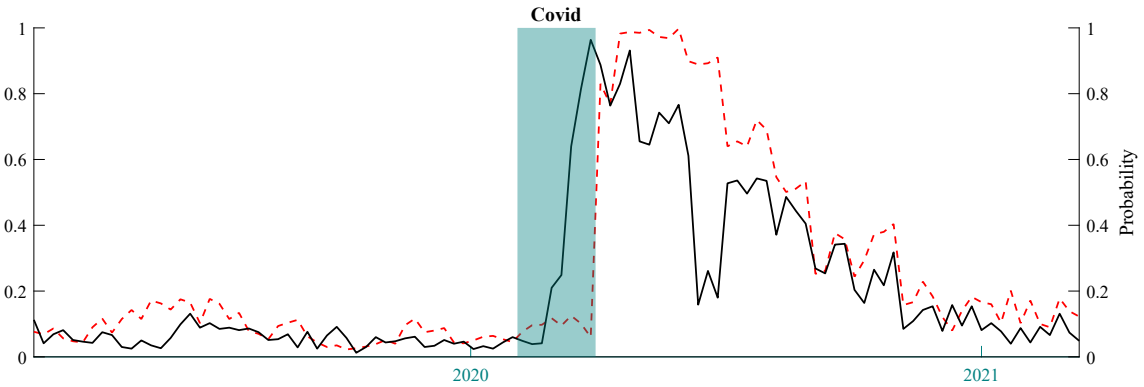

Figure 3.13: *Out-of-sample probabilities of being in a downturn episode with the GARCH specification. The dashed red line is the probability from macroeconomic variables only whereas the black solid line is the probability from macro variables and asset swap spreads.*

3.10.6. Specific downturn episodes and allocation strategies returns

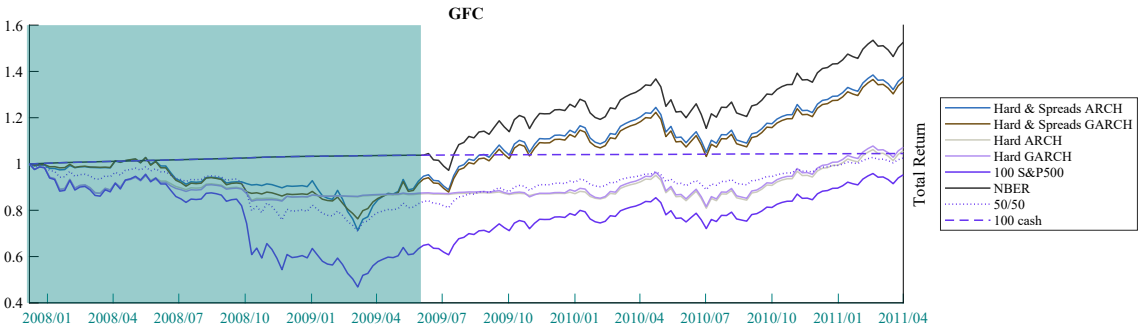

Figure 3.14: *Total cumulative return of the competitive specification during the Great Financial Crisis*

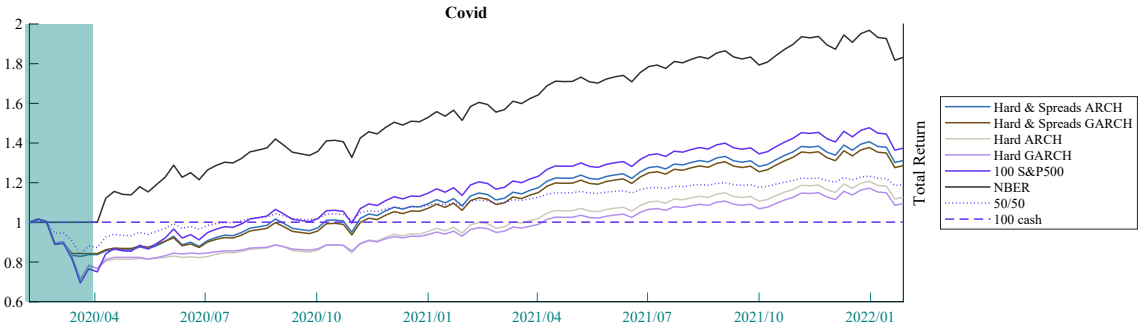

Figure 3.15: *Total cumulative return of the competitive specification during the Covid Crisis*

3.11. Rolling window returns

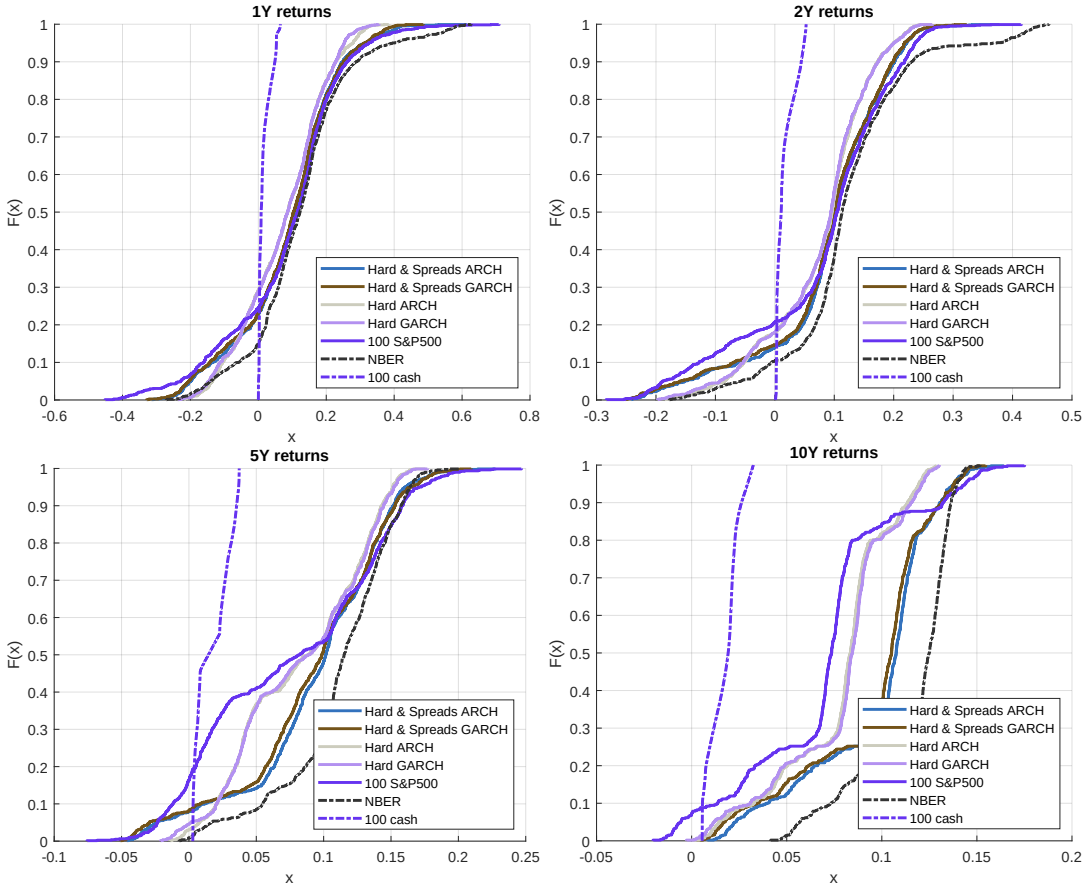

Figure 3.16: *Cumulative distribution functions of rolling window Returns from 1Y to 10Y holding horizons*

Chapter 4

Bridging business cycle dynamics and monetary policy in asset allocation

Abstract: Multi-asset allocation seeks consistent returns across business and monetary policy cycles phases. This work proposes a new allocation framework embedding market sentiment, business cycle phase and monetary policy stance signals. First, a new way of gauging monetary policy stance in a contemporaneous fashion is presented building upon Markov Switching Dynamic Factor Models. Secondly, this Chapter shows the value to combine this monetary policy signal with existing methodologies identifying in real-time regime switches in both business cycle phases and market sentiment when constructing portfolios. Encompassing macroeconomic and monetary policy regimes in building asset allocation strategies outperforms the well known 60-40 portfolio both in return maximization and risk minimization. During market downturns driven either by recession or monetary policy restriction, the proposed methodology outperforms several benchmark strategies. In more "normal" periods, the signals developed do not significantly hamper the performance of the considered portfolios compared to more "passive" strategies.

Keywords: *Bayesian Estimation; Dynamic Factor; Non-linearity; Business Cycle Analysis, Monetary Policy; Asset allocation*

4.1. Introduction

Navigating through US business cycle and monetary policy phases might be challenging for a multi-asset investor who seeks consistent risk-adjusted returns. There are evidences macroeconomic regimes determine financial returns distributions (Ang and Timmermann (2012)). Expected paths of future monetary policy rates or monetary policy regimes also play a major role in asset prices variations (Rigobon and Sack (2004)). A substantial body of literature has focused on improving portfolio returns by adapting allocation through regime identifications (Ang and Bekaert (2004)). Accounting for business cycle phases into portfolio construction was brought by Brocato and Steed (1998). Jensen and Mercer (2003) propose to rather take into account monetary policy regimes in portfolio construction. Kollar and Schmieder (2019) advocate to consider narrowing asset allocation to both business cycle phases and financial cycles in investment allocation. Kritzman et al. (2012) are the first to deploy a regime identification composed of growth, inflation and financial turbulence regimes to build an adequate allocation strategy. More recently, Kim and Kwon (2023) present an investment framework for dynamic asset allocation strategies based on changes in the growth and inflation environments (implying a monetary policy reaction). In a similar vein, Bouyé and Teiletche (2024) show macro regime-based portfolios (overheating, "goldilock", stagflation, downturn) can outperform traditional asset-based portfolios. This literature mainly faces two drawbacks: one is the frequency at which regimes are identified (mainly monthly or quarterly regimes), the other is the nature of the identification when looking at optimal portfolios, most of it is ex-post identification rather than real-time.

The race-horse 60% equity / 40% bond constant portfolio is sensitive to restrictive monetary policy phases where both equity and bond prices fall because of an increase in the discount factor. This salient fact motivates regime-contingent asset allocation in a real-time fashion. Indeed, a multi-asset investor seeking consistent return across business and monetary policy phases has to be able to identify them in a timely manner. This Chapter intends to narrow tactical dynamic long-only asset allocation to business cycle phases real-time identification, existing and new market sentiment measures as well as a novel framework gauging monetary policy stance through long-term expected real rates. Real rates variations are modelled within a four-state Markov-switching dynamic factor model (MS-DFM) encompassing hard and soft hawkish and dovish regimes. Real rates are known to move according to monetary policy and information shocks (Nakamura and Steinsson (2018)). When computed as the difference of nominal interest rates and inflation-linked swap rates they capture a market assessment of the monetary regime. A new market sentiment is also proposed in the (MS-DFM) framework building on a four-state Markov-Chain allowing for bull correction and bear rallies inter-states. Finally, we use the asset swap spreads extension of the second Chapter to assess the business cycle regime. The signals are computed on a weekly basis. The macroeconomic turning point signals and market sentiment are used to dynamically allocate equity/bond assets while the monetary policy stance signal is used as a hedging signal towards cash whenever a restrictive phase is identified.

The Chapter is organized as follows: Section 4.2 describes the Markov switching framework as well as the specifications used to build the monetary, business cycle regimes and market sentiment probabilities. Section 4.3 describes the general Bayesian estimation with details on priors and MCMC algorithms given in Appendices 4.7.1 and 4.7.2. Section 4.4 presents in-sample and out-of-sample probabilities of the monetary policy stance identifier and the market sentiment. Section 4.5 defines the allocation rules as well as the weekly backtest performances of the strategies together with an event study regarding specific macroeconomic and monetary phases. Section 4.6 concludes.

4.2. Markov-switching Models

The use of Markov-switching models to capture cyclical dynamics in market returns and macroeconomic aggregates is widespread in the literature. The work of Chauvet (1998), Kim and Nelson (1998), Camacho et al. (2014), among others, using non-linear dynamic factor models to infer business cycle phases are worthwhile. Maheu and McCurdy (2000), Maheu et al. (2012) allow for a broad partition of market returns into bull and bear regimes. The latter deploy a methodology to identify bull corrections and bear rallies. Hamilton and Gang (1996) were the first to narrow business cycle phases and market volatility regimes. Regarding Monetary policy regimes, a vast strand of the literature focuses on monetary policy rules switches via a MS-Taylor rule as in Perruchoud (2009), on a simultaneous multivariate system as in Sims and Zha (2004) or in MS-DSGE as in Chang et al. (2021). Worth noting that the first analysis of regime-switching in the term-structure of interest rates was proposed by Hamilton (1988). We introduce a new approach to identify monetary policy regimes which builds upon the market sentiment of equity returns framework presented in section 4.2.3. We will consider in this section three independent MS-DFMs to identify monetary policy phases, business cycle phases in real-time and markets stressed episodes. A market sentiment signal stemming from an univariate time series S&P 500 returns will be characterized by a textbook Hidden Markov Model (HMM) as benchmark. The general form of the models will take the following form.

Let $\boldsymbol{y}_t$ a vector of m monthly or weekly observable time series and let f_t a single latent common factor. We have the standard DFM given by :

$$\boldsymbol{y}_t = \boldsymbol{\Lambda} f_t + \boldsymbol{u}_t, \tag{4.1}$$

where $\boldsymbol{\Lambda}$ denotes the loadings matrix, $\boldsymbol{u}_t$ is orthogonal to f_t and for all $j = 1, \ldots, m$

$$\psi_j(L) u_{j,t} = e_{j,t}, \quad e_{j,t} \sim \mathcal{N}(0, \sigma^2_{e,j}), \tag{4.2}$$

let us denote $\boldsymbol{\psi}_j = (\psi_{j,1}, \ldots, \psi_{j,l})'$ the coefficients of the lag polynomial $\psi_j(L)$ of order l and let the factor follows

$$\begin{aligned} f_t &= \mu_{S_t} + \phi f_{t-1} + \varepsilon_t \\ \varepsilon_t &= \sigma_t \eta_t \end{aligned} \tag{4.3}$$

where η_t is iid $(0, 1)$ and S_t is an independent first order n-state Markov chain of constant transition probability matrix $\mathbf{P}$ with dimensions n $\times$ n. Depending on the specified model, the dynamic volatility of the dynamic factor σ_t will be conditional or Markov-switching, thus we keep the $_t$ notation in the general notation.

4.2.1. Monetary policy stance identification

As introduced by Woodford (2003) in the wake of Clarida et al. (1999), in many New Keynesian models, the real interest rate gap is a measure of monetary policy stance. The gap is defined as a difference between a real interest rate and a natural rate of interest. The forward dimension of the real interest rates is paramount as the information content of market expectations concerning inflation gives us a hint regarding the dynamics the market participants are pricing. According to Woodford (2003), the role of monetary policy is to keep agent's inflation expectations anchored at central banks' target. This theory builds upon rational expectations. Inflation expectations implied by market prices have now become a pivotal information set entering the monetary policy reaction function. A race-horse model for this reaction function is the Tayor Rule (Taylor (1993)) which specify the short-term nominal interest rate as a function of output gap and and the percentage deviation of inflation from its target.

The intuition behind the novel approach we propose is the need for practitioners to grasp the intensity or amplitude of forward real rates interest dynamics. Financial markets, compared to textbook macroeconomic models, are indeed very sensitive to forward real interest rates moves rather than absolute levels or gaps. The drifts and inertia related to real rates are moreover challenging. We draw from Orphanides (2003) approach in modelling interest rates in first difference. At the effective lower bound or very far from natural rate of interest, strong variations of real interest rates had historically a dramatic impact on risky assets, in line with the duration model proposed by Leibowitz et al. (1989) showing that equity prices display a negative sensitivity to real interest rates. We thus need to capture the common dynamics of a set of forward real interest rates. In our approach, because of data availability we will use the weekly 5 year-, 7 year-, 10 year- forward real interest rates. Those forward real interest rates are defined as the difference between the nominal interest rate of a given maturity measured in our case by Overnight Index Swap (OIS) and an inflation expectation component measured by Inflation-Linked Swap (ILS) of corresponding maturity. We take the absolute variations of the negative values of the data so that a negative variation corresponds to a restrictive movement in the forward real interest rates.

We consider the factor model presented in equations (4.1) to (4.3). The approach intends to identify four states : high or low volatile hawkish or dovish dynamics in a factor capturing the co-movement of the forward real interest rates. This can also be interpreted as "hard" or "soft" dovish or hawkish moves in markets' participants views. The first order Markov Chain displays four states $(n = 4)$. The first element of $\mathbf{\Lambda}$ is set to one for the sake of identification in equation (4.1). The residuals u_t in (4.2) follow an AR(1) process. In equation (4.3), we impose $\mu_1 < \mu_3 < 0 < \mu_2 < \mu_4$.

The volatility $\sigma_t = \sigma_{S_t}$ is also Markov-switching with $\sigma_1 > \sigma_3$ and $\sigma_2 > \sigma_4$. $\phi = 0$, the factor does not follow an autoregressive process. $\mathbf{P^{(MP)}}$ is unrestricted. The absence of restriction in $\mathbf{P^{(MP)}}$ enables to capture the idea that the chain can switch from a hard hawkish surprise to a hard dovish interpretation, as we can have noticed during the 2008-2009 great financial crisis. Given monetary policy surprises or events the market participants face and interpret, dynamics of the monetary policy stance perception can vary a lot. We will refer to the work of Jarociński and Karadi (2020) who perform a thorough analysis of markets reactions to Monetary policy communication in a structural VAR framework.

4.2.2. Business cycle turning point detection

The business cycle turning point model builds upon the second Chapter based on the first Chapter of this manuscript. It is an MS-DFM model with an ARCH extension in the volatility process for the factor. The information sample is composed of eleven monthly variables: industrial production, real manufacturing trade and sales, civilian employment, real personal income as well as seven grade buckets of USD asset swap spreads ranging from Investment grade (AAA) to Speculative grade (CCC).

We consider again the factor model presented in equations (4.1) to (4.3). The first order Markov chain displays two states ($n = 2$). The first element of $\mathbf{\Lambda}$ is set to one for the sake of identification in equation (4.1). The residuals u_t in (4.2) follow an AR(1) process. In equation (4.3), we impose $\mu_1 < \mu_0$. The volatility σ_t follows a ARCH(1) dynamic: $\sigma_t^2 = \omega + \alpha\varepsilon_{t-1}^2$ with $\omega > 0$ and $0 < \alpha < 1$. The factor follows an auto-regressive process of order 1. $\mathbf{P^{(BC)}}$ is unrestricted. We thus identify two states : a recession regime ($S_t = 1$) and an expansion regime ($S_t = 0$). We can rewrite $\mathbf{P^{(BC)}}$:

$$\mathbf{P^{(BC)}} = \begin{bmatrix} q & 1-q \\ 1-p & p \end{bmatrix}$$

The transition probabilities are defined as

$$q = \mathbb{P}(S_t = 0 | S_{t-1} = 0) \quad \text{and} \quad p = \mathbb{P}(S_t = 1 | S_{t-1} = 1),$$

The second Chapter of this manuscript shows the ability of this specification to contemporaneously capture economic downturn episodes.

4.2.3. Market sentiment

We build here on the work of Maheu et al. (2012) who introduce a framework in which bull and bear regimes in the returns of S&P 500 allow for bull corrections and bear rallies. The framework takes into account short-term reversals within each regime of the market. As such, a bull regime can face a series of persistent negative returns (a bull correction), even if the expected long-run return (primary trend) is positive in that regime. We extend this framework by taking into account a dynamic factor model approach enabling to partition the common dynamics of four equity indices

: the returns of the S&P 500, the Russell, the Dow Jones and the NASDAQ. The underlying idea is to be able to capture a global stress in the equity market which would not be tilted to a specific market profile, either Large/Small or Value/Growth, given the growing concentration of the S&P 500 index. This factor extension is different from the multivariate extension adopted by Liu et al. (2024) with a hierarchical Markov switching model. This specification assumes that a common discrete state variable drives all the asset returns from a hierarchical Markov switching model which allows the cross-section of state-specific means and variances to vary over bull and bear markets.

This factor extension can be described as follows. Taking equations (4.1) to (4.3) into consideration. The first order Markov Chain displays four states ($n = 4$). The first element of $\mathbf{\Lambda}$ is set to one for the sake of identification in equation (4.1). The residuals u_t in (4.2) follow an AR(1) process. In equation (4.3), we impose

$$\text{Bear Regime} \begin{cases} \mu_1 < 0 & \text{(bear market state)} \\ \mu_2 > 0 & \text{(bear market rally)} \end{cases}$$

$$\text{Bull Regime} \begin{cases} \mu_3 < 0 & \text{(bull market correction)} \\ \mu_4 > 0 & \text{(bull market state)} \end{cases}$$

There is no restriction on σ_t. $\phi = 0$, the factor does not follow an auto-regressive process. $\mathbf{P^{(MS)}}$ is restricted.

$$\mathbf{P^{(MS)}} = \begin{bmatrix} p_{11} & p_{12} & 0 & p_{14} \\ p_{21} & p_{22} & 0 & p_{24} \\ p_{31} & 0 & p_{33} & p_{34} \\ p_{41} & 0 & p_{43} & p_{44} \end{bmatrix}$$

The movement of a bull (bear) regime to a bear rally (bull correction) state is not allowed for identification, but Maheu et al. (2012) justify it through the data. To allow for short-term deviation from the long-term trend the authors use the Hamilton and Susmel (1994) resolution of unconditional probabilities of $\mathbf{P^{(MS)}}$ given by :

$$\mathbf{\Pi} = (\mathbf{A}'\mathbf{A})^{-1}\mathbf{A}'\mathbf{e}$$

with $\mathbf{A}' = [\mathbf{P^{(MS)}}' - \mathbf{I}, \boldsymbol{\iota}]$ and $\mathbf{e}' = [0, 0, 0, 1]$ and $\boldsymbol{\iota} = [1, 1, 1, 1]'$. This matrix of unconditional state probabilities $\mathbf{\Pi}$ allows to constrain long-run market returns in the bear and bull regimes:

$$E[f_t \mid \text{bear regime}, S_t = 1, 2] = \frac{\pi_1}{\pi_1 + \pi_2}\mu_1 + \frac{\pi_2}{\pi_1 + \pi_2}\mu_2 < 0$$

$$E[f_t \mid \text{bull regime}, S_t = 3, 4] = \frac{\pi_3}{\pi_3 + \pi_4}\mu_3 + \frac{\pi_4}{\pi_3 + \pi_4}\mu_4 < 0$$

The bull (bear) market regime is defined with long-run positive (negative) returns but the market regimes can have short-term reversals from their long-run mean. We will also consider the

univariate version of the above specification as in Maheu et al. (2012) as benchmark.

4.3. Bayesian estimation

The general model from (4.1) to (4.2) can be cast in state space form :

$$\begin{aligned} \boldsymbol{y}_t &= \boldsymbol{H}\boldsymbol{z}_t + \boldsymbol{\varsigma}_t & \boldsymbol{\varsigma}_t &\sim \mathcal{N}(0, \boldsymbol{R}) \\ \boldsymbol{z}_t &= \boldsymbol{\delta}_{S_t} + \boldsymbol{\Xi}\boldsymbol{z}_{t-1} + \boldsymbol{\zeta}_t & \boldsymbol{\zeta}_t &\sim \mathcal{N}(0, \boldsymbol{Q}_t) \end{aligned} \tag{4.4}$$

$\boldsymbol{H}$ the $(m) \times (ml+1)$ matrix, $\boldsymbol{\Xi}$ the $(ml+1) \times (ml+1)$ matrix, and $\boldsymbol{\Xi}_{j=1\ldots m}$ the $l \times l$ matrix such that

$$\boldsymbol{H} = \begin{bmatrix} \lambda_1 & \boldsymbol{h}^l & \ldots & 0 \\ \vdots & \vdots & \ddots & \vdots \\ \lambda_m & 0 & \ldots & \boldsymbol{h}^l \end{bmatrix} \quad \boldsymbol{\Xi} = \begin{bmatrix} \boldsymbol{\phi} & & & \\ & \boldsymbol{\Xi}_1 & & \\ & & \ddots & \\ & & & \boldsymbol{\Xi}_m \end{bmatrix}$$

$$\text{with} \quad \boldsymbol{\Xi}_{j=1\ldots m} = \begin{bmatrix} \psi_{j,1} & \psi_{j,2} & \ldots & \psi_{j,l-1} & \psi_{j,l} \\ 1 & 0 & \ldots & 0 & 0 \\ 0 & 1 & \ldots & 0 & 0 \\ \vdots & \vdots & \ddots & \vdots & \vdots \\ 0 & 0 & \ldots & 1 & 0 \end{bmatrix}.$$

$\lambda_1 = 1$ for identification purpose. $\boldsymbol{h}^l$ is a $1 \times l$ vector with the only first element equal to one. $\boldsymbol{\delta}_{S_t} = (\mu_{S_t}, 0, \ldots, 0)'$, $\text{diag}(\boldsymbol{Q}_t) = (\sigma_t^2, \sigma_{e,1}^2\boldsymbol{h}^l, \ldots \sigma_{e,m}^2\boldsymbol{h}^l)$. The vector $(ml+1)$ of unobserved variables $\boldsymbol{z}_t$ is given by

$$\boldsymbol{z}_t = (f_t, (1, L, \ldots, L^{l-1})u_{1,t}, \ldots, (1, L, \ldots, L^{l-1})u_{m,t})'.$$

The vector of parameters to estimate is given will be specific to the model specification we use. We denote by $\boldsymbol{\vartheta}^{(\text{MP})}$, the vector of parameters of the Monetary Policy stance model. $\boldsymbol{\vartheta}^{(\text{BC})}$ refers to the parameters vector for the business cycle phases assessor. Finally $\boldsymbol{\vartheta}^{(\text{MS})}$ will refer to the vector of parameters for the Market sentiment model. We have the following set of parameters vectors :

$$\begin{aligned} \boldsymbol{\vartheta}^{(\text{MP})} &= (\mathbf{P}^{(\mathbf{MP})}, \boldsymbol{\Psi}', \sigma_{e,1}, \ldots, \sigma_{e,m}, \boldsymbol{\Lambda}', \mu_1, \mu_2, \mu_3, \mu_4, \sigma_1, \sigma_2, \sigma_3, \sigma_4)' \\ \boldsymbol{\vartheta}^{(\text{BC})} &= (\mathbf{P}^{(\mathbf{BC})}, \boldsymbol{\Psi}', \sigma_{e,1}, \ldots, \sigma_{e,m}, \boldsymbol{\Lambda}', \mu_0, \mu_1, \phi, \omega, \alpha)' \\ \boldsymbol{\vartheta}^{(\text{MS})} &= (\mathbf{P}^{(\mathbf{MS})}, \boldsymbol{\Psi}', \sigma_{e,1}, \ldots, \sigma_{e,m}, \boldsymbol{\Lambda}', \mu_1, \mu_2, \mu_3, \mu_4, \sigma_1, \sigma_2, \sigma_3, \sigma_4)' \end{aligned}$$

Let us denote $\boldsymbol{z}^{(T)} = \{\boldsymbol{z}_1, \ldots, \boldsymbol{z}_T\}$ the unobserved state vector in equation (4.4), $\boldsymbol{y}^{(T)} = \{\boldsymbol{y}_1, \ldots, \boldsymbol{y}_T\}$ the observed data, and $S^{(T)} = \{S_1, \ldots, S_T\}$ the unobserved Markov Chain. The models are estimated using a Markov Chain Monte Carlo (MCMC) Gibbs sampling algorithm in the spirit of Kim and Nelson (1999) and Bai and Wang (2011) where conditional draws of the state vector, the Markov Chain, and the parameters vector $\boldsymbol{\vartheta}^{(\cdot)}$ are obtained sequentially.

- We generate conditional draws of the state vector from $p(\boldsymbol{z}^{(T)}|\boldsymbol{y}^{(T)}, S^{(T)}, \boldsymbol{\vartheta}^{(.)})$ using the forward-filtering backward-smoothing algorithm of Carter and Kohn (1994).
- We generate conditional draws of the Markov chain from $p(S^{(T)}|\boldsymbol{y}^{(T)}, \boldsymbol{z}^{(T)}, \boldsymbol{\vartheta}^{(.)})$ based on the Hamilton filter (Hamilton (1989)).
- We generate conditional draws for the parameters vector from $p(\boldsymbol{\vartheta}^{(.)}|\boldsymbol{y}^{(T)}, \boldsymbol{z}^{(T)}, S^{(T)})$ by sequentially drawing in the conditional distribution of components of $\boldsymbol{\vartheta}^{(.)}$

Details of priors used and the MCMC algorithms for each model specification can be found respectively in Appendices 4.7.1 and 4.7.2.

4.4. Results

4.4.1. In-sample

This section presents the in-sample probabilities of the MS-DFMs presented in Section 4.2. Figure 4.1 shows the 4 regimes identified by our monetary policy stance identifier. Five hard hawkish phases are noticeable. The first phase is the one taking place from mid-2004 until the end of the year. This event materializes policy rates normalisation following the gradual US recovery which took place from June 2004 to June 2006. We catch the early stage of the tightening with the soft hawkish probability which then transitions to hard hawkish regime as the market expectations for long-term maturities are more ample at the beginning of a hiking cycles or monetary policy shock as shown by Boeck and Feldkircher (2021). According to the authors this is not the case for short-term maturities yields that under-react first and exhibit then a period of overcompensation called delayed overshooting. The hard hawkish regime then flips again to soft hawkish regime and fades away at the end of 2004. The second hawkish regime identified corresponds to the noisy period surrounding Federal Open Market Committee (FOMC) communications during the Great Financial Crisis. Jarociński and Karadi (2020) identify likewise restrictive monetary policy shocks during this period. Moreover, the information shock as identified by the authors induces a bearish guidance regarding future activity provoking a fall in long-term inflation expectations and thus a rise in real interest rates, which in turn transposes itself into a overarching hawkish regime. From late 2010 to February 2011, the recovery and reflation expected in the US has brought a soft hawkish signal into place. Another hard hawkish period identified is the "taper tantrum" period in may 2013 triggered by Bernanke's speech regarding the possibility the Federal Reserve could reduce the speed of its balance sheet expansion. It ignited a massive bond sell-off dragging rates upwards, this is a clear hawkish perception the market had regarding the Federal Reserve even though the monetary regime was clearly dovish at the time. This is also the reason why the Federal Reserve has put a lot of effort to divorce expectations of future rate increases from balance sheet reductions afterwards (Smith and Valcarcel (2023)). The Covid outbreak in February 2020, by the uncertainty it has brought regarding economic prospects yielded hard deflationary expectations for a short period of time (before the massive monetary and fiscal stimulus). This is captured by the spike in the hard hawk probability regime and surrounded by a slight move

in the soft hawkish probability. The last hawkish period identified by our specification is the one referring to the expeditive action undertaken by the Federal Reserve from 2022 onwards to dampen the supply/demand unbalances provoked by the global economy reopening and amplified by the Russian invasion of Ukraine.

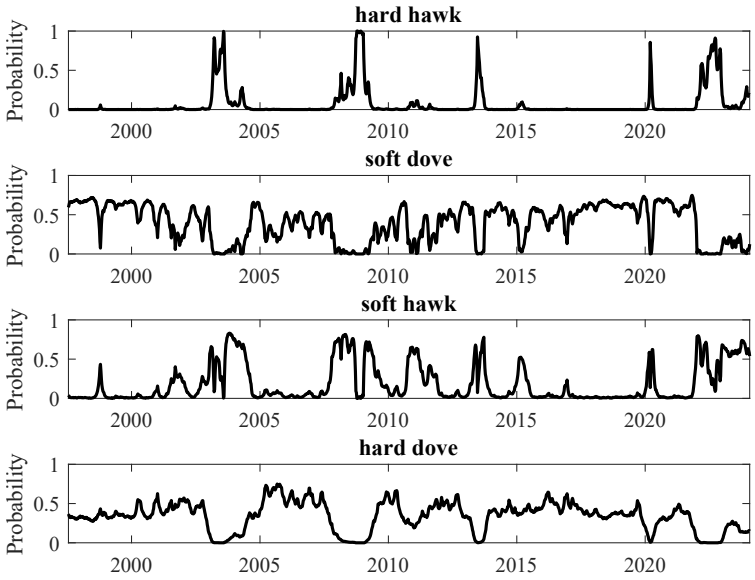

Figure 4.1: *Dovish/hawkish 4-regimes in-sample probabilities*

If we recombine the inter-state regimes into two broad measures of hawkishness and dovishness by summing up the soft/hard dovish hawkish probabilities we get the two symmetric probabilities presented in Figure 4.2. What we are interested in is the capacity of the monetary policy stance signal to detect a hawkish regime (implied by expected long-term real rates) in order to deploy a specific hedging asset allocation strategy.

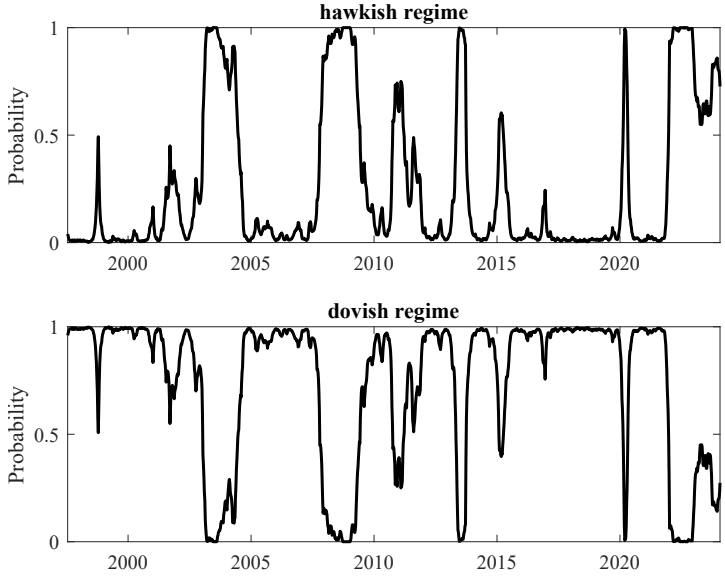

Figure 4.2: *Dovish/hawkish 2-regimes in-sample probabilities*

Figure 4.3 displays the 4-states market sentiment in-sample probabilities. The bear regime probability manages to capture seven ample market downturns from 1989 to 2023. Those downturns are the dotcom bubble burst in march 2000 and specific stresses associated to it afterwards, specifically in 2002. The Great financial crisis and the market stress associated to it is labelled as bear regime in early September 2008 until March 2009. Lastly the Covid outbreak in China followed by a broad shutdown in world economy provoked a fall in equity markets from 19th February until the massive Monetary and State supports announced mid-march 2020. Bull correction phases appear more frequently in our dataset. Significant periods are the 1990 recession in the US in the wake of the Gulf crisis and the rise in oil products as consequence. 1998 is worth to be noted as a pre-dotcom bubble burst triggered by the Russian debt crisis. A significant bull correction regime appears during the beginning of June 2004 hiking cycle. The Great Financial Crisis is captured as a bull correction from October 2007 to September 2008. The "flash crash" of May 2010 and the correction of 2011 in the wake of the Greek debt stress and European debt crisis are captured as bull correction events. The "taper tantrum" is also identified as bull correction regime. The 2015 slowing in corporate earnings is labelled as bull correction phase. The 2018 market correction is associated with fears regarding Federal Reserve decisions and the uncertainty in the tariffs war between Trump's administration and China. Finally, one can observe that the correction induced by the Federal Reserve expeditive action to dampen 2022 inflationary pressures is labelled as bull correction regime.

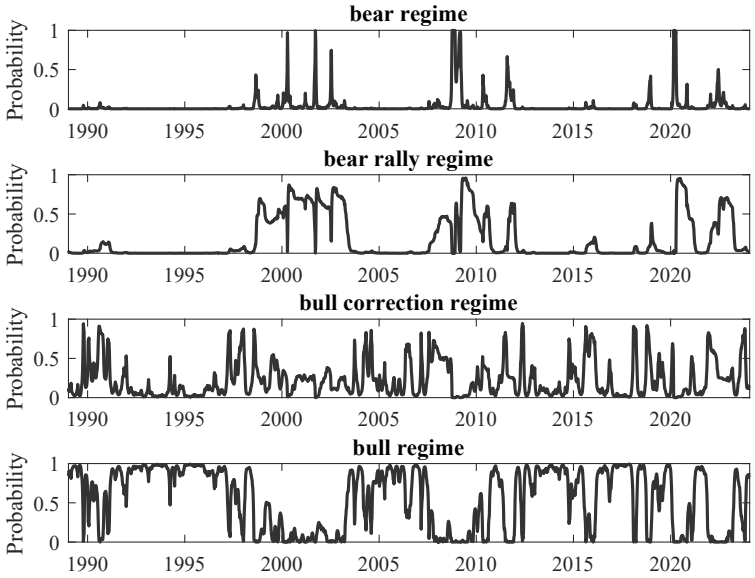

Figure 4.3: *In-sample probabilities from the multivariate specification of the market sentiment*

Figure 4.4 displays the recombined bull/bear market sentiment in-sample probabilities. This partitioning is globally consistent with the multivariate bull/bear approach probabilities obtained by Liu et al. (2024) on this specific time span.

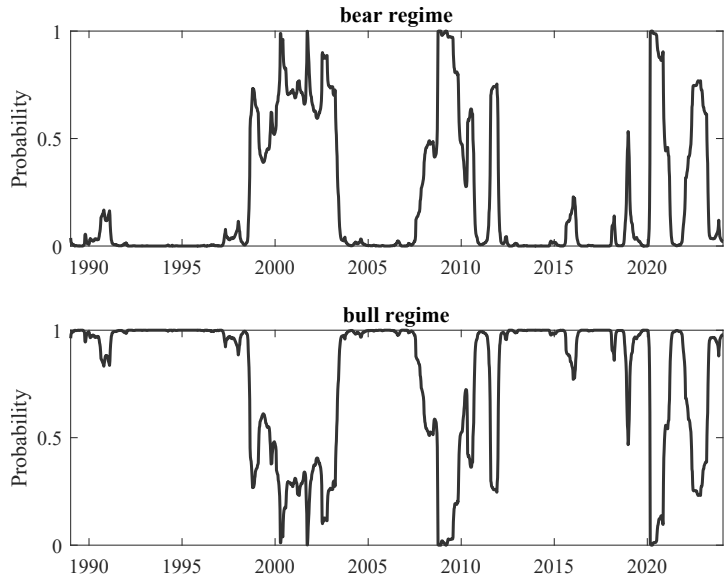

Figure 4.4: *Bull/bear in-sample probabilities from the multivariate specification of the market sentiment*

Figures 4.13 and 4.14 in Appendix 4.7.3 display the 4-states market sentiment in-sample probabilities and the recombined bull/bear probabilities based on the univariate specification as in Maheu et al. (2012), taking only into account the S&P500 time series.

4.4.2. Out-of-sample

This section presents the out-of-sample exercise undertaken on a weekly basis from January the 7th 2000 until 24th February 2023. Figure 4.5 displays the real-time probabilities to be in a hard hawkish regimes. The signal manages to capture, from a real-time market perspective the restrictive monetary policy events described in subsection 4.4.1 and thus, validating the proposed approach.

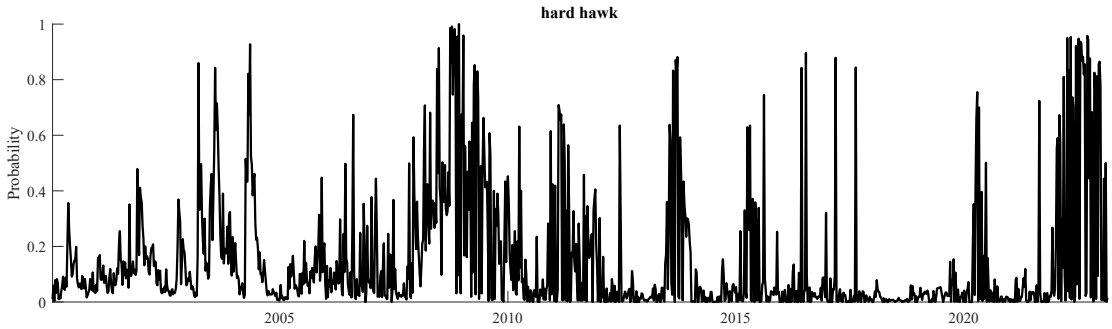

Figure 4.5: *Hard hawkish regime out-of-sample probabilities*

Figures 4.6 and 4.7 show the real-time probabilities of the market sentiment signal. Compared to the in-sample probabilities displayed in Figures 4.3 and 4.4, we get a more sensitive signal which manages to identify in a timely manner the bearish events described in subsection 4.4.1.

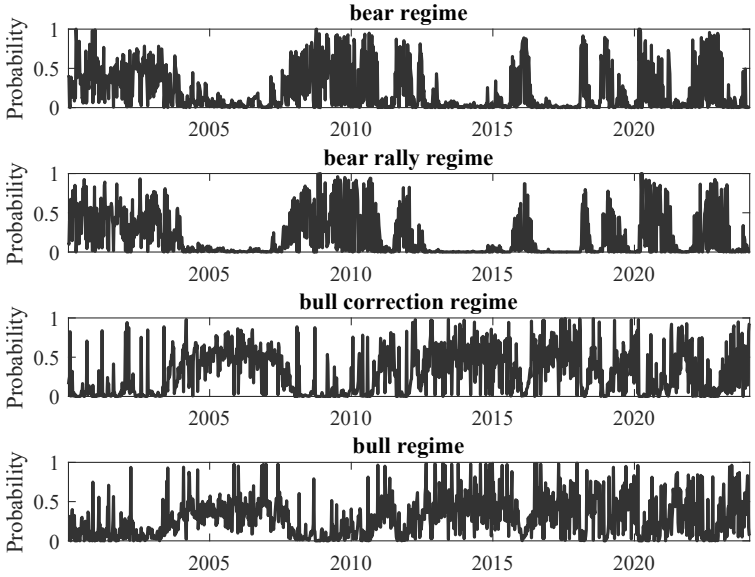

Figure 4.6: *Real-time probabilities from the multivarite specification of the market sentiment*

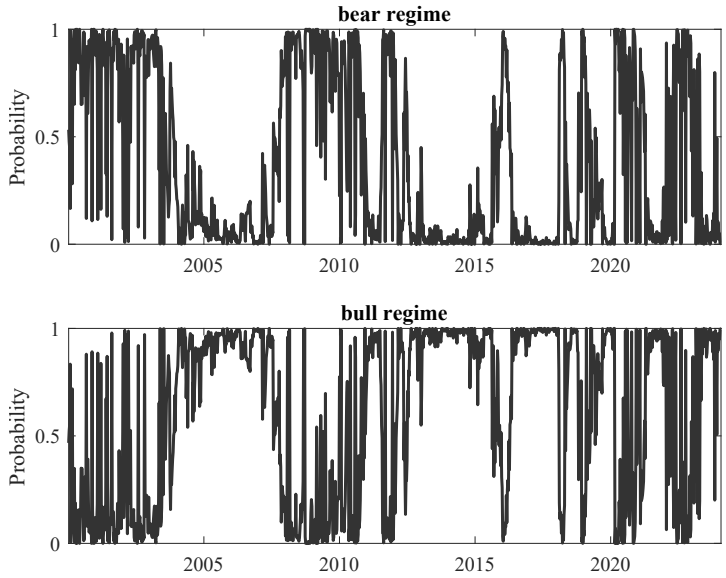

Figure 4.7: *Real-time bull/bear probabilities from the multivariate specification of the market sentiment*

4.5. Asset allocation

A substantial litterature has focused on relationships between monetary policy and equity prices (Thorbecke (1997), Bernanke and Kuttner (2005), among others). We can mention Hamilton and de Longis (2015) who bring a coherent allocation strategy along business cycle phases measured on a real-time monthly basis. The need to take into account business cycle phases into portfolio construction has been documented by Brocato and Steed (1998). Jensen and Mercer (2003) advocate taking into account the monetary policy cycle into portfolio optimization would be of a

better help than the latter approach. The need to bridge asset allocation to both business cycle phases and financial cycles has been put forward by Kollar and Schmieder (2019). Kritzman et al. (2012) identify monthly or quarterly regimes defined as financial market turbulences, inflation and economic growth and deploy a tactical asset allocation. To the best of our knowledge, this is the first try to narrow in a single allocation framework macroeconomic turning point real-time signals, monetary policy stance regimes and market sentiment on a weekly rebalancing basis, making our investment strategy "live".

This section introduces rules of allocation based on signals extracted in the former section. A race-horse allocation strategy in the asset management industry consists in attributing a constant 60% weight to equity and a 40% weight to bonds. This allocation rule is attributed to the Modern Portfolio theorists in the 50's. This strategy has proven to be efficient to capture equity markets long run returns as well as offering the safe heaven characteristics of the bond market when it comes to risky assets downturns. This induces a less volatile profile of total long run returns. This strategy shows nonetheless a vulnerable return profile during monetary policy restrictive periods or hawkish phases in the market. As interest rates increase, bond prices fall as well as equity prices. We propose an asset allocation to circumvent this issue. By taking into account a monetary policy stance signal, the investor can opt for a hedging strategy to cap the losses incurred by reducing its exposure to the equity/bond market. We define in this section a range of alternative portfolio strategies that mimic the 60 % equities / 40 % bonds strategy by allowing weights to be dynamic. The turning point probability and the market sentiment probability are used as inputs in the dynamic weighting scheme. Moreover, the monetary stance probability will be used as hedging weight when incorporated to the allocation decision. We compare the constructed portfolios to well-known benchmark strategies : 100% cash, 100% equity, 60% equity / 40% bond. Rebalancing of the portfolio is implemented on a weekly basis, at the time when the market sentiment, business cycle phase assessor and monetary policy stance signal are computed. Finally, we apply a 2 basis point transaction cost to the S&P500 rebalancing and none for cash or 10 Year US Treasuries, given the liquidity of those markets.

4.5.1. Rules

We consider a set of rules taking into account a portfolio universe composed of a risky asset (S&P500 index), a fixed income asset (10 Year US Bond) and Cash (3-month Treasury Bill). Business cycle and market sentiment regimes will serve as weights in the equity/bonds allocation weights, making the 60 % equities / 40 % bonds allocation portfolio dynamic. If a stressed market or a recession signal occur, the weight applied to the risky asset can be reduced up to 0%. High volatile markets are generally associated with negative future returns. This stylized fact, known as leverage effect has been extensively studied in the literature. One can refer to Black (1976), Kim et al. (2000) for the volatility feedback analysis.

Business cycle phases also play a major role in equity returns profiles. When a fear of a downturn or

a recession occurs, expected revenues of firms fall triggering equity prices to drop. As mentioned by Siegel (1991) there is a positive relationship between firm profits and earnings as well as dividends for stakeholders. Balance sheet effects through increase of debt ratio also amplify the deterioration in valuation ratios. On the other hand, bond markets are then considered as a safer place for investors, especially for Government debt with good credit grades. This so-called "flight to quality" phenomenon tends to reduce bond yields and increase the market price of the already-issued bonds.

A restrictive monetary policy is carried out in a inflationary regime central banks want to cool down. The main tool is the increase of the cost of credit by setting its policy rates higher. It tames the aggregate demand into a better balance with respect to the aggregate supply of the economy. The impact of such moves is an increase of bond yields across the maturity curve. It implies a drop in bond indices prices. In such events, equity markets tend also to suffer as the discount factors in cash flow models increase. The anticipated slowdown in activity also brings the expected revenues of firms down. One of the only asset class which does not suffer from such restrictive monetary environments is cash. Short-term rates increase, making the carry of money markets attractive compared to deterioration in other asset classes valuations, especially the most risky ones. A 60 % equities / 40 % bonds portfolio, in a restrictive monetary environment, faces negative returns on each leg of the asset allocation rule.

We will thus build up some allocation rules taking into account monetary policy stance and giving a specific weight to cash. In the remaining part of the Chapter, we will always consider long-only portfolios. We define w_t^{cash} as the weight allocated to cash at time t, w_t^{equity} the weight for the S&P 500 and w_t^{bond} the weight attributed to the 10 Year Treasury bond. Moreover $w_t^{equity} + w_t^{cash} + w_t^{bond} = 1$. Finally, $P(S_t^{BC} = 1 \mid I_t)$ will denote the filtered probability to be in a recession phase, $P(S_t^{MS} = \{1,2\} \mid I_t)$ in a bear regime phase, $P(S_t^{MS} = \{1,3\} \mid I_t)$ the probability to be in a negative return equity market regime and $P(S_t^{MP} = \{1\} \mid I_t)$ to be in a restrictive monetary regime. Five broad asset allocation cases will be considered. One which takes only the probability of being in a bear regime or a negative return market. The second approach will modulate the latter probability by averaging the signal with a business cycle regime. The third approach will take into account Monetary policy stance with the market sentiment. The fourth one will mix the three axes. Finally the latter approach will exclude the market sentiment and look at the utility of business cycle and monetary policy stance together.

4.5.1.1. Market sentiment only

We consider two alternative signals. The multivariate model presented in section 4.2.3 and the univariate specification as the one introduced by Maheu et al. (2012). It aims at comparing the added value of considering a broad definition of US equity markets compared to the single S&P 500 total return index when extracting a sentiment index. The weighting scheme of bond and equity is either given by :

$$w_t^{bond} = P(S_t^{MS} = \{1,2\} \mid I_t) \quad w_t^{equity} = P(S_t^{MS} = \{3,4\} \mid I_t)$$

looking specifically to bull/bear partition or

$$w_t^{bond} = P(S_t^{MS} = \{1,3\} \mid I_t) \quad w_t^{equity} = P(S_t^{MS} = \{2,4\} \mid I_t)$$

when trying to capture negative return phases, allowing for within-regime partitions.

4.5.1.2. Market sentiment and Business cycle

Based on both univariate and multivariate market sentiment specifications as well as bull/bear or positive/negative return partitions, we then consider using the turning point signal to mitigate market stress not induced by macroeconomic fundamentals. The weighting scheme is given by:

$$\begin{aligned} w_t^{bond} &= \frac{P(S_t^{MS} = \{1,2\} \mid I_t) + P(S_t^{BC} = 1 \mid I_t)}{2} \\ w_t^{equity} &= \frac{P(S_t^{MS} = \{3,4\} \mid I_t) + P(S_t^{BC} = 0 \mid I_t)}{2} \end{aligned}$$

considering bull/bear partition or

$$\begin{aligned} w_t^{bond} &= \frac{P(S_t^{MS} = \{1,3\} \mid I_t) + P(S_t^{BC} = 1 \mid I_t)}{2} \\ w_t^{equity} &= \frac{P(S_t^{MS} = \{2,4\} \mid I_t) + P(S_t^{BC} = 0 \mid I_t)}{2} \end{aligned}$$

looking for a positive/negative short-term returns.

4.5.1.3. Market sentiment and Monetary Policy stance

The set of rules described in this section intends to gauge whether adding the monetary policy stance is valuable. The market sentiment defines the equity/bond allocation, the cash is weighted by the monetary policy stance signal, used as a hedging extension. The weighting scheme of bond, equity and cash is either given by :

$$\begin{aligned} w_t^{bond} &= P(S_t^{MS} = \{1,2\} \mid I_t) \times (1 - P(S_t^{MP} = 1 \mid I_t)) \\ w_t^{equity} &= P(S_t^{MS} = \{3,4\} \mid I_t) \times (1 - P(S_t^{MP} = 1 \mid I_t)) \\ w_t^{cash} &= 1 - w_t^{bond} - w_t^{equity} \end{aligned}$$

through the bull/bear partition or

$$\begin{aligned} w_t^{bond} &= P(S_t^{MS} = \{1,3\} \mid I_t) \times (1 - P(S_t^{MP} = 1 \mid I_t)) \\ w_t^{equity} &= P(S_t^{MS} = \{2,4\} \mid I_t) \times (1 - P(S_t^{MP} = 1 \mid I_t)) \\ w_t^{cash} &= 1 - w_t^{bond} - w_t^{equity} \end{aligned}$$

considering specifically the positive/negative return partition.

4.5.1.4. Business cycle and Monetary policy stance

The rules in this section enable to gauge the benefit of using the market sentiment. The multi-asset allocation is only driven by fundamental macroeconomic signals and the monetary policy stance. The underlying hypothesis is that once looking at macroeconomic or monetary policy stress, there is no need to take into account other kind of market stress not attributable to the former ones. Hence, the unique set of rules is given by:

$$\begin{aligned} w_t^{bond} &= P(S_t^{BC} = 1 \mid I_t) \times (1 - P(S_t^{MP} = 1 \mid I_t)) \\ w_t^{equity} &= P(S_t^{BC} = 0 \mid I_t) \times (1 - P(S_t^{MP} = 1 \mid I_t)) \\ w_t^{cash} &= 1 - w_t^{bond} - w_t^{equity} \end{aligned}$$

The equity/bond weighting scheme is defined by the real-time turning point signal whereas the monetary policy stance signal enables to migrate the allocation towards cash whenever a monetary policy appears to be increasingly tight.

4.5.1.5. Market sentiment, Business cycle and Monetary policy stance

Finally, a last set of rules we characterize as all-weather will embrace the three signals used concomitantly. The weighting scheme is a mix of the intuitions described in subsections 4.5.1.2 and 4.5.1.3. The macroeconomic turning point signal mitigate the market sentiment in the equity/bond allocation while the monetary policy stance signal allows for a dynamic hedging with cash. The weighting scheme is given by:

$$\begin{aligned} w_t^{bond} &= \frac{P(S_t^{MS} = \{1,2\} \mid I_t) + P(S_t^{BC} = 1 \mid I_t)}{2} \times (1 - P(S_t^{MP} = 1 \mid I_t)) \\ w_t^{equity} &= \frac{P(S_t^{MS} = \{3,4\} \mid I_t) + P(S_t^{BC} = 0 \mid I_t)}{2} \times (1 - P(S_t^{MP} = 1 \mid I_t)) \\ w_t^{cash} &= 1 - w_t^{bond} - w_t^{equity} \end{aligned}$$

when focusing on a market bull/bear partition or by :

$$\begin{aligned} w_t^{bond} &= \frac{P(S_t^{MS} = \{1,3\} \mid I_t) + P(S_t^{BC} = 1 \mid I_t)}{2} \times (1 - P(S_t^{MP} = 1 \mid I_t)) \\ w_t^{equity} &= \frac{P(S_t^{MS} = \{2,4\} \mid I_t) + P(S_t^{BC} = 0 \mid I_t)}{2} \times (1 - P(S_t^{MP} = 1 \mid I_t)) \\ w_t^{cash} &= 1 - w_t^{bond} - w_t^{equity} \end{aligned}$$

when concentrating on a positive/negative return real-time identification.

4.5.2. Performance comparison

We compare the performances of the competing strategies in a real-time backtest exercise. The backtest is ran from 7th January 2000 to 24th February 2023 on weekly basis. The portfolios rebalancing occurs at the end of a given week. The macroeconomic turning point signal stems

from the second Chapter real-time backtest. The filtered probabilities $P(S_t^{BC} \mid I_t)$, $P(S_t^{MS} \mid I_t)$ and $P(S_t^{MP} \mid I_t)$ are computed at the same date t.
We denote $\boldsymbol{w_t} = [w_t^{bond}, w_t^{equity}, w_t^{cash}]$ and the return of each asset $\boldsymbol{r_t} = [r_t^{bond}, r_t^{equity}, r_t^{cash}]$. The weekly total return of a specific asset a, is given by $r_t^a = (P_t^a/P_{t-1}^a) - 1$, P_t^a being the price of asset a at time t. For the Market sentiment strategies and the Market sentiment and Business cycle strategies in sections 4.5.1.1 and 4.5.1.2, $w_t^{bond} = 0$. The return of a strategy s between $t-1$ and t, $r_{t,s}$ is given by $\boldsymbol{w_{t-1}r_t'}$. In this section, we will focus on annualised returns, volatilities, Sharpe ratios (Sharpe (1994)) and maximum drawdowns as well as the same statistics for portfolio holding rolling windows ranging from 1 year to 10 years. Given that first moments of the descriptive statistics are auto-correlated on the rolling window holding periods, we will focus on empirical cumulative distributions albeit we put the average statistics in the performance comparison tables. Moreover, we will use Fleming et al. (2003) approach to measure the economic utility for an investor to hold a specific portfolio. This approach relates to the mean-variance analysis and the quadratic utility framework. The realized weekly utility generated by a strategy s is given by :

$$U(r_{t,s}) = W_0 \left((1 + r_t^f + r_{t,s}) - \frac{\gamma}{2(1+\gamma)} (1 + r_t^f + r_{t,s})^2 \right) \tag{4.5}$$

W_0 is the initial wealth invested, r_t^f the 3-month cash return, $r_{t,s}$ the portfolio return and γ a fixed aversion parameter. To measure the value of a strategy compared to another one, we can define a constant Δ which equalizes :

$$\sum_{t=1}^{T} U(r_{t,s1}) = \sum_{t=1}^{T} U(r_{t,s2} - \Delta)$$

This constant Δ can be considered as the maximum performance fee that an investor would agree to pay for switching from strategy $s1$ to $s2$ under the hypothesis that he is indifferent between both. The higher the Δ, the more strategy $s2$ is valuable for the investor.

Table 4.1 displays the annualised performances for the five groups of competing strategies. Bold lines highlight the strategies for which the annualised Sharpe ratio is maximised. From the Modern Portfolio Theory (Markowitz (1952)), an investor is interested in maximizing the risk-adjusted return of his/her portfolio, and will not be eager to increase return if it comes at a higher cost in terms of returns dispersion, e.g. volatility. The strategy embedding the bull/bear sentiment, the macroeconomic real-time downturn signal and the Monetary policy stance signal (MS-Bull-Bear-Return-Uni-MP-BC) tend to outperform the other strategies. The strategy only relying on the market sentiment (MS-Bull-Bear-Return-Uni) is the one which performs worst compared to its counterparts incorporating either a monetary policy stance signal, a business cycle phase assessor or both. From the tabled results, the multivariate extension of the equity market sentiment does not improve the performances statistics. Moreover, the strategy consisting in taking exposure to the risky asset whenever a signal of bear rally materialize appears to be inefficient. This is attributable to the fact that short-term reversal identified are not persistent enough to yield higher returns.

Bottom line of those preliminary annualised results is: each highlighted strategy outperforms the benchmarks of holding a constant 100% exposure to the risky asset, 100% exposure to cash or 60 % equities / 40 % bonds. Remarkably, the constant 60 % equities/40 % bonds portfolio tends to underperform a vast majority of competitive specifications, highlighting the necessity to adopt a dynamic weighting scheme based on regime identification. The Market Sentiment-Business Cycle-Monetary Policy strategy is nearly two times higher in terms of annualised Sharpe ratio compared to this race-horse allocation.

The 1-year to 10-year portfolio holding rolling windows depicted in Appendix 4.7.4.1 validate partially this first assessment. Tables 4.11 to 4.14 show the superiority of the highlighted strategies for each holding period considered. The strategy based on the univariate bull/bear market sentiment, the business cycle phase assessor and the monetary policy stance signal maximize the rolling Sharpe ratios. For 1-year to 2-year rolling holding periods, the strategy composed of the equity market sentiment and the monetary policy stance is the second best. For longer rolling holding periods however, the strategy based on the univariate bull/bear market sentiment performs quite well even though it remains below the 3-signal allocation approach. Finally, the more the holding period increases (e.g. from rolling 1-year to rolling 10-year) the better strategies incorporating monetary policy stance and business cycle phase assessors perform.

Table 4.1: *Annualised performances for the five groups of competing strategies and benchmarks from January 2000 to February 2023*

	Ann. Return	**Ann. Vol**	**Ann. SR**	**Ann. Max DD**
MS-Sign-Return-Multi	5.1%	9.8%	0.33	25.4%
MS-Bull-Bear-Return-Multi	5.6%	10.0%	0.37	22.8%
MS-Sign-Return-Uni	2.6%	11.0%	0.06	40.3%
MS-Bull-Bear-Return-Uni	**5.7%**	**9.3%**	**0.41**	**25.8%**
MS-Sign-Return-Multi-BC	5.9%	12.1%	0.33	37.2%
MS-Bull-Bear-Return-Multi-BC	7.4%	12.8%	0.43	36.9%
MS-Sign-Return-Uni-BC	5.4%	11.9%	0.30	36.8%
MS-Bull-Bear-Return-Uni-BC	**6.8%**	**10.6%**	**0.46**	**27.6%**
MS-Sign-Return-Multi-MP	4.1%	9.4%	0.23	24.8%
MS-Bull-Bear-Return-Multi-MP	6.3%	10.7%	0.41	21.9%
MS-Sign-Return-Uni-BC	3.6%	8.1%	0.21	21.4%
MS-Bull-Bear-Return-Uni-MP	**5.8%**	**8.2%**	**0.48**	**15.9%**
MP-BC	**7.4%**	**12.8%**	**0.43**	**42.6%**
MS-Sign-Return-Multi-MP-BC	5.8%	10.4%	0.38	33.3%
MS-Bull-Bear-Return-Multi-MP-BC	6.9%	11.3%	0.44	32.8%
MS-Sign-Return-Uni-MP-BC	5.6%	9.4%	0.40	27.9%
MS-Bull-Bear-Return-Uni-MP-BC	**6.8%**	**9.3%**	**0.52**	**22.9%**
S&P500	6.5%	18.1%	0.26	54.7%
60%Equity/40%Bond	4.8%	10.4%	0.28	32.1%
Cash3m	1.7%			

The Figure 4.8 displays the cumulative distribution of the rolling window Sharpe Ratios from

1 year to 10 year holding periods. An investor seeks thin left tails and the most right-skewed cumulative distributions. Albeit 1 year and 2 year rolling Sharpe ratios tend to display quite similar distributive patterns, longer rolling holding periods show that strategies implementing a broader set of signals yield a greater Sharpe ratio on a large part of the distribution support. The Market Sentiment-Business Cycle-Monetary Policy strategy yield on each point of the support a higher Sharpe ratio on a 10 year holding period. The longer the holding period, the more likely the investor will face an adverse shock, arising from a monetary policy restriction or a macroeconomic downturn. Thus, strategies incorporating business cycle or monetary policy regimes will be able to cope with those negative shocks by rebalancing the portfolio in a timely manner.

Figure 4.17 in Appendix 4.7.4.2 shows the cumulative distribution of rolling returns for the 1 year to 10 year portfolio holding periods. Again we seek strategies with thin left tails (capped drawdowns) and right-skewed profile. Strategies taking into account market sentiment and either business cycle regimes, monetary policy stance or both highlight globally lower downside risks for the entire holding periods considered.

Figure 4.9 shows the log-total cumulative return of the strategies backtested on a weekly basis from 7th January 2000 to 24th February 2023. Strikingly, being capable of timely identifying monetary and macroeconomic regimes yield far better long-term returns than the considered benchmarks. The log-scale enables to capture accelerations in the cumulative returns, this is the reason why fixed income assets (bond or cash) display flattened curves. Hence the pay-off is linear as the composed yield is timely incremental.

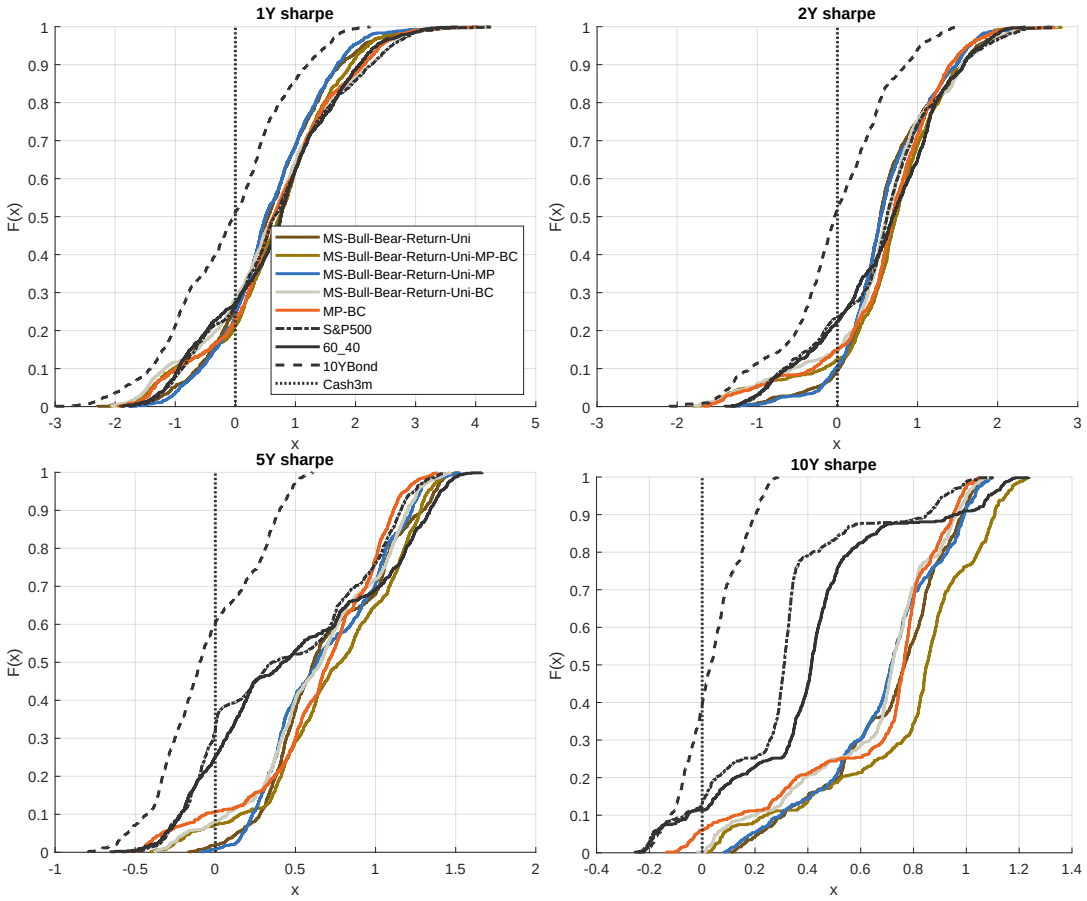

Figure 4.8: *Cumulative distribution functions of rolling window Sharpe ratios from 1 year to 10 year holding horizons*

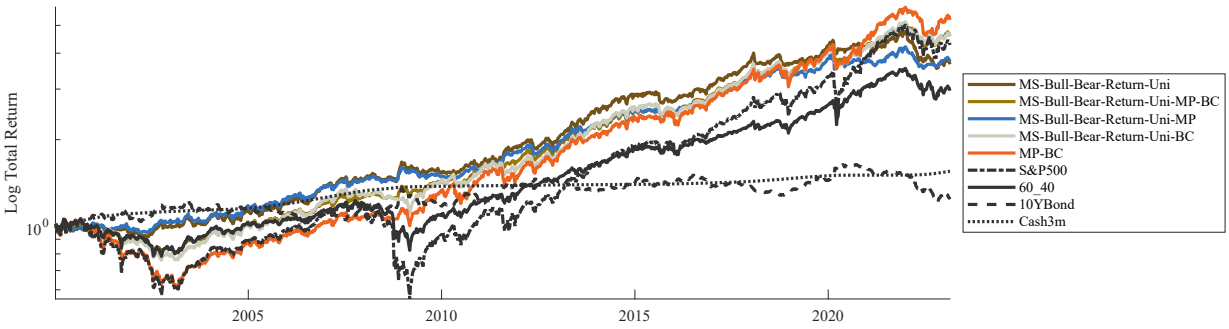

Figure 4.9: *Log total cumulative return of the selected strategies and benchmarks from 7th January 2000 to 24th February 2023.*

We now focus on the economic utility for the investor to invest in a specific strategy. Tables 4.2 and 4.3 report the rolling annual average fees Δ for respectively 1-year and 10-year holding periods. The values in the columns are the strategy fees that would make an investor with a given risk aversion indifferent between the strategy and the benchmark allocation. For each benchmark, two columns are presented referring to two aversion parameters γ in the quadratic utility in equation

(4.5). On a 1 year rolling holding period (4.2), and for each aversion coefficient, an investor will tend to prefer any competitive strategy compared to holding a constant 100% exposure to S&P500 or a fixed 60 % equities / 40 % bonds allocation. Ranking strategies based on absolute values of annual average fees Δs, one can highlight that an investor with low risk aversion ($\gamma = 1$) will tend to prefer a strategy mainly composed of the business cycle phase assessor and the monetary policy stance signal (MP-BC). An investor with a higher risk aversion ($\gamma = 10$) will prefer the strategy adding the market sentiment to the monetary policy stance signal (MS-Bull-Bear-Return-Uni-MP). The 3-signal approach (MS-Bull-Bear-Return-Uni-MP-BC) compares fairly well to the other strategies as it is globally always the second preferred except for a switch with low aversion from a 100% cash strategy, making it the most robust strategy.

Table 4.2: *1-year rolling window fees*

1Y	**S&P500**		**60/40**		**Cash**	
γ	1	10	1	10	1	10
MS-Bull-Bear-Return-Uni	0.92%	13.80%	1.69%	2.60%	5.17%	1.16%
MS-Bull-Bear-Return-Uni-BC	0.66%	11.98%	2.00%	1.72%	5.99%	0.84%
MS-Bull-Bear-Return-Uni-MP	0.65%	14.45%	1.38%	3.14%	4.75%	1.55%
MP-BC	1.26%	10.59%	2.65%	0.42%	6.81%	-0.32%
MS-Bull-Bear-Return-Uni-MP-BC	0.97%	13.93%	2.03%	3.03%	5.78%	1.84%

On a 10 year rolling holding period (4.3), and for each aversion coefficient, an investor prefers any competitive strategy compared to holding a constant 100% exposure to S&P500 or a fixed 60 % equities / 40 % bonds allocation. Ranking strategies based on absolute values of annual average fees Δs again, an investor with low risk aversion ($\gamma = 1$) prefers a strategy mainly composed of the business cycle phase assessor and the monetary policy stance signal. An investor with a higher risk aversion ($\gamma = 10$) will prefer the strategy adding the market sentiment to the two signals mentioned previously (MS-Bull-Bear-Return-Uni-MP-BC). Globally, the strategy applying the 3-signal approach compares very well and is the most reliable strategy when considering different aversion profiles and holding periods.

Table 4.3: *10-year rolling window fees*

10 Year	**S&P500**		**60/40**		**Cash**	
γ	1	10	1	10	1	10
MS-Bull-Bear-Return-Uni	1.20%	13.21%	2.49%	3.32%	6.37%	2.40%
MS-Bull-Bear-Return-Uni-BC	1.41%	12.46%	2.72%	2.63%	6.63%	1.73%
MS-Bull-Bear-Return-Uni-MP	0.28%	13.24%	1.56%	3.36%	5.40%	2.43%
MP-BC	2.24%	11.79%	3.57%	2.00%	7.52%	1.12%
MS-Bull-Bear-Return-Uni-MP-BC	1.39%	14.04%	2.70%	4.09%	6.60%	3.18%

4.5.3. Event study

In this subsection we focus on specific monetary and macroeconomic events to understand precisely the added value of the 3-signal strategy compared to the alternative ones. In our dataset, there

are three occurrences of macroeconomic downturns. The Dot com recession in 2001, the Great Financial Crisis from December of 2007 to May 2009 and the Covid recession. From the monetary policy standpoint, our dataset is composed of four rate hiking cycles as well as four cutting cycles. We have first the January to May 2000 monetary restriction phase, which in fact started in June 1999, intended to deflate the Dot com growing bubble and cooling down an economy at the time around its potential. The equity bubble started to crack in March 2000 and slowly to diffuse into the real economy, hence forcing the Federal Reserve to react and cut rates from January 2001 to December 2001, fighting the 8-month long recession and following a Taylor-type rule (Taylor (2007)). The recovery at the time was muted (jobless recovery as mentioned by Bernanke (2010)) and the geopolitical uncertainty brought by middle east wars made the Federal Market Committee decide two rate cuts in November 2002 and June 2003 to fight deflation fears. Starting from this final cut, US growth picked up again in 2004 and 2005. In the wake of this economic expansion, real estate imbalances started to appear obliging the Fed to dampen inflationary pressures from June 2004 to June 2006. The following housing burst started to spread to real economy with rising unemployment and triggered an easing cycle starting from September 2007 to April 2008. The Fed paused the easing cycle afterwards to evaluate the effects of its action. Recession began in December 2007 inducing financial confusion translating into the worst banking crisis in history deepening the macroeconomic downturn and forcing the Fed to reach the zero-lower bound (first-time in history) and to provide ample liquidity to the markets by implementing balance-sheet tools. By its amplitude and duration, the great financial recession became the worst economic downturn in US economic history. Hence bringing the necessity for monetary policy to use a set of new tools such as forward guidance and quantitative easing (Bernanke (2020)). After a false hawkish signal known as "taper tantrum" in May 2013 and in the wake of a recovering economy the FOMC proceeded to a gradual policy normalisation from December 2015 to December 2018. Growing concerns about inflation path and economic uncertainty induced by the Trade War between the US and China drove the FOMC to proceed to a "mid-cycle policy adjustment" in 2019. The outbreak of Covid-19 led to a two-month recession far fom historical standards by its duration and amplitude but obliged the FOMC to reach the zero-lower bound and provide historically ample liquidity to the markets again. The historic expansive policy mix in a supply-constrained world economy, amplified by the energy shock provoked by Ukraine War in February 2022 forced the FOMC to proceed to an expeditive monetary restriction from March 2022 to July 2023.

Figure 4.9 shows us that S&P500 was the asset class benefiting the most of the sequence described above compared to cash or long-term treasury bonds. The 60 % equities / 40 % bonds portfolio suffers from being constantly underexposed to the equity market. This fact is also depicted in Table 4.1. We now turn to the analysis of the strategies during "normal" and "abnormal" times. We characterize "abnormal" times as periods during which macroeconomic downturns occur or tightening monetary policy are implemented. "Normal" times are periods of economic expansion and either neutral monetary policy stance or easing ones. Only two years over our 23 year long sample have experienced a monetary easing cycle: 2007 and 2019.

Table 4.4 displays annual Sharpe ratios during recession years. Given the "safe heaven" nature of long-term Treasury bonds, this is the only asset class which performs on average positively during recession years. Moreover, recession periods are accompanied with monetary policy easing to counter deflationary pressures or unsustainable high employment with respect to the Federal Reserve dual mandate. Yet, the profile remain very heterogeneous across downturn years as the 2009 recovery has pushed long term yields up,as part of market reflation expectations mechanism. Equity indices suffer from macroeconomic headwinds, on average the Sharpe ratios are slightly negative. Yet, 2009 recession exit and ample monetary support made the S&P500 skyrocket in the second part of the year, thus yielding a positive annual Sharpe ratio (the 2009 market recovery was steady as displayed in Figure 4.10). Likewise, the 2020 recession brought the Sharpe ratio in positive territories given the historical monetary and budgetary stimulus in US economy (as the cumulative returns show in Figure 4.11). The constant 60 % equities / 40 % bonds portfolio also displays a slightly negative Sharpe ratio on average during recession years. Two competitive strategies outperform the 60 % equities / 40 % bonds constant portfolio on average during recession years: the strategy implementing a monetary stance/business cycle detection (MP-BC) with a positive Sharpe ratio on average. The second best remains the strategy adding the Market sentiment to the above mentioned 2 signals (MS-Bull-Bear-Return-Uni-MP-BC). This result is also even more striking when looking at returns themselves in Table 4.16 showed in Appendix 4.7.4.3.

Table 4.4: *Annual Sharpe Ratios during recessions*

	2001	**2008**	**2009**	**2020**	**Average**
MS-Bull-Bear-Return-Uni	-1.24	1.16	-0.86	-0.11	-0.26
MS-Bull-Bear-Return-Uni-BC	-1.34	-1.53	1.29	0.13	-0.36
MS-Bull-Bear-Return-Uni-MP	-1.15	1.05	-1.05	-0.24	-0.35
MP-BC	**-1.29**	**0.44**	**1.15**	**0.39**	**0.17**
MS-Bull-Bear-Return-Uni-MP-BC	**-1.56**	**0.84**	**0.54**	**0.15**	**-0.01**
S&P500	-0.65	-1.29	1.20	0.50	-0.06
60/40	-0.78	-1.17	0.87	0.83	-0.06
10 Year Bond	-0.63	1.54	-1.28	1.28	0.23

Table 4.5 displays annual Sharpe ratios during monetary tightening cycles. Long term Treasuries generally suffer from Monetary policy tightening cycles as yield rise along the maturity curve. This explains the negative average Sharpe ratio. The 60 % equities / 40 % bonds portfolio suffers from this Bond dynamic. Surprisingly the S&P500 index resists quite well to those monetary restriction periods with a positive average Sharpe ratio. The Table shows nonetheless the ability of strategies incorporating business cycle phases and monetary policy stance or the 3-signal approach to outperform the 60 % equities / 40 % bonds portfolio. When looking at yearly returns in Table 4.17, Appendix 4.7.4.3, adding the monetary policy stance signal always enable to limit losses. 2022 is a text-book case of restrictive monetary policy. Table 4.17 shows the ability of strategies incorporating either the market sentiment and monetary policy stance or the 3-signal approach to drastically reduce the loss incurred. The profile of the cumulative returns shown in Figure 4.12 confirm this fact. Adding the monetary policy stance to the market sentiment or to the market sentiment and business cycle phase assessor combined during 2022 allows the investor with

a quadratic utility function to always prefer being invested in those strategies compared to the S&P500 or the 60 % equities / 40 % bonds portfolio (Table 4.7). The results in the Table 4.7 are quite intuitive: the investor would always have chosen to remain fully cash invested, no matter his aversion profile. Nonetheless, compared to the other two benchmark strategies and for each aversion parameter γ, he would have chosen a strategy capable of tracking the monetary policy risk. This is in line with Cochrane (1999) who highlights that risk-averse investors might favour a portfolio with lower Sharpe ratio in a context of time-varying risk and return, if it is able to offer a hedge during times of financial distress.

Table 4.5: *Annual Sharpe Ratios during monetary policy tightening*

	2000	**2004**	**2005**	**2006**	**2015**	**2016**	**2017**	**2018**	**2022**	**Average**
MS-Bull-Bear-Return-Uni	-0.73	0.73	0.10	1.03	-0.61	1.45	3.56	-0.40	-2.40	0.30
MS-Bull-Bear-Return-Uni-BC	-0.59	0.94	0.12	1.05	-0.21	0.94	3.56	-0.44	-1.18	0.47
MS-Bull-Bear-Return-Uni-MP	-0.69	1.06	0.09	0.76	-0.42	1.55	3.40	-0.37	-1.66	0.41
MP-BC	**-0.46**	**1.31**	**0.11**	**0.77**	**0.17**	**0.81**	**3.41**	**-0.37**	**-0.95**	**0.53**
MS-Bull-Bear-Return-Uni-MP-BC	**-0.55**	**1.19**	**0.10**	**0.77**	**-0.06**	**1.22**	**3.40**	**-0.39**	**-1.38**	**0.48**
S&P500	-0.62	1.02	0.14	1.05	0.03	0.80	3.57	-0.41	-0.89	0.52
60/40	-0.52	0.94	-0.21	0.41	0.05	0.76	3.19	-0.59	-1.33	0.30
10 Year Bond	0.32	-0.30	-1.00	-1.78	-0.07	-0.28	-0.28	-1.14	-2.11	-0.74

Table 4.6 displays the annual Sharpe ratios of the competing strategies in normal times. At first glance, the 60 % equities / 40 % bonds portfolio is the one yielding the higher risk-scaled return on average. S&P 500 is the second asset class with regard to historical standards. The strategies we propose exhibit Sharpe ratios superior to 1 and beat the 100% Bond portfolio. This result validates the idea that the investor pays an insurance fee against "abnormal episodes". If the economic and monetary cycles were only composed of steady expanding periods one could consider the 60 % equities / 40 % bonds portfolio as the best solution for asset allocation. This is also the reason why this allocation strategy has been the race-horse for decades in asset management industry. The annual returns in "normal" periods displayed in Appendix 4.7.4.3, Table 4.15 confirm the S&P500 yields the better performance. At a cost of higher volatility, all alternative strategies except the one incorporating the risk sentiment and the monetary policy stance signal tend to outperform the 60 % equities / 40 % bonds portfolio on average.

Table 4.6: *Annual Sharpe Ratios during "normal times"*

	2002	**2003**	**2007**	**2010**	**2011**	**2012**	**2013**	**2014**	**2019**	**2021**	**Average**
MS-Bull-Bear-Return-Uni	0.88	0.33	0.05	0.91	1.55	0.25	3.1	1.16	1.91	1.48	1.17
MS-Bull-Bear-Return-Uni-BC	-1.56	1.68	-0.04	0.72	0.23	0.71	3.2	1.27	2.29	2.36	1.09
MS-Bull-Bear-Return-Uni-MP	1.23	0.07	-0.04	0.84	1.81	0.18	2.5	1.13	1.89	1.51	1.12
MP-BC	**-1.62**	**1.63**	**-0.07**	**0.61**	**0.14**	**1.06**	**2.6**	**1.38**	**2.70**	**2.55**	**1.10**
MS-Bull-Bear-Return-Uni-MP-BC	**-1.39**	**1.51**	**-0.06**	**0.92**	**0.99**	**0.71**	**2.6**	**1.25**	**2.47**	**2.16**	**1.12**
S&P500	-1.25	1.69	0.06	0.77	0.08	1.16	3.3	1.38	2.74	2.51	1.24
60/40	-1.17	1.70	0.08	1.11	0.70	1.72	2.1	2.12	3.36	2.18	1.39
10 Year Bond	1.17	-0.33	-0.14	0.64	1.51	0.34	-1.4	1.30	0.82	-0.71	0.32

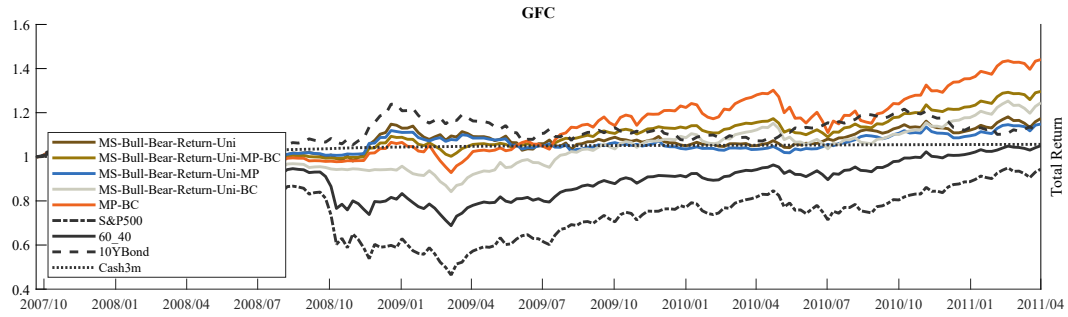

Figure 4.10: *Cumulative return of the selected strategies and benchmarks during the Great Financial Crisis and its aftermath*

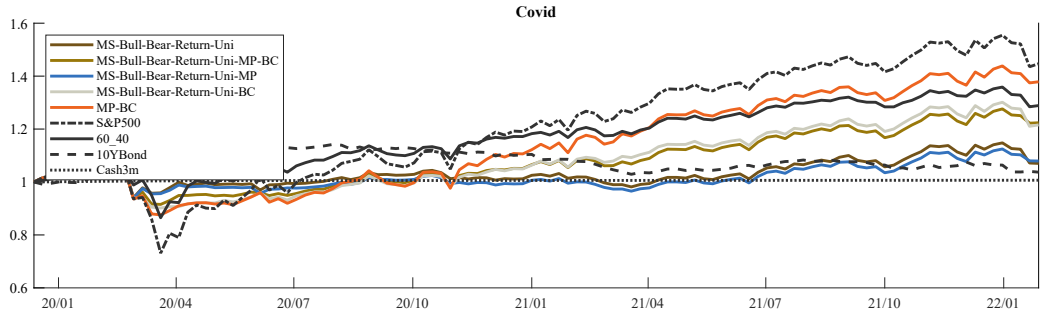

Figure 4.11: *Cumulative return of the selected strategies and benchmarks during the Covid crisis and its aftermath*

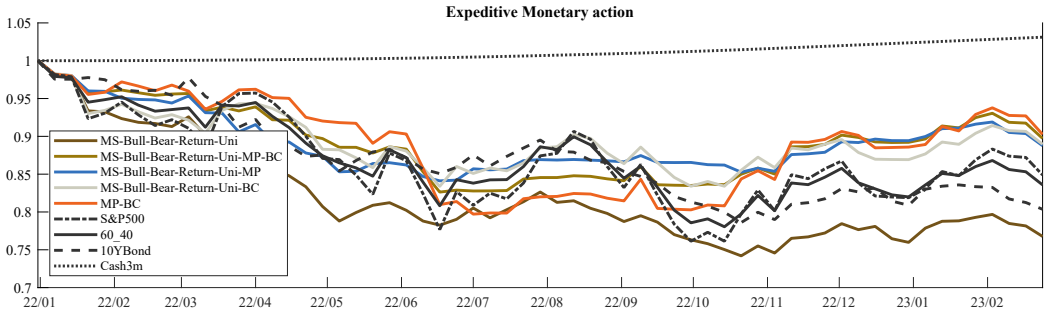

Figure 4.12: *Cumulative return of the selected strategies and benchmarks during the 2022 monetary policy tightening*

Table 4.7: *2022 annual fees*

2022	**S&P500**		**60/40**		**Cash**	
γ	1	10	1	10	1	10
MS-Bull-Bear-Return-Uni	-7.39%	10.13%	-7.18%	-2.63%	-25.32%	-29.34%
MS-Bull-Bear-Return-Uni-BC	6.02%	23.53%	6.27%	9.19%	-14.45%	-20.82%
MS-Bull-Bear-Return-Uni-MP	8.91%	32.70%	9.17%	17.45%	-12.11%	-14.52%
MP-BC	8.13%	23.88%	8.38%	9.45%	-12.74%	-20.73%
MS-Bull-Bear-Return-Uni-MP-BC	8.77%	30.94%	9.03%	15.85%	-12.22%	-15.76%

4.6. Conclusion

Investors seeking consistent returns across economic phases, both from a business cycle and monetary policy perspective, face challenging questions regarding portfolio construction. Trying to time the occurrence of the phases on each of those axes can be of a great relevance to that aim. This work shows the added value for an investor who wants to diversify its portfolio to take into account business cycle dynamics, market sentiment and monetary policy stance. The Chapter contributions to the regime-contingent asset allocation literature are three-fold.

It first introduces a novel approach to gauge the monetary policy regime through real interest rates dynamics using a Markov-switching dynamic factor model capturing the co-movement of long-term maturities real yields. This model proves to be reliable in identifying monetary policy restriction signals both in-sample and out-of-sample using weekly market data.

It then extends Maheu et al. (2012) bull/bear specification into a dynamic factor model in order to capture a multivariate equity market sentiment allowing for bull corrections and bear rallies. This signal succeeds in capturing an underlying market sentiment across four major US equity indices.

This Chapter finally combines the monetary policy stance signal with the market sentiment and a weekly real-time business cycle phase assessor within a long-only asset allocation framework. The benefit for an investor to take into account those three dimensions is paramount to weigh dynamically its portfolio. The regimes along those axes and their underlying market prices dynamics warrant allocations beyond the traditional fixed 60 % equities / 40 % bonds portfolio. The backtests implemented show that taking into account the three-signal approach in a dynamic equity/bond/cash hedging strategy maximizes the Sharpe ratio between the 7th of January 2000 to the 24th February 2023. Moreover, no matter the portfolio holding period considered (rolling 1 year to 10 year windows) or the monetary/economic regime faced the returns and Sharpe ratios are higher than the 60 % equities / 40 % bonds benchmark advocating this approach is reliable for an investor who seeks steady returns. The economic utility of the investor in strategies incorporating those three cycles shows to be maximal on 1 year to 10 year rolling windows regardless of his/her risk aversion profile.

This promising framework could be used in a bigger investment universe. One could also consider the assets weighting scheme being defined by traditional portfolio construction optimizations such as mean-variance, constant volatility or a risk parity approach. A multi-country adaptation of this model would be relevant to allow for a geographical diversification. Those questions are left for further research.

4.7. Appendix

4.7.1. Priors

4.7.1.1. Monetary policy stance identification

This section describes the priors used for the distributions of the parameter vector $\boldsymbol{\vartheta}^{(MP)}$.
λ_1 is set to one for identification purposes. For all $j = 2, \ldots, m$, we use the following prior to sample λ_j the j-th element of the factor loading matrix $\boldsymbol{\Lambda}$ in (4.1)

$$\lambda_j \sim \mathcal{N}(a_j, A_j) \tag{4.6}$$

where hyperparameters are set to $a_j = 0$ and $A_j = 1$. To sample the parameters linked to the residuals $u_{j,t}$ in (4.2), we use the following priors, for $l = 1$,

$$\begin{aligned} \psi_{j,l} \sim &\quad \mathcal{N}(\pi, \Pi) \quad \pi = 0, \Pi = 1 \\ \sigma^2_{e,j} \sim &\quad IG(\nu_i, Z_i) \quad \nu_i = 20, Z_i = 20 \end{aligned} \tag{4.7}$$

where IG denotes the inverse-gamma distribution. Each row of $\mathbf{P^{(MP)}}$ follows a Dirichlet distribution.

$$\begin{aligned} \{p_{1,1}, p_{1,2}, p_{1,3}, p_{1,4}\} &\sim Dir(2000, .5, 150, .5) \\ \{p_{2,1}, p_{2,2}, p_{2,3}, p_{2,4}\} &\sim Dir(.5, 2000, .5, 150) \\ \{p_{3,1}, p_{3,2}, p_{3,3}, p_{3,4}\} &\sim Dir(150, 15, 2000, 100) \\ \{p_{4,1}, p_{4,2}, p_{4,3}, p_{4,4}\} &\sim Dir(.5, 150, 100, 2000) \end{aligned}$$

The prior for the Markov-switching intercept in equation (4.3) is given by :

$$\boldsymbol{\mu} = (\mu_1, \mu_2, \mu_3, \mu_4)' \sim \mathcal{N}(\alpha^*, A^*) \tag{4.8}$$

with $\alpha^* = (-1, 1, 0, 0)'$ and $A^* = \mathbf{I}_4$.

The prior for the factor variance in equation (4.3) is given by, for $i = 1, ..., 4$:

$$\sigma_i^2 \sim \quad IG(\nu_i^*, Z_i^*) \quad \nu_i^* = 20, Z_i^* = 20$$

4.7.1.2. Business Cycle turning point detection

This section describes the priors used for the distributions of the parameter vector $\boldsymbol{\vartheta}^{(BC)}$.
λ_1 is set to one for identification purposes. For all $j = 2, \ldots, m$, we use the following prior to sample λ_j the j-th element of the factor loading matrix $\boldsymbol{\Lambda}$ in (4.1)

$$\lambda_j \sim \mathcal{N}(a_j, A_j) \tag{4.9}$$

where hyperparameters are set to $a_j = 0$ and $A_j = 0.1$. To sample the parameters linked to the residuals $u_{j,t}$ in (4.2), we use the following priors, for $l = 1, 2$,

$$\begin{aligned} \psi_{j,l} \sim &\quad \mathcal{N}(\pi, \Pi) \quad \pi = 0, \Pi = 0.1 \\ \sigma^2_{e,j} \sim &\quad IG(\nu_i, Z_i) \quad \nu_i = 2, Z_i = 1 \end{aligned} \tag{4.10}$$

where IG denotes the inverse-gamma distribution. Additionally, independent beta distributions can be used as conjugate prior for each transition probability

$$\pi(q, p) \propto q^{u_{00}}(1-q)^{u_{01}} p^{u_{11}}(1-p)^{u_{10}} \tag{4.11}$$

As in Doz et al. (2020), we put an informative prior and set $u_{00} = 470, u_{01} = 9, u_{10} = 9, u_{11} = 90$ in order to take into account the relative persistence of each of the regimes as observed on macroeconomic data. The prior for the Markov-switching intercept in equation (4.3) is given by :

$$\boldsymbol{\mu} = (\mu_0, \mu_1)' \sim \mathcal{N}(\alpha^*, A^*) \tag{4.12}$$

with $\alpha^* = (.3, -.3)'$ and $A^* = \text{diag}(0.04, 0.04)$. We acknowledge that, in the spirit of Leiva-Leon et al. (2020), relatively tight priors are used for identification purposes. The informativeness brought by the first moment is indeed needed to discriminate between the regimes over the parameters space. The prior for the autoregressive parameter ϕ in equation (4.3) is given by

$$\phi \sim \mathcal{N}(\alpha, A) \tag{4.13}$$

where $\alpha = 0$, $A = 0.1$. In the case of a MS-DFM-ARCH, we use the following prior for the vector $\boldsymbol{\theta}^{(\text{ARCH})} = (\omega, \alpha)$

$$\log \boldsymbol{\theta}^{(\text{ARCH})} \sim \mathcal{N}(\theta_0^{(\text{ARCH})}, V_\theta) \mathbb{1}(\alpha < 1).$$

$\boldsymbol{\theta}^{(\text{ARCH})}$ thus follows a truncated log-normal distribution with the stationarity restriction that $\alpha < 1$. We set the hyperparameters to $\theta_0^{(\text{ARCH})} = \log(1, 0.5)$ and $V_\theta = \text{diag}(1, 1)$.

4.7.1.3. Market sentiment

This section describes the priors used for the distributions of the parameter vector $\boldsymbol{\vartheta}^{(MP)}$.
λ_1 is set to one for identification purposes. For all $j = 2, \ldots, m$, we use the following prior to sample λ_j the j-th element of the factor loading matrix $\boldsymbol{\Lambda}$ in (4.1)

$$\lambda_j \sim \mathcal{N}(a_j, A_j) \tag{4.14}$$

where hyperparameters are set to $a_j = 0$ and $A_j = 1$. To sample the parameters linked to the residuals $u_{j,t}$ in (4.2), we use the following priors, for $l = 1$,

$$\begin{aligned} \psi_{j,l} \sim &\quad \mathcal{N}(\pi, \Pi) \quad \pi = 0, \Pi = 1 \\ \sigma^2_{e,j} \sim &\quad IG(\nu_i, Z_i) \quad \nu_i = 2, Z_i = \sigma^2_{y_j} \end{aligned} \tag{4.15}$$

where IG denotes the inverse-gamma distribution. Each row of $\mathbf{P^{(MS)}}$ follows a Dirichlet distribution.

$$\begin{aligned}
\{p_{1,1}, p_{1,2}, p_{1,4}\} &\sim Dir(8, 1.5, 0.5) \\
\{p_{2,1}, p_{2,2}, p_{2,4}\} &\sim Dir(1.5, 8, 0.5) \\
\{p_{3,1}, p_{3,3}, p_{3,4}\} &\sim Dir(0.5, 8, 1.5) \\
\{p_{4,1}, p_{4,3}, p_{4,4}\} &\sim Dir(0.5, 1.5, 8)
\end{aligned}$$

The prior for the Markov-switching intercept in equation (4.3) is given by :

$$\boldsymbol{\mu} = (\mu_1, \mu_2, \mu_3, \mu_4)' \sim \mathcal{N}(\alpha^*, A^*) \tag{4.16}$$

with $\alpha^* = (-.7, .2, -.2, .3)'$ and $A^* = \mathbf{I}_4$.

The prior for the factor variance in equation (4.3) is given by, for $i = 1, ..., 4$:

$$\sigma_i^2 \sim \quad IG(\nu_i^*, Z_i^*) \quad \nu_i^* = 2, Z_i^* = \sigma_{y_1}^2$$

4.7.2. Bayesian Estimation

Let $\boldsymbol{z}^{(T)} = \{\boldsymbol{z}_1, ..., \boldsymbol{z}_T\}$ the unobserved state, $\boldsymbol{y}^{(T)} = \{\boldsymbol{y}_1, ..., \boldsymbol{y}_T\}$ the observed data and $S^{(T)} = \{S_1, ..., S_T\}$ the first order Markov-Chain. We describe the Gibbs sampler steps based on Kim and Nelson (1999) and follow their notations. The Gibbs sampler consists of iterating between the three following steps sequentially.

4.7.2.1. Generation of the state vector

The joint distribution of $\boldsymbol{z}^{(T)}$, given $\boldsymbol{y}^{(T)}$, $S^{(T)}$ and $\boldsymbol{\vartheta}^{(.)}$ can be defined as

$$p(\boldsymbol{z}^{(T)} \mid \boldsymbol{y}^{(T)}, S^{(T)}, \boldsymbol{\vartheta}^{(.)}) = p(\boldsymbol{z}_T \mid \boldsymbol{y}^{(T)}, S^{(T)}, \boldsymbol{\vartheta}^{(.)}) \prod_{t=1}^{T-1} p(\boldsymbol{z}_t \mid \boldsymbol{y}^{(t)}, S^{(t)}, \boldsymbol{\vartheta}^{(.)}, \boldsymbol{z}_{t+1})$$

which boils down to generating $\boldsymbol{z}_t$ for $t = T, T-1, ..., 1$ from

$$\begin{aligned}
&\boldsymbol{z}_T \mid \boldsymbol{y}^{(T)}, S^{(T)}, \boldsymbol{\vartheta}^{(.)} \sim \mathcal{N}(\boldsymbol{z}_{T|T}, \boldsymbol{V}_{T|T}) \\
&\boldsymbol{z}_t \mid \boldsymbol{y}^{(t)}, S^{(t)}, \boldsymbol{z}_{t+1}, \boldsymbol{\vartheta}^{(.)} \sim \mathcal{N}(\boldsymbol{z}_{t|t,\boldsymbol{z}_{t+1}}, \boldsymbol{V}_{t|t,\boldsymbol{z}_{t+1}})
\end{aligned} \tag{4.17}$$

where $\boldsymbol{z}_{t|t} = E(\boldsymbol{z}_t \mid \boldsymbol{y}^{(t)})$ and $\boldsymbol{V}_{t|t} = Var(\boldsymbol{z}_t \mid \boldsymbol{y}^{(t)})$ for $t = 1, ..., T$. In equation (4.17), $\boldsymbol{z}_T \mid \boldsymbol{y}^{(T)}, S^{(T)}, \boldsymbol{\vartheta}^{(.)}$ can be generated using the Multi-move Gibbs sampling introduced by Carter and Kohn (1994) as follows

1. We use the Kalman filter to obtain $\boldsymbol{z}_{t|t}$ and $\boldsymbol{V}_{t|t}$ for $t = 1, ..., T$. The last iteration of the filter gives $\boldsymbol{z}_{T|T}$ and $\boldsymbol{V}_{T|T}$ which are then used to generate $\boldsymbol{z}_T$.

2. For $t = T-1, T-2, ..., 1$, $\boldsymbol{z}_{t|t}$ and $\boldsymbol{V}_{t|t}$, $\boldsymbol{z}_{t+1}$ can be considered as an incremental vector of observations in the system. The distribution $p(\boldsymbol{z}_t \mid \boldsymbol{y}^{(T)}, S^{(t)}, \boldsymbol{\vartheta}^{(.)}, \boldsymbol{z}_{t+1})$ is then deduced from the Kalman smoother. From equation (4.4), updating equation are then given by

$$\begin{aligned}\boldsymbol{z}_{t|t,\boldsymbol{z}_{t+1}} &= \boldsymbol{z}_{t|t} + \boldsymbol{V}_{t|t}\boldsymbol{\Xi}\tilde{\boldsymbol{\varsigma}}_t/R_t \\ \boldsymbol{V}_{t|t,\boldsymbol{z}_{t+1}} &= \boldsymbol{V}_{t|t} - \boldsymbol{V}_{t|t}\boldsymbol{\Xi}'\boldsymbol{\Xi}\boldsymbol{V}'_{t|t}/R_t\end{aligned}$$

where $\tilde{\boldsymbol{\varsigma}}_t = \boldsymbol{z}_{t+1} - \boldsymbol{\delta}_{S_{t+1}} - \boldsymbol{\Xi}\boldsymbol{z}_{t|t}$ and $R_t = \boldsymbol{\Xi}\boldsymbol{V}_{t|t}\boldsymbol{\Xi}' + \sigma^2_{t+1}$.

4.7.2.2. Generation of the Markov Chain

Once $\boldsymbol{z}^{(T)}$ has been simulated, given $\boldsymbol{\vartheta}^{(.)}$, the Markov Chain $S^{(T)}$ can be generated from the following distribution

$$\begin{aligned}p(S^{(T)} \mid \boldsymbol{y}^{(T)}, \boldsymbol{z}^{(T)}, \boldsymbol{\vartheta}^{(.)}) &= p(S_T \mid \boldsymbol{y}^{(T)}, \boldsymbol{z}^{(T)}, \boldsymbol{\vartheta}^{(.)}) \prod_{t=1}^{T-1} p(S_t \mid \boldsymbol{y}^{(t)}, \boldsymbol{z}^{(t)}, S_{t+1}, \boldsymbol{\vartheta}^{(.)}) \\ &= p(S_T \mid \boldsymbol{z}^{(T)}, \boldsymbol{\vartheta}^{(.)}) \prod_{t=1}^{T-1} p(S_t \mid \boldsymbol{z}^{(t)}, S_{t+1}, \boldsymbol{\vartheta}^{(.)})\end{aligned}$$

as the distribution of $S^{(T)}$ is orthogonal to $\boldsymbol{y}^{(T)}$ given $\boldsymbol{z}^{(T)}$. We can thus obtain conditional draws for $S^{(T)}$ as follows

1. We use the Hamilton (1989) filter on (4.3) to generate $p(S_t \mid \boldsymbol{z}^{(t)}, \boldsymbol{\vartheta}^{(.)})$ for $t = 1, 2, ..., T$ and save them. The last iteration gives $p(S_T \mid \boldsymbol{z}^{(T)}, \boldsymbol{\vartheta}^{(.)})$ from which we get S_T.

2. To draw S_t given $\boldsymbol{z}^{(T)}$ and S_{t+1}, for $t = T-1, T-2, ..., 1$ the following result is used

$$p(S_t \mid \boldsymbol{z}^{(t)}, S_{t+1}, \boldsymbol{\vartheta}^{(.)}) = \frac{p(S_{t+1} \mid S_t) p(S_t \mid \boldsymbol{z}^{(t)}, \boldsymbol{\vartheta}^{(.)})}{p(S_{t+1} \mid \boldsymbol{z}^{(t)}, \boldsymbol{\vartheta}^{(.)})} \propto p(S_{t+1} \mid S_t) p(S_t \mid Z^{(t)}, \boldsymbol{\vartheta}^{(.)})$$

   where $p(S_{t+1} \mid S_t)$ is the transition probability in $\boldsymbol{\vartheta}^{(.)}$ and $p(S_t \mid \boldsymbol{z}^{(t)}, \boldsymbol{\vartheta}^{(.)})$ is obtained form the values saved in the previous step.

3. The last step consists in drawing from

$$Pr(S_t = 1 \mid \boldsymbol{z}^{(t)}, S_{t+1}, \boldsymbol{\vartheta}^{(.)}) = \frac{p(S_{t+1} \mid S_t = 1) p(S_t = 1 \mid \boldsymbol{z}^{(t)}, \boldsymbol{\vartheta}^{(.)})}{\sum_{j=0}^{1} p(S_{t+1} \mid S_t = j) p(S_t = j \mid \boldsymbol{z}^{(t)}, \boldsymbol{\vartheta}^{(.)})}$$

   where S_t is drawn from a uniform distribution $S_t \sim \mathcal{U}(0,1)$. If the generated number is smaller than $Pr(S_t = 1 \mid S_{t+1}, \boldsymbol{z}^{(t)}, \boldsymbol{\vartheta}^{(.)})$, $S_t = 1$, otherwise $S_t = 0$.

4.7.2.3. Generation of the parameters vector

4.7.2.3.1 Monetary policy stance identification

To generate $\mathbf{P}^{(\mathbf{MP})}$, we follow Geweke (2005). We denote the sum of transitions from the state $S_{t-1} = i$ to $S_t = j$ by n_{ij}. Each row of $^{(\mathbf{MP})}$ are drawn from posteriors:

$$
\begin{aligned}
&Dir(2000 + n_{11}, .5 + n_{12}, 150 + n_{13}, .5 + n_{14}) \\
&Dir(.5 + n_{21}, 2000 + n_{22}, .5 + n_{23}, 150 + n_{24}) \\
&Dir(150 + n_{31}, 15 + n_{32}, 2000 + n_{33}, 100 + n_{34}) \\
&Dir(.5 + n_{41}, 150 + n_{42}, 100 + n_{43}, 2000 + n_{44})
\end{aligned}
$$

Given $\boldsymbol{y}^{(T)}$ and $f^{(T)}$, we can rewrite equation-by-equation equation (4.1) with

$$
y^*_{j,t} = \lambda_j f^*_{j,t} + e_{j,t}
$$

for $j = 2, \ldots, m$, where $y^*_{j,t}$ and $f^*_{j,t}$ are the j-the respective components of

$$
\begin{aligned}
\boldsymbol{y}^*_t = &\quad \boldsymbol{y}_t - \bar{\boldsymbol{\psi}}_1 \circ \boldsymbol{y}_{t-1} \\
\boldsymbol{f}^*_t = &\quad \boldsymbol{e}_m f_t - \bar{\boldsymbol{\psi}}_1 f_{t-1}
\end{aligned}
\tag{4.18}
$$

with $\boldsymbol{e}_m$ denoting a vector of 1 of length m qnd $\bar{\boldsymbol{\psi}}_l = (\psi_{1,l}, \ldots, \psi_{m,l})$, $l = 1$ being the order of the AR specification in equation (4.2). From (4.6) and (4.18), we obtain conditional draws for λ_j from the posterior distribution

$$
\mathcal{N}\left[\left(A_j^{-1} + \sigma_{e,j}^{-2} f_j^{*(T)'} f_j^{*(T)}\right)^{-1} \left(A_j a_j + \sigma_{e,j}^{-2} f_j^{*(T)'} y_j^{*(T)}\right), \left(A_j^{-1} + \sigma_{e,j}^{-2} f_j^{*(T)'} f_j^{*(T)}\right)^{-1}\right].
$$

Given $\boldsymbol{y}^{(T)}$ and $f^{(T)}$, from (4.1) we can measure $\boldsymbol{u}^{(T)}$ and from equation (4.2) and the prior distribution (4.10), for all $j = 1, \ldots, m$, we can draw $\boldsymbol{\psi}_j$ from the posterior distribution

$$
\mathcal{N}\left[\left(\boldsymbol{\Pi}_j^{-1} + \sigma_{e,j}^{-2} \boldsymbol{w}_j^{(T)'} \boldsymbol{w}_j^{(T)}\right)^{-1} \left(\boldsymbol{\Pi}_j^{-1} \boldsymbol{\pi}_j + \sigma_{e,j}^{-2} \boldsymbol{w}_j^{(T)'} u_j^{(T)}\right), \left(\boldsymbol{\Pi}_j^{-1} + \sigma_{e,j}^{-2} \boldsymbol{w}_j^{(T)'} \boldsymbol{w}_j^{(T)})^{-1}\right)\right]
$$

where $\boldsymbol{w}_{j,t} = (u_{j,t-1}, u_{j,t-2})'$. Similarly, from the generated $\boldsymbol{\psi}_j$ and from (4.10), we can draw $\sigma^2_{e,j}$ from the posterior distribution

$$
IG\left(\nu_j + \frac{T}{2}, Z_j + \frac{\left(u_j^{(T)} - \boldsymbol{\psi}_j' \boldsymbol{w}_j^{(T)}\right)' \left(u_j^{(T)} - \boldsymbol{\psi}_j' \boldsymbol{w}_j^{(T)}\right)}{2}\right).
$$

Finally, we turn to the generation of (μ_0, μ_1, ϕ). Rewriting equation (4.3), we have

$$
\frac{f_t}{\sigma_{S_t}} = \frac{\mu_{S_t}}{\sigma_{S_t}} + \eta_t
$$

Let us denote G^*_t the left-hand side of the above equation and

$$
Q^{*(T)} = \left[\begin{array}{cccc} S^{(T)} = 1 & S^{(T)} = 2 & S^{(T)} = 3 & S^{(T)} = 4 \end{array}\right]
$$

From the prior distribution (4.12), $\boldsymbol{\mu}$ can be drawn from the posterior distribution :

$$\boldsymbol{\mu} \sim \mathcal{N}((A^{*-1} + Q^{*(T)\prime}Q^{*(T)})^{-1}(A^{*-1}\alpha + Q^{*(T)\prime}G^{*(T)}), (A^{*-1} + Q^{*(T)\prime}Q^{*(T)})^{-1}),$$

and only draws verifying the condition $\mu_1 < \mu_3 < 0 < \mu_4 < \mu_2$ are kept. For $i = 1...n$, $\sigma^2_{S_t=i}$ is drawn from the posterior distribution:

$$IG\left(.5 + \frac{\sum_{t=1}^{T}(S_t = i)}{2}, 20 + \frac{\left(f_{S^{(T)}=i} - \mu_{S_t=i}\right)'\left(f_{S^{(T)}=i} - \mu_{S_t=i}\right)}{2}\right).$$

and only draws verifying the condition $\sigma_1 > \sigma_3$ and $\sigma_2 > \sigma_4$

4.7.2.3.2 Business Cycle turning point detection

We now turn to the generation of draws for the vector of parameters. To do so, we will sequentially draw components of the $\boldsymbol{\vartheta}$ vector as follows.
We obtain conditional draws for the transition probabilities p and q following Albert and Chib (1993). In particular, given $S^{(T)}$ and the initial state, we denote the sum of transitions from the state $S_{t-1} = i$ to $S_t = j$ by n_{ij}, the log-likelihood is given by

$$L(q, p) = q^{n_{00}}(1-q)^{n_{01}}p^{n_{11}}(1-p)^{n_{10}}.$$

By combining the likelihood function and the conjugate priors presented in the previous section, from equation (4.11), we get the conditional distributions of (p, q) as the product of the independent beta distributions from which we generate p and q as

$$\begin{aligned} q \mid S^{(T)} &\sim \text{Beta}(u_{00} + n_{00}, u_{01} + n_{01}) \\ p \mid S^{(T)} &\sim \text{Beta}(u_{11} + n_{11}, u_{10} + n_{10}). \end{aligned}$$

Given $\boldsymbol{y}^{(T)}$ and $f^{(T)}$, we can rewrite equation-by-equation equation (4.1) with

$$y^*_{j,t} = \lambda_j f^*_{j,t} + e_{j,t}$$

for $j = 2, \ldots, m$, where $y^*_{j,t}$ and $f^*_{j,t}$ are the j-the respective components of

$$\begin{aligned} \boldsymbol{y}^*_t &= \boldsymbol{y}_t - \bar{\boldsymbol{\psi}}_1 \circ \boldsymbol{y}_{t-1} \\ \boldsymbol{f}^*_t &= \boldsymbol{e}_m f_t - \bar{\boldsymbol{\psi}}_1 f_{t-1} \end{aligned} \tag{4.19}$$

with $\boldsymbol{e}_m$ denoting a vector of 1 of length m qnd $\bar{\boldsymbol{\psi}}_l = (\psi_{1,l}, \ldots, \psi_{m,l})$, $l = 1$ being the order of the AR specification in equation (4.2). From (4.9) and (4.19), we obtain conditional draws for λ_j from the posterior distribution

$$\mathcal{N}\left[\left(A_j^{-1} + \sigma_{e,j}^{-2} f_j^{*(T)'} f_j^{*(T)}\right)^{-1}\left(A_j a_j + \sigma_{e,j}^{-2} f_j^{*(T)'} y_j^{*(T)}\right), \left(A_j^{-1} + \sigma_{e,j}^{-2} f_j^{*(T)'} f_j^{*(T)}\right)^{-1}\right].$$

Given $\boldsymbol{y}^{(T)}$ and $f^{(T)}$, from (4.1) we can measure $\boldsymbol{u}^{(T)}$ and from equation (4.2) and the prior distribution (4.10), for all $j = 1, \ldots, m$, we can draw $\boldsymbol{\psi}_j$ from the posterior distribution

$$\mathcal{N}\left[\left(\boldsymbol{\Pi}_j^{-1} + \sigma_{e,j}^{-2}\boldsymbol{w}_j^{(T)'}\boldsymbol{w}_j^{(T)}\right)^{-1}\left(\boldsymbol{\Pi}_j^{-1}\boldsymbol{\pi}_j + \sigma_{e,j}^{-2}\boldsymbol{w}_j^{(T)'}u_j^{(T)}\right), \left(\boldsymbol{\Pi}_j^{-1} + \sigma_{e,j}^{-2}\boldsymbol{w}_j^{(T)'}\boldsymbol{w}_j^{(T)})^{-1}\right)\right]$$

where $\boldsymbol{w}_{j,t} = (u_{j,t-1}, u_{j,t-2})'$. Similarly, from the generated $\boldsymbol{\psi}_j$ and from (4.10), we can draw $\sigma_{e,j}^2$ from the posterior distribution

$$IG\left(\nu_j + \frac{T}{2}, Z_j + \frac{\left(u_j^{(T)} - \boldsymbol{\psi}_j'\boldsymbol{w}_j^{(T)}\right)'\left(u_j^{(T)} - \boldsymbol{\psi}_j'\boldsymbol{w}_j^{(T)}\right)}{2}\right).$$

Finally, we turn to the generation of $(\mu_0, \mu_1, \phi, \boldsymbol{\theta}^{(ARCH)'})$. The parameters are drawn from the three full conditional distributions $p(\boldsymbol{\mu} \mid \boldsymbol{z}^{(T)}, S^{(T)}, \phi, \boldsymbol{\theta}^{(\text{ARCH})})$, $p(\phi \mid \boldsymbol{z}^{(T)}, S^{(T)}, \boldsymbol{\theta}^{(\text{ARCH})})$ and $p(\boldsymbol{\theta}^{(\text{ARCH})} \mid \boldsymbol{z}^{(T)}, S^{(T)}, \phi)$ sequentially. Since μ_{S_t} and ϕ appear in the conditional variance equation, those distributions are non-standard, as noted by Chan and Grant (2016), and Metropolis Hastings algorithms are required. Rewriting equation (4.3), we have

$$\frac{f_t - \phi f_{t-1}}{\sigma_t} = \frac{\mu_0(1 - S_t) + \mu_1 S_t}{\sigma_t} + \eta_t$$

Let us denote G_t^* the left-hand side of the above equation and Let us denote G_t^* the left-hand side of the above equation and

$$Q^{*(T)} = \begin{bmatrix} 1 - S^{(T)} & S^{(T)} \end{bmatrix}$$

From the prior distribution (4.12), to sample $\boldsymbol{\mu}$, we use a multivariate Gaussian proposal :

$$\mathcal{N}\left[(A^{*-1} + Q^{*(T)\prime}Q^{*(T)})^{-1}(A^{*-1}\alpha + Q^{*(T)\prime}G^{*(T)}), (A^{*-1} + Q^{*(T)\prime}Q^{*(T)})^{-1}\right]$$

and only keep draws verifying $\mu_0 > \mu_1$. Rewriting again equation (4.3) yields

$$\frac{f_t - \mu_0(1 - S_t) - \mu_1 S_t}{\sigma_t} = \phi\frac{f_{t-1}}{\sigma_t} + \eta_t.$$

Denoting $\tilde{G}_t$ the left-hand side of the above equation and $\tilde{Q}_t$ the right-hand side. To sample ϕ we use a Gaussian proposal with mean $\bar{\phi}$ and variance V_ϕ given by

$$\begin{aligned} \bar{\phi} = &\quad (A^{-1} + \tilde{Q}'\tilde{Q})^{-1}(A^{-1}\alpha + \tilde{Q}'\tilde{G}) \\ V_\phi = &\quad (A^{-1} + \tilde{Q}'\tilde{Q})^{-1}. \end{aligned}$$

Only draws satisfying the stationarity condition $|\phi| < 1$ are kept. Finally to sample $\boldsymbol{\theta}^{(\text{ARCH})}$, we use a Gaussian proposal centered at the mode of $p(\boldsymbol{\theta}^{(\text{ARCH})} \mid \boldsymbol{z}^{(T)}, S_t, \phi)$ with covariance matrix set to be the outer product of the scores.

4.7.2.3.3 Market sentiment

To generate $\mathbf{P}^{(\mathbf{MS})}$, we follow Geweke (2005). We denote the sum of transitions from the state $S_{t-1} = i$ to $S_t = j$ by n_{ij}. Each row of $\mathbf{P}^{(\mathbf{MS})}$ are drawn from posteriors:

$$Dir(8 + n_{11}, 1.5 + n_{12}, 0.5 + n_{14})$$
$$Dir(1.5 + n_{21}, 8 + n_{22}, 0.5 + n_{24})$$
$$Dir(0.5 + n_{31}, 8 + n_{33}, 1.5 + n_{34})$$
$$Dir(0.5 + n_{41}, 1.5 + n_{43}, 8 + n_{44})$$

Given $\boldsymbol{y}^{(T)}$ and $f^{(T)}$, we can rewrite equation-by-equation equation (4.1) with

$$y^*_{j,t} = \lambda_j f^*_{j,t} + e_{j,t}$$

for $j = 2, \ldots, m$, where $y^*_{j,t}$ and $f^*_{j,t}$ are the j-the respective components of

$$\begin{aligned} \boldsymbol{y}^*_t = &\quad \boldsymbol{y}_t - \bar{\boldsymbol{\psi}}_1 \circ \boldsymbol{y}_{t-1} \\ \boldsymbol{f}^*_t = &\quad \boldsymbol{e}_m f_t - \bar{\boldsymbol{\psi}}_1 f_{t-1} \end{aligned} \tag{4.20}$$

with $\boldsymbol{e}_m$ denoting a vector of 1 of length m qnd $\bar{\boldsymbol{\psi}}_l = (\psi_{1,l}, \ldots, \psi_{m,l})$, $l = 1$ being the order of the AR specification in equation (4.2). From (4.14) and (4.20), we obtain conditional draws for λ_j from the posterior distribution

$$\mathcal{N}\left[\left(A_j^{-1} + \sigma_{e,j}^{-2} f_j^{*(T)'} f_j^{*(T)}\right)^{-1} \left(A_j a_j + \sigma_{e,j}^{-2} f_j^{*(T)'} y_j^{*(T)}\right), \left(A_j^{-1} + \sigma_{e,j}^{-2} f_j^{*(T)'} f_j^{*(T)}\right)^{-1}\right].$$

Given $\boldsymbol{y}^{(T)}$ and $f^{(T)}$, from (4.1) we can measure $\boldsymbol{u}^{(T)}$ and from equation (4.2) and the prior distribution (4.10), for all $j = 1, \ldots, m$, we can draw $\boldsymbol{\psi}_j$ from the posterior distribution

$$\mathcal{N}\left[\left(\boldsymbol{\Pi}_j^{-1} + \sigma_{e,j}^{-2} \boldsymbol{w}_j^{(T)'} \boldsymbol{w}_j^{(T)}\right)^{-1} \left(\boldsymbol{\Pi}_j^{-1} \boldsymbol{\pi}_j + \sigma_{e,j}^{-2} \boldsymbol{w}_j^{(T)'} u_j^{(T)}\right), \left(\boldsymbol{\Pi}_j^{-1} + \sigma_{e,j}^{-2} \boldsymbol{w}_j^{(T)'} \boldsymbol{w}_j^{(T)})^{-1}\right)\right]$$

where $\boldsymbol{w}_{j,t} = (u_{j,t-1}, u_{j,t-2})'$. Similarly, from the generated $\boldsymbol{\psi}_j$ and from (4.10), we can draw $\sigma^2_{e,j}$ from the posterior distribution

$$IG\left(\nu_j + \frac{T}{2}, Z_j + \frac{\left(u_j^{(T)} - \boldsymbol{\psi}_j' \boldsymbol{w}_j^{(T)}\right)' \left(u_j^{(T)} - \boldsymbol{\psi}_j' \boldsymbol{w}_j^{(T)}\right)}{2}\right).$$

Finally, we turn to the generation of (μ_0, μ_1, ϕ). Rewriting equation (4.3), we have

$$\frac{f_t}{\sigma_{S_t}} = \frac{\mu_{S_t}}{\sigma_{S_t}} + \eta_t$$

Let us denote G^*_t the left-hand side of the above equation and

$$Q^{*(T)} = \left[\begin{array}{cccc} S^{(T)} = 1 & S^{(T)} = 2 & S^{(T)} = 3 & S^{(T)} = 4 \end{array}\right]$$

From the prior distribution (4.12), $\boldsymbol{\mu}$ can be drawn from the posterior distribution :

$$\boldsymbol{\mu} \sim \mathcal{N}((A^{*-1} + Q^{*(T)\prime}Q^{*(T)})^{-1}(A^{*-1}\alpha + Q^{*(T)\prime}G^{*(T)}), (A^{*-1} + Q^{*(T)\prime}Q^{*(T)})^{-1}),$$

and only draws verifying the condition $\mu_1 < 0, \mu_2 > 0, \mu_3 < 0, \mu_4 > 0$, and the long run conditions $\frac{\pi_1}{\pi_1+\pi_2}\mu_1 + \frac{\pi_2}{\pi_1+\pi_2}\mu_2 > 0$, $\frac{\pi_3}{\pi_3+\pi_4}\mu_3 + \frac{\pi_4}{\pi_3+\pi_4}\mu_4 < 0$. For $i = 1...n$, $\sigma^2_{S_t=i}$ is drawn from the posterior distribution:

$$IG\left(.5 + \frac{\sum_{t=1}^{T}(S_t = i)}{2}, 20 + \frac{(f_{S^{(T)}=i} - \mu_{S_t=i})'(f_{S^{(T)}=i} - \mu_{S_t=i})}{2}\right).$$

For the univariate specification of the market sentiment, the dynamic factor structure presented in equations (4.1) to (4.3) is not used. We have $y_t \mid S_t \sim \mathcal{N}(\mu_{S_t}, \sigma^2_{S_t})$. We thus discard the step generating the state vector presented in 4.7.2.1.

4.7.2.4. Posterior distributions of the parameters

Table 4.8: *Monetary Policy stance model parameters posteriors*

Variables	Parameters	Mean	Std
5Y	λ	1	0
7Y	λ	0.96	0.02
10Y	λ	0.88	0.02
5Y	ψ	-0.27	0.04
7Y	ψ	-0.28	0.06
10Y	ψ	-0.13	0.03
5Y	σ_e^2	0.15	0.01
7Y	σ_e^2	0.10	0.01
10Y	σ_e^2	0.32	0.02
Factor			
	μ_1	-0.31	0.17
	μ_2	0.02	0.02
	μ_3	-0.06	0.05
	μ_4	0.05	0.03
	σ_1	4.10	0.72
	σ_2	0.54	0.13
	σ_3	1.08	0.17
	σ_4	0.36	0.05
	P_{11}	0.93	0.01
	P_{12}	0.00	0.00
	P_{13}	0.07	0.01
	P_{14}	0.00	0.00
	P_{21}	0.00	0.00
	P_{22}	0.93	0.01
	P_{23}	0.00	0.00
	P_{24}	0.07	0.01
	P_{31}	0.06	0.01
	P_{32}	0.01	0.00
	P_{33}	0.89	0.01
	P_{34}	0.04	0.00
	P_{41}	0.00	0.00
	P_{42}	0.07	0.01
	P_{43}	0.04	0.00
	P_{44}	0.89	0.01

Table 4.9: *Multivariate Market Sentiment model parameters posteriors*

Variables	Parameters	Mean	Std
S&P500	λ	1	0
Russell	λ	1.1524	0.0172
Nasdaq	λ	1.0996	0.0126
Dow Jones	λ	0.946	0.0294
S&P500	ψ	-0.2953	0.0506
Russell	ψ	-0.0123	0.0288
Nasdaq	ψ	0.0466	0.0463
Dow Jones	ψ	-0.379	0.0221
S&P500	σ_e^2	0.0536	0.0059
Russell	σ_e^2	0.3298	0.0146
Nasdaq	σ_e^2	0.1081	0.0078
Dow Jones	σ_e	1.6205	0.0548
Factor			
	μ_1	-0.7168	0.3338
	μ_2	0.1294	0.104
	μ_3	-0.0453	0.066
	μ_4	0.191	0.0232
	σ_1	6.9455	1.9506
	σ_2	1.3513	0.25
	σ_3	1.0703	0.2164
	σ_4	0.2868	0.0315
	P_{11}	0.7823	0.0751
	P_{12}	0.2001	0.0736
	P_{14}	0.0176	0.0233
	P_{21}	0.0263	0.0191
	P_{22}	0.9468	0.0255
	P_{24}	0.0269	0.0186
	P_{31}	0.0188	0.0112
	P_{33}	0.8818	0.0412
	P_{34}	0.0994	0.0377
	P_{41}	0.0014	0.0016
	P_{43}	0.0519	0.0201
	P_{44}	0.9467	0.0203

Table 4.10: *Univariate Market Sentiment model parameters posteriors*

Parameters	Mean	Std
μ_1	-0.65	0.34
μ_2	0.10	0.07
μ_3	0.02	0.09
μ_4	0.02	0.04
σ_1	7.05	2.43
σ_2	1.25	0.16
σ_3	0.97	0.47
σ_4	0.27	0.08
P_{11}	0.78	0.08
P_{12}	0.21	0.08
P_{14}	0.01	0.02
P_{21}	0.02	0.01
P_{22}	0.96	0.02
P_{24}	0.02	0.01
P_{31}	0.02	0.01
P_{33}	0.89	0.06
P_{34}	0.10	0.05
P_{41}	0.00	0.01
P_{43}	0.09	0.07
P_{44}	0.90	0.08

4.7.3. Market sentiment univariate specification in-sample and out-of-sample probabilities

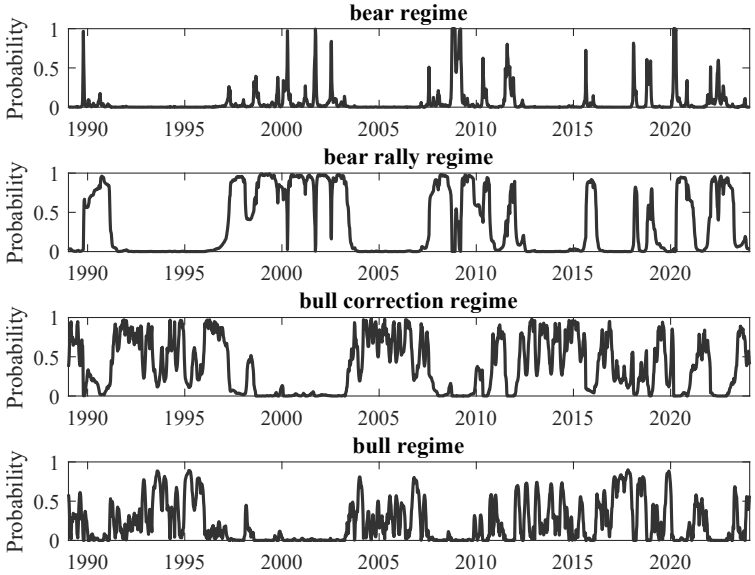

Figure 4.13: *In-sample probabilities from the univariate specification of the market sentiment*

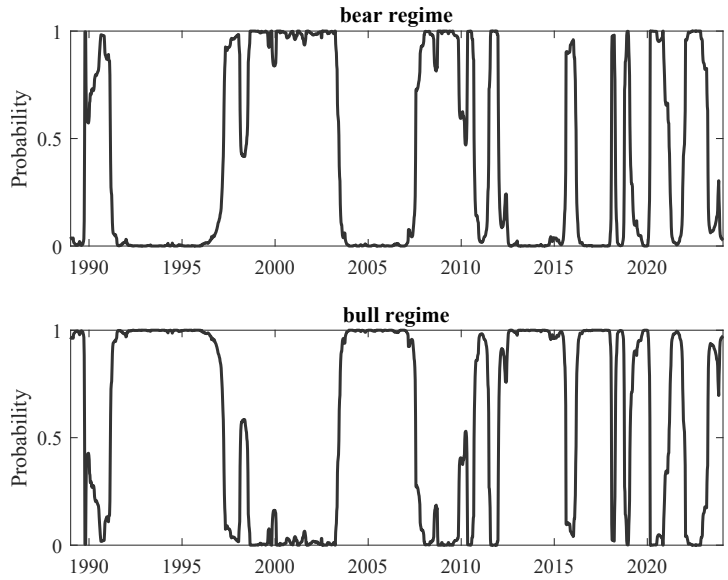

Figure 4.14: *Bull/bear in-sample probabilities from the univariate specification of the market sentiment*

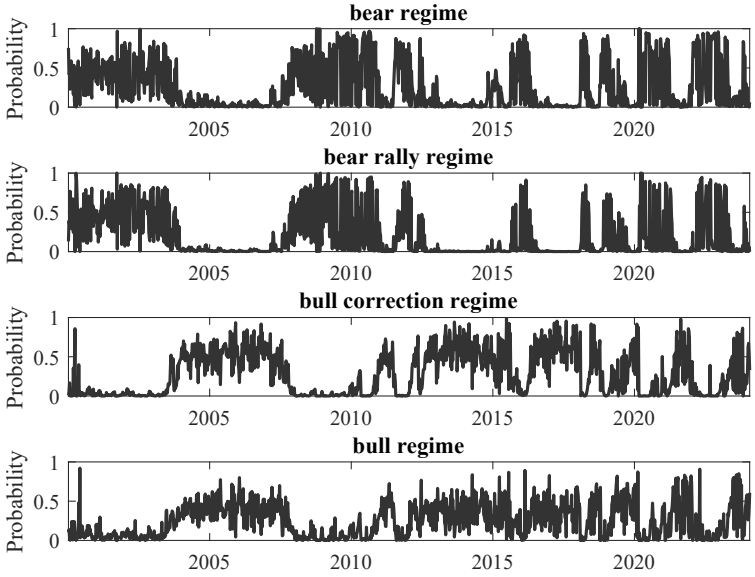

Figure 4.15: *Real-time probabilities from the univariate specification of the market sentiment*

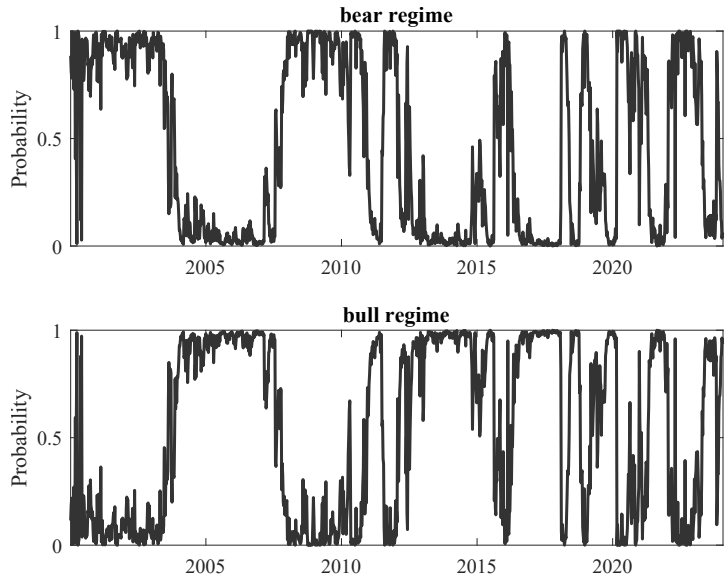

Figure 4.16: *Real-time bull/bear probabilities from the univariate specification of the market sentiment*

4.7.4. Performances of the portfolios

4.7.4.1. Rolling window performances

Table 4.11: *1Y rolling performances for the five groups of competing strategies and benchmarks*

	1 Y Return	**1 Y Vol**	**1 Y SR**	**1 Y Max DD**
MS-Sign-Return-Multi	6.1%	8.6%	0.51	6.5%
MS-Bull-Bear-Return-Multi	6.5%	9.7%	0.49	7.8%
MS-Sign-Return-Uni	3.8%	9.2%	0.22	8.2%
MS-Bull-Bear-Return-Uni	**6.7%**	**9.0%**	**0.56**	**7.2%**
MS-Sign-Return-Multi-BC	7.0%	11.4%	0.46	10.0%
MS-Bull-Bear-Return-Multi-BC	8.2%	11.7%	0.55	9.9%
MS-Sign-Return-Uni-BC	6.3%	10.8%	0.43	9.5%
MS-Bull-Bear-Return-Uni-BC	**7.5%**	**10.3%**	**0.56**	**8.6%**
MS-Sign-Return-Multi-MP	4.8%	8.8%	0.35	7.5%
MS-Bull-Bear-Return-Multi-MP	6.9%	9.5%	0.54	8.0%
MS-Sign-Return-Uni-BC	4.1%	7.3%	0.32	6.3%
MS-Bull-Bear-Return-Uni-MP	**6.3%**	**8.0%**	**0.58**	**6.1%**
MP-BC	**8.3%**	**12.0%**	**0.55**	**10.1%**
MS-Sign-Return-Multi-MP-BC	6.5%	9.8%	0.49	8.3%
MS-Bull-Bear-Return-Multi-MP-BC	7.6%	10.2%	0.57	8.6%
MS-Sign-Return-Uni-MP-BC	6.1%	8.7%	0.51	7.1%
MS-Bull-Bear-Return-Uni-MP-BC	**7.3%**	**8.9%**	**0.63**	**7.0%**
S&P500	8.3%	16.3%	0.42	14.3%
60Bond/40Equity	5.6%	9.2%	0.42	8.2%
Cash3m	1.6%			

Table 4.12: *2Y rolling performances for the five groups of competing strategies and benchmarks*

	2 Y Return	**2 Y Vol**	**2 Y SR**	**2 Y Max DD**
MS-Sign-Return-Multi	6.4%	8.5%	0.54	8.4%
MS-Bull-Bear-Return-Multi	7.2%	9.7%	0.56	9.5%
MS-Sign-Return-Uni	4.0%	9.4%	0.23	11.2%
MS-Bull-Bear-Return-Uni	**7.7%**	**9.1%**	**0.65**	**8.2%**
MS-Sign-Return-Multi-BC	7.1%	11.4%	0.47	13.8%
MS-Bull-Bear-Return-Multi-BC	8.2%	11.7%	0.55	13.4%
MS-Sign-Return-Uni-BC	6.4%	10.8%	0.43	13.1%
MS-Bull-Bear-Return-Uni-BC	**7.8%**	**10.3%**	**0.59**	**11.1%**
MS-Sign-Return-Multi-MP	5.1%	8.9%	0.37	10.0%
MS-Bull-Bear-Return-Multi-MP	6.9%	9.4%	0.55	10.2%
MS-Sign-Return-Uni-BC	4.3%	7.3%	0.35	8.3%
MS-Bull-Bear-Return-Uni-MP	**6.9%**	**8.1%**	**0.64**	**7.0%**
MP-BC	**8.4%**	**11.9%**	**0.56**	**13.2%**
MS-Sign-Return-Multi-MP-BC	6.8%	9.8%	0.52	11.1%
MS-Bull-Bear-Return-Multi-MP-BC	7.7%	10.2%	0.59	11.1%
MS-Sign-Return-Uni-MP-BC	6.4%	8.6%	0.55	9.0%
MS-Bull-Bear-Return-Uni-MP-BC	**7.8%**	**8.9%**	**0.68**	**8.6%**
S&P500	8.1%	16.5%	0.39	20.2%
60Bond/40Equity	6.0%	9.3%	0.45	11.2%
Cash3m	1.6%			

Table 4.13: *5Y rolling performances for the five groups of competing strategies and benchmarks*

	5 Y Return	**5 Y Vol**	**5 Y SR**	**5 Y Max DD**
MS-Sign-Return-Multi	5.4%	8.5%	0.42	13.5%
MS-Bull-Bear-Return-Multi	7.7%	9.7%	0.62	11.1%
MS-Sign-Return-Uni	2.1%	9.8%	0.03	19.9%
MS-Bull-Bear-Return-Uni	**8.3%**	**9.1%**	**0.71**	**9.1%**
MS-Sign-Return-Multi-BC	7.6%	11.1%	0.53	19.4%
MS-Bull-Bear-Return-Multi-BC	8.7%	11.2%	0.62	18.3%
MS-Sign-Return-Uni-BC	5.9%	10.8%	0.38	21.5%
MS-Bull-Bear-Return-Uni-BC	**8.4%**	**10.1%**	**0.66**	**14.0%**
MS-Sign-Return-Multi-MP	5.4%	8.4%	0.44	12.5%
MS-Bull-Bear-Return-Multi-MP	7.2%	8.6%	0.63	11.6%
MS-Sign-Return-Uni-BC	3.3%	6.9%	0.22	12.5%
MS-Bull-Bear-Return-Uni-MP	**7.4%**	**8.0%**	**0.71**	**7.7%**
MP-BC	**9.0%**	**11.4%**	**0.64**	**16.2%**
MS-Sign-Return-Multi-MP-BC	7.3%	9.3%	0.60	13.3%
MS-Bull-Bear-Return-Multi-MP-BC	8.2%	9.4%	0.68	13.5%
MS-Sign-Return-Uni-MP-BC	6.2%	8.1%	0.55	12.2%
MS-Bull-Bear-Return-Uni-MP-BC	**8.3%**	**8.5%**	**0.77**	**9.4%**
S\&P500	7.5%	16.6%	0.35	31.4%
60Bond/40Equity	5.6%	9.2%	0.42	17.5%
Cash3m	1.7%			

Table 4.14: *10 year rolling performances for the five groups of competing strategies and benchmarks*

	10 Y Return	**10 Y Vol**	**10 Y SR**	**10 Y Max DD**
MS-Sign-Return-Multi	6.3%	9.3%	0.49	18.7%
MS-Bull-Bear-Return-Multi	7.3%	9.8%	0.57	13.1%
MS-Sign-Return-Uni	1.2%	11.5%	-0.04	36.8%
MS-Bull-Bear-Return-Uni	**8.2%**	**9.1%**	**0.71**	**10.2%**
MS-Sign-Return-Multi-BC	7.7%	11.5%	0.52	27.3%
MS-Bull-Bear-Return-Multi-BC	8.9%	11.8%	0.61	24.3%
MS-Sign-Return-Uni-BC	5.5%	11.6%	0.33	34.0%
MS-Bull-Bear-Return-Uni-BC	**8,4%**	**10,2%**	**0,66**	**18,2%**
MS-Sign-Return-Multi-MP	5,5%	8,6%	0,44	16.6%
MS-Bull-Bear-Return-Multi-MP	7.5%	9.0%	0.63	13.3%
MS-Sign-Return-Uni-BC	3.0%	7.3%	0.17	19.9%
MS-Bull-Bear-Return-Uni-MP	**7.2%**	**7.9%**	**0.69**	**9.0%**
MP-BC	**9.3%**	**11.6%**	**0.66**	**19.6%**
MS-Sign-Return-Multi-MP-BC	7.5%	9.4%	0.61	16.4%
MS-Bull-Bear-Return-Multi-MP-BC	8.5%	9.7%	0.69	16.5%
MS-Sign-Return-Uni-MP-BC	6.3%	8.3%	0.55	16.3%
MS-Bull-Bear-Return-Uni-MP-BC	**8.4%**	**8.5%**	**0.79**	**10.7%**
S\&P500	7.0%	18.1%	0.29	49.9%
60Bond/40Equity	5.6%	10.0%	0.38	29.4%
Cash3m	1.7%			

4.7.4.2. Cumulative distributions of rolling window returns for selected strategies

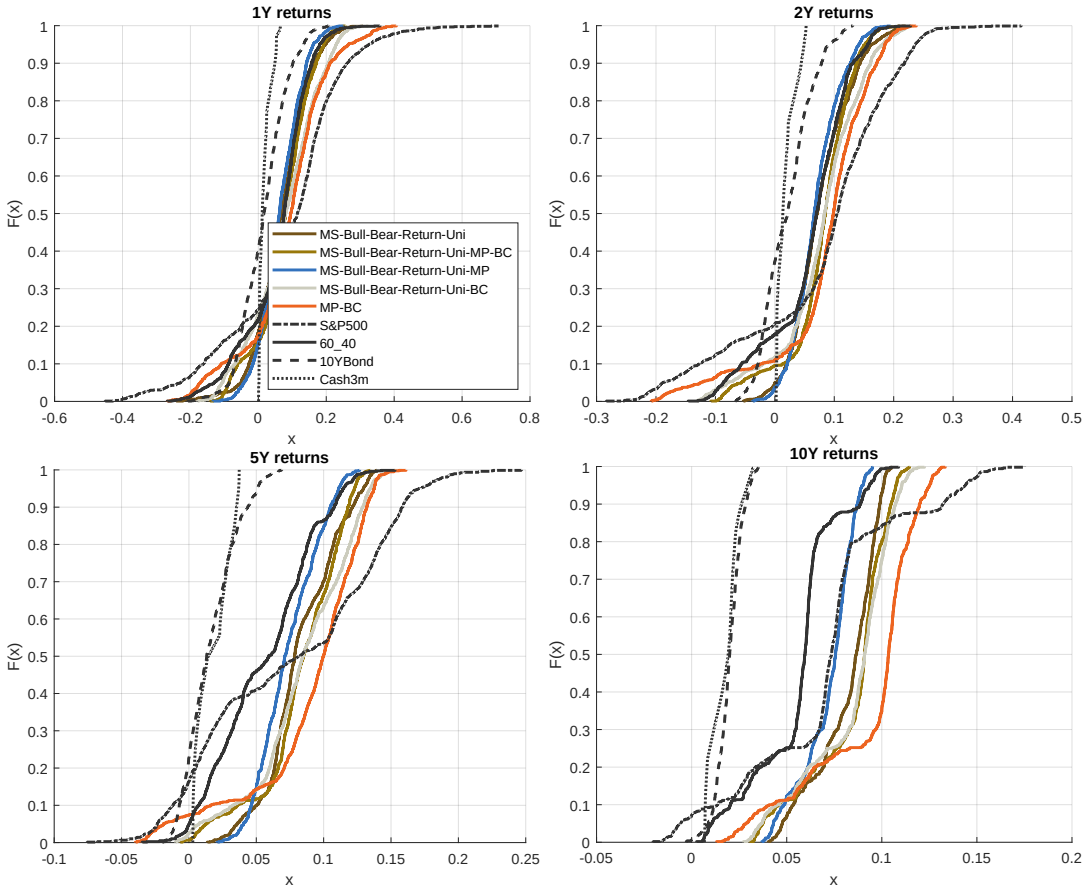

Figure 4.17: *Cumulative distribution functions of rolling window Returns from 1 year to 10 year holding horizons*

4.7.4.3. Yearly returns of the strategies in "normal" and "abnormal" times

Table 4.15: *Annual returns during "normal" times*

	2002	2003	2007	2010	2011	2012	2013	2014	2019	2021	Average
MS-Bull-Bear-Return-Uni	7.1%	3.8%	5.7%	6.1%	16.0%	2.6%	30.7%	12.2%	15.4%	12.9%	11.3%
MS-Bull-Bear-Return-Uni-BC	-12.1%	16.6%	4.9%	7.5%	3.1%	7.6%	31.9%	13.8%	22.2%	23.0%	11.9%
MS-Bull-Bear-Return-Uni-MP	8.0%	1.5%	4.9%	5.3%	16.1%	1.9%	22.2%	11.5%	14.9%	12.7%	9.9%
MP-BC	**-21.6%**	**20.8%**	**4.5%**	**9.7%**	**2.4%**	**12.0%**	**24.1%**	**14.7%**	**30.4%**	**28.8%**	**12.6%**
MS-Bull-Bear-Return-Uni-MP-BC	**-7.6%**	**11.0%**	**4.7%**	**7.8%**	**9.4%**	**6.9%**	**23.1%**	**13.1%**	**22.4%**	**20.5%**	**11.1%**
S&P500	-23.0%	26.8%	6.1%	13.4%	2.1%	13.8%	33.4%	15.4%	32.3%	29.3%	15.0%
60/40	-10.4%	15.1%	5.8%	10.5%	7.5%	9.6%	14.3%	12.4%	22.2%	15.3%	10.2%
10 Year Bond	10.2%	-1.9%	4.5%	4.9%	13.6%	2.7%	-9.7%	7.3%	7.8%	-3.4%	3.6%

Table 4.16: *Annual returns during recession periods*

	2001	**2008**	**2009**	**2020**	**Average**
MS-Bull-Bear-Return-Uni	-6.7%	14.0%	-7.7%	-1.0%	-0.3%
MS-Bull-Bear-Return-Uni-BC	-10.0%	-4.4%	16.0%	2.5%	1.0%
MS-Bull-Bear-Return-Uni-MP	-4.6%	10.3%	-6.8%	-2.8%	-1.0%
MP-BC	**-15.7%**	**6.0%**	**15.8%**	**8.0%**	**3.5%**
MS-Bull-Bear-Return-Uni-MP-BC	**-10.0%**	**8.2%**	**4.3%**	**2.8%**	**1.3%**
S&P500	-10.7%	-39.0%	31.5%	16.1%	-0.5%
60/40	-6.6%	-19.1%	13.0%	15.5%	0.7%
10 Year Bond	-2.0%	18.3%	-12.7%	10.5%	3.6%

Table 4.17: *Annual returns during tightening cylces*

	2000	**2004**	**2005**	**2006**	**2015**	**2016**	**2017**	**2018**	**2022**	**Average**
MS-Bull-Bear-Return-Uni	1.2%	8.4%	4.4%	15.0%	-5.3%	12.3%	21.0%	-1.6%	-23.6%	3.5%
MS-Bull-Bear-Return-Uni-BC	-0.6%	10.9%	4.6%	15.3%	-1.9%	9.7%	21.1%	-3.4%	-12.8%	4.8%
MS-Bull-Bear-Return-Uni-MP	1.8%	10.1%	4.2%	11.5%	-2.6%	12.5%	19.6%	-1.2%	-10.4%	5.1%
MP-BC	**-2.4%**	**13.2%**	**4.4%**	**11.6%**	**2.2%**	**10.2%**	**19.8%**	**-4.1%**	**-11.2%**	**4.9%**
MS-Bull-Bear-Return-Uni-MP-BC	**0.1%**	**11.7%**	**4.3%**	**11.6%**	**-0.1%**	**11.4%**	**19.7%**	**-2.4%**	**-10.6%**	**5.1%**
S&P500	-7.4%	12.1%	4.8%	15.5%	0.8%	10.6%	21.4%	-5.1%	-17.8%	3.9%
60/40	-0.7%	7.1%	2.2%	7.8%	0.8%	6.1%	12.3%	-3.9%	-17.7%	1.6%
10 Year Bond	8.5%	-0.4%	-1.9%	-3.1%	-0.2%	-1.0%	-0.2%	-3.1%	-18.8%	-2.2%

Bibliography

Albert, J. H. and Chib, S. (1993). Bayesian analysis of binary and polychotomous response data. *Journal of the American Statistical Association*, 88(422):669–679.

Ang, A. and Bekaert, G. (2004). How do regimes affect asset allocation. *Financial Analysts Journal*, 60:86–99.

Ang, A. and Timmermann, A. (2012). Regime changes and financial markets. *Annual Review of Financial Economics*, 4(1):313–337.

Antolin-Diaz, J., Drechsel, T., and Petrella, I. (2017). Tracking the Slowdown in Long-Run GDP Growth. *The Review of Economics and Statistics*, 99(2):343–356.

Antolin-Diaz, J., Drechsel, T., and Petrella, I. (2023). Advances in Nowcasting Economic Activity: The Role of Heterogeneous Dynamics and Fat Tails. CEPR Discussion Papers 17800, C.E.P.R. Discussion Papers.

Aussenegg, W., Goetz, L., and Jelic, R. (2016). European asset swap spreads and the credit crisis. *The European Journal of Finance*, 22(7):572–600.

Bai, J. and Ng, S. (2008). Large dimensional factor analysis. *Foundations and Trends(R) in Econometrics*, 3(2):89–163.

Bai, J. and Wang, P. (2011). Conditional markov chain and its application in economic time series analysis. *Journal of Applied Econometrics*, 26(5):715–734.

Bai, J. and Wang, P. (2015). Identification and bayesian estimation of dynamic factor models. *Journal of Business & Economic Statistics*, 33(2):221–240.

Barigozzi, M. and Hallin, M. (2023). Dynamic Factor Models: a Genealogy. Working Papers ECARES 2023-15, ULB – Universite Libre de Bruxelles.

Bańbura, M., Giannone, D., Modugno, M., and Reichlin, L. (2013). Now-casting and the real-time data flow. In Elliott, G. and Timmermann, A., editors, *Handbook of Economic Forecasting*, volume 2, pages 195–237.

Bernanke, B. (2010). Monetary policy and the housing bubble: a speech at the annual meeting of the american economic association, atlanta, georgia, january 3, 2010. (499).

Bernanke, B. and Gertler, M. (1989). Agency Costs, Net Worth, and Business Fluctuations. *American Economic Review*, 79(1):14–31.

Bernanke, B. and Kuttner, K. (2005). What explains the stock market's reaction to federal reserve policy? *Journal of Finance*, 60(3):1221–1257.

Bernanke, B. S. (2020). The new tools of monetary policy. *American Economic Review*, 110(4):943–83.

Black, F. (1976). Studies of stock price volatility changes, proceedings of the business and economic statistical section. *American Statistical Association*, pages 177–181.

Boeck, M. and Feldkircher, M. (2021). The impact of monetary policy on yield curve expectations. *Journal of Economic Behavior and Organization*, 191:887–901.

Bollerslev, T. (1986). Generalized autoregressive conditional heteroskedasticity. *Journal of Econometrics*, 31(3):307–327.

Bouyé, E. and Teiletche, J. (2024). Regime-based strategic asset allocation. *The World Bank, Treasury, RAMP.*

Brocato, J. and Steed, S. (1998). Optimal Asset Allocation over the Business Cycle. *The Financial Review*, 33(3):129–148.

Burns, A. F. and Mitchell, W. C. (1946). Measuring business cycles. *National Bureau of Economic Research.*

Camacho, M., Perez-Quiros, G., and Poncela, P. (2014). Green shoots and double dips in the euro area: A real time measure. *International Journal of Forecasting*, 30(3):520–535.

Camacho, M., Perez-Quiros, G., and Poncela, P. (2018). Markov-switching dynamic factor models in real time. *International Journal of Forecasting*, 34(4):598–611.

Camacho, M., Perez-Quiros, G., and Poncela, P. (2015). Extracting nonlinear signals from several economic indicators. *Journal of Applied Econometrics*, 30(7):1073–1089.

Campbell, J. Y. and Shiller, R. J. (1988). The dividend-price ratio and expectations of future dividends and discount factors. *The review of financial studies*, 1(3):195–228.

Carriero, A., Clark, T. E., Marcellino, M., and Mertens, E. (2022). Addressing COVID-19 Outliers in BVARs with Stochastic Volatility. *The Review of Economics and Statistics*, pages 1–38.

Carter, C. K. and Kohn, R. (1994). On Gibbs sampling for state space models. *Biometrika*, 81(3):541–53.

Chan, J. C. (2017). The stochastic volatility in mean model with time-varying parameters: An application to inflation modeling. *Journal of Business & Economic Statistics*, 35(1):17–28.

Chan, J. C. (2023). Comparing stochastic volatility specifications for large Bayesian VARs. *Journal of Econometrics*, 235(2):1419–1446.

Chan, J. C. and Eisenstat, E. (2018). Bayesian model comparison for time-varying parameter VARs with stochastic volatility. *Journal of Applied Econometrics*, 33(4):509–532.

Chan, J. C. and Grant, A. L. (2016). Modeling energy price dynamics: GARCH versus stochastic volatility. *Energy Economics*, 54:182–189.

Chan, J. C. and Jeliazkov, I. (2009). Efficient simulation and integrated likelihood estimation in state space models. *International Journal of Mathematical Modelling and Numerical Optimisation*, 1(1-2):101–120.

Chang, Y., Maih, J., and Tan, F. (2021). Origins of monetary policy shifts: A new approach to regime switching in dsge models. *Journal of Economic Dynamics and Control*, 133(C).

Chauvet, M. (1998). An econometric characterization of business cycle dynamics with factor structure and regime switches. *International Economic Review*, 39(4):969–996.

Chauvet, M. and Piger, J. (2008). A comparison of the real-time performance of business cycle dating methods. *Journal of Business & Economic Statistics*, 26(1):42–49.

Chauvet, M. and Senyuz, Z. (2016). A dynamic factor model of the yield curve components as a predictor of the economy. *International Journal of Forecasting*, 32(2):324–343.

Clarida, R., Gali, J., and Gertler, M. (1999). The science of monetary policy: A new keynesian perspective. *Journal of Economic Literature*, 37(4):1661–1707.

Clark, T. E. (2011). Real-time density forecasts from Bayesian Vector Autoregressions with stochastic volatility. *Journal of Business & Economic Statistics*, 29(3):327–341.

Clark, T. E. and Ravazzolo, F. (2015). Macroeconomic forecasting performance under alternative specifications of time-varying volatility. *Journal of Applied Econometrics*, 30(4):551–575.

Cochrane, J. H. (1999). Portfolio Advice for a Multifactor World. *NBER Working Papers*, (7170).

de Longis, A. and Ellis, D. (2023). Tactical asset allocation, risk premia, and the business cycle: A macro regime approach. *Journal of Portfolio Management*, 49(4).

De Santis, R. A. (2016). Credit spreads, economic activity and fragmentation. *European Central Bank Working Paper Series*, 1930.

De Santis, R. A. (2018). Unobservable country bond premia and fragmentation. *Journal of International Money and Finance*, 82(C):1–25.

Diebold, F. X. and Rudebusch, G. D. (1996). Measuring business cycles: A modern perspective. *The Review of Economics and Statistics*, 78(1):67–77.

Doz, C., Ferrara, L., and Pionnier, P.-A. (2020). Business cycle dynamics after the Great Recession: An extended Markov-switching dynamic factor model. Working Paper 02443364, Paris School of Economics.

Doz, C. and Fuleky, P. (2019). Dynamic factor models. Working Papers 2019-4, University of Hawaii Economic Research Organization, University of Hawaii at Manoa.

Doz, C., Giannone, D., and Reichlin, L. (2011). A two-step estimator for large approximate dynamic factor models based on kalman filtering. *Journal of Econometrics*, 164(1):188–205.

Driessen, J. (2005). Is default event risk priced in corporate bonds? *The Review of Financial Studies*, 18(1):165–195.

Engle, R. F. (1982). Autoregressive conditional heteroscedasticity with estimates of the variance of United Kingdom inflation. *Econometrica*, 50(4):987–1007.

Eo, Y. and Kim, C.-J. (2016). Markov-switching models with evolving regime-specific parameters: are postwar booms or recessions all alike? *The Review of Economics and Statistics*, 98(5):940–949.

Evans, M. (2005). Where are we now? Real-time estimates of the macroeconomy. *International Journal of Central Banking*, 2(1):127–175.

Fama, E. F. (1981). Stock returns, real activity, inflation, and money. *American Economic Review*, 71(4):545–565.

Faust, J., Gilchrist, S., Wright, J. H., and Zakrajšek, E. (2011). Credit spreads as predictors of real-time economic activity: A bayesian model-averaging approach. *National Bureau of Economic Research Working Paper*, 16725.

Fleming, J., Kirby, C., and Ostdiek, B. (2003). The economic value of volatility timing using "realized" volatility. *Journal of Financial Economics*, 67(3):473–509.

Furno, F. and Giannone, D. (2024). Nowcasting recession risk. *Research Methods and Applications on Macroeconomic Forecasting*.

Geweke, J. (1977). The dynamic factor analysis of economic timeseries models. *Latent variables in socio-economic models*, pages 365–383.

Geweke, J. F. (2005). Contemporary bayesian econometrics and statistics. *Wiley series in probability and statistics*.

Giannone, D., Reichlin, L., and Small, D. (2008). Nowcasting: The real-time informational content of macroeconomic data. *Journal of Monetary Economics*, 55(4):665–676.

Gilchrist, S. and E.Zakrajšek (2012). Credit spreads and business cycle fluctuations. *American Economic Review*, 102(4):1692–1720.

Gilchrist, S., Yankov, V., and Zakrajšek, E. (2009). Credit market shocks and economic fluctuations: Evidence from corporate bond and stock markets. *Journal of Monetary Economics*, 56:471–493.

Hamilton, J. (1988). Rational-expectations econometric analysis of changes in regime: An investigation of the term structure of interest rates. *Journal of Economic Dynamics and Control*, 12(2-3):385–423.

Hamilton, J. and Gang, L. (1996). Stock market volatility and the business cycle. *Journal of Applied Econometrics*, 11(5):573–93.

Hamilton, J. D. (1989). A new approach to the economic analysis of nonstationary time series and the business cycle. *Econometrica*, 57(2):357–384.

Hamilton, J. D. (2011). Calling recessions in real time. *International Journal of Forecasting*, 27(4):1006–1026.

Hamilton, J. D. and Kim, D. H. (2002). A reexamination of the predictability of economic activity using the yield spread. *Journal of Money, Credit, and Banking*, 34(2):340–360.

Hamilton, J. D. and Susmel, R. (1994). Autoregressive conditional heteroskedasticity and changes in regime. *Journal of Econometrics*, 64(1):307–333.

Hamilton, M. and de Longis, A. (2015). Dynamic asset allocation through the business cycle: A macro regime approach. *OppenheimerFunds*.

Harvey, C. R. (1988). The real term structure and consumption growth. *Journal of Financial Economics*, 22(2):305–333.

Heinlein, R. and Lepori, G. M. (2022). Do financial markets respond to macroeconomic surprises? Evidence from the UK. *Empirical Economics*, 62(5):2329–2371.

Jarociński, M. and Karadi, P. (2020). Deconstructing monetary policy surprises—the role of information shocks. *American Economic Journal: Macroeconomics*, 12(2):1–43.

Jensen, G. R. and Mercer, J. M. (2003). New evidence on optimal asset allocation. *The Financial Review*, 38(3):435–454.

Kim, C.-J. (1994). Dynamic linear models with Markov-switching. *Journal of Econometrics*, 60(1-2):1–22.

Kim, C.-J., Morley, J. C., and Nelson, C. (2000). Is There a Positive Relationship between Stock Market Volatility and the Equity Premium? *Working Papers*, (0023).

Kim, C.-J. and Nelson, C. R. (1998). Business cycle turning points, a new coincident index and tests of duration dependence based on a dynamic factor model with regime switching. *The Review of Economics and Statistics*, 80(2):188–201.

Kim, C.-J. and Nelson, C. R. (1999). *State space models with regime switching*. The MIT Press, Cambridge, Massachusetts.

Kim, M. J. and Kwon, D. (2023). Dynamic asset allocation strategy: an economic regime approach. *Journal of Asset Management*, 24(2):136–147.

Kim, M.-J. and Yoo, J.-S. (1995). New index of coincident indicators: A multivariate markov switching factor model approach. *Journal of Monetary Economics*, 36(3):607–630.

Kiyotaki, N. and Moore, J. (1997). Credit cycles. *Journal of Political Economy*, 105(2):211–48.

Kollar, M. and Schmieder, C. (2019). Macro-based asset allocation: An empirical analysis. EIB Working Papers 2019/11, European Investment Bank (EIB).

Kritzman, M., Page, S., and Turkington, D. (2012). Regime shifts: Implications for dynamic strategies. *Financial Analysts Journal*, 68(3):22–39.

Kroencke, T. A. (2022). Recessions and the stock market. *Journal of Monetary Economics*, 131:61–77.

Leibowitz, M. L., Sorensen, E. H., Arnott, R. D., and Hanson, H. N. (1989). A total differential approach to equity duration. *Financial Analysts Journal*, 45(5):30–37.

Leiva-Leon, D., Pérez-Quirós, G., and Rots, E. (2020). Real-time weakness of the global economy: A first assessment of the coronavirus crisis. *Working Paper Series, European Central Bank*, 2381.

Leiva-León, D., Pérez-Quirós, G., Sapriza, H., Vazquez-Grande, F., and Zakrajšek, E. (2022). Introducing the credit market sentiment index. *Richmond Fed Economic Brief*, 22(33).

Li, W. K. and Mak, T. (1994). On the squared residual autocorrelations in non-linear time series with conditional heteroskedasticity. *Journal of Time Series Analysis*, 15(6):627–636.

Liu, J., Maheu, J., and Song, Y. (2024). Identification and forecasting of bull and bear markets using multivariate returns. Technical report.

López-Salido, D., Stein, J. C., and Zakrajšek, E. (2016). Credit-market sentiment and the business cycle. *NBER Working Papers*, 21879.

Maheu, J. and McCurdy, T. (2000). Identifying bull and bear markets in stock returns. *Journal of Business & Economic Statistics*, 18(1):100–112.

Maheu, J., McCurdy, T., and Song, Y. (2012). Components of bull and bear markets: Bull corrections and bear rallies. *Journal of Business & Economic Statistics*, 30(3):391–403.

Marcellino, M., Porqueddu, M., and Venditti, F. (2016). Short-term gdp forecasting with a mixed-frequency dynamic factor model with stochastic volatility. *Journal of Business & Economic Statistics*, 34(1):118–127.

Mariano, R. S. and Murasawa, Y. (2003). A new coincident index of business cycles based on monthly and quarterly series. *Journal of Applied Econometrics*, 18(4):427–443.

Markowitz, H. (1952). Portfolio selection. *The Journal of Finance*, 7(1):77–91.

McCracken, M. W. and Ng, S. (2016). FRED-MD: A monthly database for macroeconomic research. *Journal of Business & Economic Statistics*, 34(4):574–589.

McQueen, G. and Roley, V. V. (1993). Stock prices, news, and business conditions. *Review of Financial Studies*, 6(3):683–707.

Nakamura, E. and Steinsson, J. (2018). High-frequency identification of monetary non-neutrality: The information effect. *The Quarterly Journal of Economics*, 133(3):1283–1330.

Ng, S. (2021). Modeling macroeconomic variations after COVID-19. Working Paper 29060, National Bureau of Economic Research.

O'Kane, D. (2000). Introduction to asset swaps. *Lehman Brothers*.

Orphanides, A. (2003). Historical monetary policy analysis and the Taylor rule. *Journal of Monetary Economics*, 50(5):983–1022.

Perruchoud, A. (2009). Estimating a taylor rule with markov switching regimes for switzerland. *Swiss Journal of Economics and Statistics (SJES)*, 145(II):187–220.

Philippon, T. (2009). The bond market's q. *The Quarterly Journal of Economics*, 124(3):1011–1056.

Rigobon, R. and Sack, B. (2004). The impact of monetary policy on asset prices. *Journal of Monetary Economics*, 51(8):1553–1575.

Sargent, T. and Sims, C. (1977). Business cycle modeling without pretending to have too much a priori economic theory. *Federal Reserve Bank of Minneapolis*, (55).

Sharpe, W. F. (1994). The sharpe ratio. pages 169–178.

Shiller, R. J. et al. (1981). Do stock prices move too much to be justified by subsequent changes in dividends?

Siegel, J. J. (1991). Does it pay stock investors to forecast the business cycle? *The Journal of Portfolio Management*, 18(1):27–34.

Sims, C. and Zha, T. (2004). Were there regime switches in u.s. monetary policy? FRB Atlanta Working Paper 2004-14, Federal Reserve Bank of Atlanta.

Smith, A. L. and Valcarcel, V. J. (2023). The financial market effects of unwinding the federal reserve's balance sheet. *Journal of Economic Dynamics and Control*, 146:104582.

Spearman, C. (1904). The proof and measurement of association between two things. *The American Journal of Psychology*, 15(1):72–101.

Stock, J. and Watson, M. W. (1991). *A Probability Model of the Coincident Economic Indicators*, pages 63–90. Cambridge University Press.

Stock, J. H. and Watson, M. W. (1989). New Indexes of Coincident and Leading Economic Indicators. In *NBER Macroeconomics Annual 1989, Volume 4*, NBER Chapters, pages 351–409. National Bureau of Economic Research, Inc.

Stock, J. H. and Watson, M. W. (2003). Forecasting output and inflation: The role of asset. *Journal of Economic Literature*, 41(3):788–829.

Taylor, J. (2007). Housing and monetary policy. *NBER Working Papers*, (13682).

Taylor, J. B. (1993). Discretion versus policy rules in practice. *Carnegie-Rochester Conference Series on Public Policy*, 39:195–214.

Thorbecke, W. (1997). On Stock Market Returns and Monetary Policy. *Journal of Finance*, 52(2):635–654.

van Vliet, P. and Blitz, D. (2011). Dynamic strategic asset allocation: Risk and return across the business cycle. *Journal of Asset Management*, 12(5):360–375.

Woodford, M. (2003). Interest and prices: Foundations of a theory of monetary policy. *Princeton University Press*, page 462–468.

ECOLE
DOCTORALE

Titre : La non-linéarité cyclique, prévision en temps réel et son application à la gestion d'actifs

Mots clés : Prévision en temps réel; Inférence Bayesienne; Modèles à Facteurs Dynamiques; Chaînes de Markov; Cycle des affaires; Allocation d'Actifs

Résumé : Ce manuscrit de thèse se donne pour objet de rapprocher le cadre méthodologique d'identification en temps réel des dynamiques du cycle économique à la gestion d'actifs. Le cycle économique est caractérisé par des phases d'expansion et de récession dont la durée et l'amplitude sont hétérogènes. Les données macroéconomiques qui servent à identifier les phases du cycle sont marquées par des délais de publication et une asynchronicité dans leur disponibilité. Les modèles à facteurs dynamiques à changements de régimes markoviens sont une solution privilégiée pour gérer ces spécificités. Dans le sillage de l'événement extrême du Covid-19 (du point de vue de l'amplitude du choc et de sa relative courte durée), une grande partie des modèles employés jusque-là pour identifier et dater les changements de régimes dans le cycle économique sont devenus inaptes à capter des retournements de plus faible envergure.
Le premier chapitre de cette thèse s'emploie à développer une extension des modèles mentionnés plus haut par le biais d'une volatilité dynamique dans le mouvement du cycle économique sous-jacent. Cette solution minore l'impact des chocs extrêmes dans le processus d'identification des régimes tout en les conservant dans le but d'établir une détection plus robuste des futurs retournements conjoncturels.
Le délai et l'asynchronicité de disponibilité des données macroéconomiques sont un enjeu crucial pour les décideurs politiques et les agents de marché. Le deuxième chapitre de ce manuscrit introduit et démontre l'utilité de considérer des données de prix de marchés afin d'établir une mesure plus concomitante des retournements conjoncturels. Une classe particulière d'actifs, les "asset swap spreads", lorsqu'ils sont agrégés, se révèlent produire des évaluations coïncidentes des retournements conjoncturels. Ces prix permettent de mitiger le coût d'opportunité induit par l'absence ou le délai d'information conjoncturelle officielle. Appliqués dans le cadre de stratégies de couverture, ces signaux se révèlent être d'une grande utilité pour l'investisseur.
L'allocation d'actifs se doit de prendre en compte les dynamiques conjoncturelles mais ce seul facteur n'est pas suffisant dans le processus de construction de portefeuille. Le troisième chapitre déploie une allocation de portefeuille basée sur l'identification de régimes macroéconomiques en ajoutant des signaux relatifs au sentiment de marché ainsi qu'à la posture de politique monétaire. Comparées à celles d'un portefeuille classique 60% actions/40% obligations, les performances basées sur l'approche à trois signaux permettent à l'investisseur d'optimiser le couple rendement/risque tant dans les périodes de stress que de croissance.

Title : Cyclical non-linearity, nowcasting and asset allocation

Keywords : Nowcasting; Bayesian Inference; Dynamic Factor Models; Markov Switching; Business Cycle; Asset Allocation

Abstract : This thesis aims to reconcile real-time identification of business cycle phases with asset management. The business cycle is characterized by phases of expansion and recession, with varying durations and amplitudes. Macroeconomic data used to identify these phases are marked by publication delays and asynchronicity in their availability. Markov-switching dynamic factor models are a typical econometric framework to manage these characteristics. In the wake of the extreme event of Covid-19 (in terms of the shock's magnitude and its relatively short duration), many models previously employed to identify and date regime changes in the economic cycle have become inadequate for capturing smaller-scale reversals.
The first chapter of this thesis develops an extension of the aforementioned methodological framework by introducing dynamic volatility into the unobserved business cycle dynamics. This solution reduces the impact of extreme shocks in the regime identification process while retaining them to establish a more robust detection of future cyclical reversals. The delay and asynchronicity of macroeconomic data availability are crucial issues for policymakers and market participants.
The second chapter of this manuscript introduces and demonstrates the utility of considering market price data to establish a more concurrent measure of cyclical downturns. A particular class of assets, the "Asset Swap spreads" (a risk premium fixed between two counterparts exchanging future corporate bond coupons for a risk-free rate), when aggregated, produce coincident evaluations of macroeconomic recessions. These prices help mitigate the opportunity cost induced by the absence or delay of official macroeconomic information. When applied in the context of hedging strategies, these signals prove to be highly useful for investors. Asset allocation must take into account economic downturns, but this factor alone is not sufficient in the portfolio construction process.
The third chapter deploys a portfolio allocation based on the identification of macroeconomic regimes, adding signals related to market sentiment and monetary policy stance. Compared to a classic 60% equities/40% bonds portfolio, the performance based on the three-signal approach allows investors to optimize the risk-adjusted return during both stressed and expansion periods.

Institut Polytechnique de Paris
91120 Palaiseau, France